FACULTEIT GENEESKUNDE EN GEZONDHEIDSWETENSCHAPPEN

Laboratorium voor Experimentele Hematologie

Driving neuro-inflammation towards neuro-protection:

IL13-mediated alternative activation of microglia and macrophages

Proefschrift voorgelegd tot het behalen van de graad van doctor in de Medische Wetenschappen aan de Universiteit Antwerpen, te verdedigen door

Debbie Le Blon

PROMOTOREN

Prof. Dr. Peter Ponsaerts

Prof. Dr. Zwi Berneman

Antwerpen, 2016

COVER

Cover illustration	Debbie Le Blon
Printing and cover design	Anita Muys, Nieuwe Media Dienst, UA

COMMENTS TO COVER ILLUSTRATION

A representative IL13-expressing mesenchymal stem cell graft in the central nervous system of an eGFP bone marrow chimeric mouse. Different activated cell types are visualized: all infiltrating blood-derived macrophages are green, all M2-activated cells are red and all MHCII-activated cells are blue.

DOCTORAL COMMITTEE

Promotors:	Prof. dr. Peter Ponsaerts, Universiteit Antwerpen
	Prof. dr. Zwi Berneman, Universiteit Antwerpen
Chairman:	Prof. dr. Paul Van de Heyning, Universiteit Antwerpen
Members:	Prof. dr. Paul Van de Heyning, Universiteit Antwerpen
	Prof. dr. Nadia Zakaria, Universiteit Antwerpen
External members:	Prof. dr. Niels Hellings, Universiteit Hasselt
	Prof. dr. Mathias Hoehn, Max Planck Institute

Table of contents

List of abbreviations

Arg-1	Arginase-1
BFP	blue fluorescent protein
BM	bone marrow
BMT	bone marrow transplantation
BW	body weight
CC	corpus callosum
CEM	complete expansion medium
CNS	central nervous system
CPMG	Carr-Purcell-Meiboom-Gill
CPZ	cuprizone
CX3CL1	CX3C chemokine ligand 1 (fractalkine)
CX3CR1	CX3C chemokine receptor 1
DKI	diffusion kurtosis imaging
EAE	experimental autoimmune encephalomyelitis
EC	external capsule
EDTA	ethylenediaminetetraacetic acid
eGFP	enhanced green fluorescent protein
FBS	fetal bovine serum
FCS	fetal calf serum
FITC	fluorescein isothiocyanate
FOV	field of view
GEE	generalized estimating equations
GFAP	glial fibrillary acidic protein
HS	horse serum
Iba1	ionized calcium binding adaptor molecule 1
IFN-γ	interferon-γ
IL	interleukin
IL13	interleukin 13
IL13R	interleukin 13 receptor
IMDM	Iscove's modified Dulbecco's medium
IRES	internal ribosome entry site
LPS	lipopolysaccharide
Iv	intravenous
KO	knock-out
Luc	luciferase
LVv	lentiviral vector
MBP	myelin basic protein
MEF	mouse embryonic fibroblast
MHCII	major histocompatibility complex class II
MRI	magnetic resonance imaging
MCP-1	monocyte chemotactic protein-1
MS	multiple sclerosis
MSC	mesenchymal stem cell

MSME	Multi-slice multi-echo
NA	number of averages
NS	number of slices
NSC	neural stem cell
PBS	phosphate buffered saline
PE	phycoerythrin
PFA	paraformaldehyde
RFP	red fluorescent protein
ROI	region of interest
RT	room temperature
S100β	S100 calcium binding protein β
SCI	spinal cord injury
SD	standard deviation
BBB	blood-brain-barrier
TBS	tris buffered saline
TE	echo times
TGF-β	transforming growth factor-β
TNF-α	tumor necrosis factor-α
TR	repetition time
UA	university of Antwerp
VEGF	vascular endothelial growth factor
Wt	wild type

Summary

Mesenchymal stem cell (MSC) transplantation is widely suggested to become a promising strategy for future cell-based therapeutic intervention following injury or disease of the central nervous system (CNS). However, preceding data by our laboratory has demonstrated the initiation of strong glial cell responses following transplantation of MSC in CNS. Until recently, we were unable to distinguish brain-resident microglial cells from blood-derived infiltrating macrophages. Therefore, in the first part of this thesis, we investigated whether microglia and macrophages can act differently in MSC graft remodeling through the use of a bone marrow transplantation procedure. Following transplantation of MSC in the CNS of enhanced green fluorescent protein $(eGFP)^+$ bone marrow chimeras or $CX_3CR1^{eGFP/+}$ transgenic mice, we demonstrated that MSC implants become infiltrated by peripheral macrophages and surrounded by brain-resident microglia. These findings are of high importance, as they implicate differential roles for microglia and macrophages in MSC graft remodeling responses. A newer approach for the treatment of neuro-inflammatory diseases is the transplantation of genetically-modified MSC in the CNS to deliver immune-modulating proteins. In the second part of this thesis, we investigated whether genetic modification of MSC with the immune modulating cytokine, interleukin (IL)13, can alter CNS inflammation and demyelination in the cuprizone (CPZ) mouse model. Experimentally, MSC or IL13-producing MSC were grafted in the splenium of the corpus callosum at the onset of CPZ-induced pathology. Upon grafting of IL13-MSC, T_2-weighted magnetic resonance imaging and quantitative histology demonstrated significantly reduced inflammation and demyelination in the splenium, compared to control MSC. Moreover, we demonstrated that MSC graft-associated microglia and infiltrating macrophages are forced into alternative activation upon grafting of IL13-MSC, but not of control MSC. Although further investigation is necessary to reveal the mode of action of IL13, our two main hypotheses are (i) the direct action of IL13, inducing death of activated microglia in the demyelinated splenium, and (ii) the indirect action of IL13-induced M2-activated macrophages, creating a protective environment. Surely, a combination of both proposed working mechanisms is also very plausible. Hence, local MSC-mediated delivery of IL13 might become part of a novel strategy to modulate detrimental neuroinflammatory responses in a variety of neuropathologies.

Samenvatting

Transplantatie van mesenchymale stamcellen (MSC) wordt meer en meer aanzien als een mogelijke strategie voor toekomstige celtherapieën bij aandoeningen van het centrale zenuwstelsel (CZS). Nochtans heeft voorgaande data binnen ons laboratorium aangetoond dat er sterke reacties optreden van gliale cellen na transplantatie van MSC in het CZS. Tot voor kort was het nog niet mogelijk om een onderscheid te maken tussen CZS-afgeleide microglia en bloed-afgeleide macrofagen. In het eerste deel van deze thesis hebben we dan ook onderzocht of microglia en macrofagen zich anders gedragen bij modulatie van een MSC transplant. Zo werd aangetoond dat na transplantatie van MSC in het CZS van *enhanced green fluorescent protein* $(eGFP)^+$ beenmerg chimeren of transgene $CX_3CR1^{eGFP/+}$ muizen, MSC transplanten volledig geïnfiltreerd worden door perifere macrofagen en omringd worden door microglia. Deze resultaten zijn van groot belang binnen dit onderzoek, aangezien ze suggereren dat microglia en macrofagen verschillende rollen kunnen spelen bij de modulatie van MSC-transplanten. Een nieuwere strategie voor de behandeling van neuro-inflammatoire ziekten is de transplantatie van genetisch gemodificeerde MSC in het CZS. Op die manier kunnen immuun-modulerende stoffen lokaal worden toegediend. In het tweede deel van deze thesis, werd onderzocht of genetische modificatie van MSC met het immuun-modulerende cytokine, interleukine (IL)13, inflammatie en demyelinisatie van het CZS kan beïnvloeden in het cuprizone (CPZ) muismodel. Hiervoor werden experimenten uitgevoerd waarbij MSC of IL13-producerende MSC getransplanteerd werden in het splenium van het corpus callosum, bij aanvang van de CPZ-geïnduceerde pathologie. Na transplantatie van IL13-MSC, werd via T2-gewogen magnetische resonantie beeldvorming en kwantitatieve histologie bewezen dat inflammatie en demyelinisatie significant verminderd was in vergelijking met controle MSC. Bovendien werd aangetoond dat MSC transplant-geassocieerde microglia en infiltrerende macrofagen tot alternatieve activering werden gedwongen na transplantatie van IL13-MSC, en niet na transplantatie van controle MSC. Hoewel verder onderzoek nodig is om het werkingsmechanisme van IL13 te achterhalen, stellen we twee hypothesen voorop, zijnde (i) de directe werking van IL13 op geactiveerde microglia in het gedemyeliniseerde splenium, wat leidt tot celdood van deze inflammatoire cellen, en (ii) de indirecte werking van IL13-geïnduceerde M2-geactiveerde macrofagen, waardoor vervolgens een neuro-protectieve omgeving ontstaat. Uiteraard is het niet uitgesloten dat het werkingsmechanisme een

combinatie van beide voorgestelde hypothesen kan zijn. Ten slotte kan uit de resultaten van deze thesis worden besloten dat lokale toediening van IL13 via MSC transplantatie nieuwe mogelijkheden biedt voor de modulatie van schadelijke neuro-inflammatie binnen verscheidene hersenaandoeningen.

Chapter I
Introduction

1.1. GENERAL INTRODUCTION

Mainly since the discovery of the unique features of endogenous stem cells[1], which form an *in vivo* source for new cells in case of tissue damage, research towards the development of cellular therapies using *ex vivo* cultured stem cells has exponentially grown over the last decades[2]. Stem cells can be isolated out of the forming blastocyst during embryogenesis. These embryonic stem cells, which can still differentiate into all cell types of the three germ layers, are called pluripotent stem cells. Additionally, stem cell populations can be isolated from various adult tissues, although in this case the obtained cell populations are more limited in their differentiation capacity[1]. As such, multipotent stem cell populations, like hematopoietic stem/progenitor cells and mesenchymal stromal/stem cells, but also already more specified stem cell populations, e.g. cardiac stem cells and liver stem cells, can only terminally differentiate towards cell types within a specific germ layer. While it was already accepted ages ago that regeneration is possible in certain organs, such as the liver or the skin[3, 4], it is rather recent that niches of neural stem cells (NSC) were discovered in the central nervous system (CNS), suggesting that endogenous repair may be possible in case of brain injury[5]. However, in most known CNS injuries and/or diseases the limited source of endogenous NSC and/or their developmental restrictions are not able to overcome severe damage[6, 7]. Therefore, many research studies became devoted to the transplantation of exogenous NSC in animal models of neuropathologies, hypothesizing that they would be able to repair and replace the damaged CNS tissue[8-11]. Despite that partial recovery and/or improvement of (histo)pathology was observed in a variety of animal models, only a limited number of grafted NSC were able to survive and in most cases no differentiation and/or integration was truly validated[9, 12]. Highly similar results were published by our own group, demonstrating by multiple imaging methods that only 1-2% of grafted autologous NSC survives after 2 weeks in the CNS because of hypoxia and apoptotic cell death[13, 14]. Consequently, the cell graft becomes completely infiltrated and surrounded by astrocytes and microglia[13], a feature being neglected in most – if not all – preceding NSC transplantation studies[8-11]. At the same time that NSC grafting studies were finding their place in the field of cellular therapies for CNS diseases, equal interest was devoted to another type of stem cell population, more easily expanded *ex vivo*, namely mesenchymal stem cells (MSC). Although MSC are not naturally found in the CNS, as they reside within the bone marrow, adipose tissue,

dental pulp, etc.[15], their intrinsic properties to secrete a variety of soluble factors involved in tissue protection, repair and immunomodulation[16-18], make them an attractive cell population to be therapeutically applied and studied in several models of disease, injury and organ transplantation[19-22]. Indeed, very similar to NSC grafting studies, many pre-clinical animal studies showed improvement in animal models of various traumata following MSC grafting[21, 22]. Again, several published reports from our group demonstrated that only a small amount (dependent on the study 5-25%) of grafted autologous MSC can survive the transplantation procedure[23, 24, 14]. This limited survival was mainly attributed to cellular hypoxia and apoptotic cell death, again resulting in invasion of the MSC graft by immune cells and encapsulation by astrocytic scar tissue[24, 25]. Nevertheless, the observation that cell grafts are able to survive upon grafting in CNS tissue, although less than one would desire, is the starting point of this doctoral thesis.

1.2. PRINCIPLE AIMES OF THIS STUDY

From a simplified point-of-view, most - if not all - CNS diseases and traumata are associated with a certain degree of neuroinflammation[26-31]. While in stroke, traumatic brain injury and spinal cord injury, acute neuroinflammatory response immediately contribute to the pathology[28-30], in neurodegenerative and autoimmune diseases, like multiple sclerosis, chronic inflammatory responses highly contribute to disease progression[27, 31]. Nevertheless, in both cases brain-resident microglia and blood-borne macrophages, despite both being difficult to distinguish from each other[32, 33], are key players in CNS immune responses. Given numerous reports suggesting that pathologic activation of microglia or macrophages can be altered through secretion of immune-modulating and/or regeneration-inducing factors by grafted MSC in the CNS, in the first part of this thesis we aim to further characterize the immunological events directly related to cell grafting in CNS. In the second part of this thesis, we aim to investigate whether genetic engineering of grafted MSC with the immunomodulating cytokine interleukin 13 (IL13) can modulate at one end MSC graft associated microglia and macrophage responses, and at the other end to a to a broader perspective can enhance the therapeutic potential of MSC grafting in the injured CNS.

1.3. GENERAL EXPERIMENTAL OUTLINE OF THIS DOCTORAL THESIS

In figure 1 we provide a flowchart overview indicating the main experimental path followed within the course of this thesis.

Starting this doctoral thesis, we first aimed to investigate whether previously observed and published[24, 25] cellular responses occurring following MSC grafting would be significantly reduced when performing MSC grafting experiments in CX_3CR1 knock out (KO) mice[34]. As the CX_3CR1-CX_3CL1 signaling pathway is highly important for cellular communication between microglia and neurons during tissue homeostasis and upon injury or disease, and in addition plays a major role in microglia activation and migration[35], we assumed that disruption of the CX_3CR1-CX_3CL1 pathway may lead to reduced MSC graft-induced immune response. However, following completion of MSC grafting experiments in $CX_3CR1^{eGFP/eGFP}$ and $CX_3CR1^{eGFP/+}$ mice, which are respectively homozygous and heterozygous KO for CX_3CR1, no clear effect on the *in vivo* cellular response towards MSC grafts could be observed in the absence of CX_3CR1 signaling or in the presence of reduced CX_3CR1 signaling. Nevertheless, these experiments led to an interesting observation in both homozygous and heterozygous CX_3CR1 KO mice. As such, it was clear that grafted MSC become surrounded, but not infiltrated, by CX_3CR1-expressing microglia, while Iba1-expressing myeloid cells, comprising both microglia and macrophages, were found both within and around the MSC graft site. Based on these results we further investigated two hypotheses: (i) at one end there is a possibility that grafted MSC downregulate CX_3CR1 expression on MSC graft-infiltrating microglia, or (ii) on the other end it are not CX_3CR1-expressing microglia that infiltrate the MSC graft but the MSC graft site becomes infiltrated by peripheral CX_3CR1^{-} macrophages. In order to investigate both hypotheses, we next generated enhanced green fluorescent protein (eGFP) bone marrow (BM) chimeric mice by means of bone marrow transplantation (BMT) experiments[36]. In the CNS of these BM chimeric mice Iba1+ myeloid cells can be further subspecified into eGFP-negative microglia and eGFP-positive BM-derived macrophages. Following grafting of MSC in the CNS of these BM chimeric mice, $eGFP^{+}$ macrophages were predominantly found within the MSC graft site, while in agreement with above-described experiments in $CX_3CR1^{eGFP/eGFP}$ and $CX_3CR1^{eGFP/+}$ mice microglia were predominantly surrounding the MSC graft site. Clearly, MSC grafting in the CNS leads to more complex

immunological events as previously assumed and will require the study of both microglia and macrophages separately in future research strategies.

*These results, as described in detail in **chapter 2** of this doctoral thesis, were summarized in a research manuscript published in 2014 in "Immunology and Cell Biology" as an "Outstanding Observation". Moreover, these data further contribute to the long-lasting aim of the host laboratory to characterize and understand the cellular events following cell grafting in the CNS. A review manuscript (currently submitted for publication) comprising all preceding and novel knowledge, as well as a critical reflection to past and current literature reports, is presented in **chapter 3** of this doctoral thesis.*

In the second part of this doctoral thesis, we aimed to investigate whether genetic modification of MSC with well-established immune modulating factors, could alter the above-described microglia and macrophage immune responses directed against the MSC itself, and to a further extent modulate pathology-associated neuroinflammatory immune responses. A first series of experiments were performed in order to determine our most preferential immunomodulatory factor for genetic engineering of MSC grafts. For this, we generated three primary mouse embryonic fibroblast (MEF) lines expressing one of the following immunomodulating factors: interleukin 4 (IL4)[37], interleukin 10 (IL10)[38] and interleukin 13 (IL13)[37]. Following grafting of these genetically engineered MEF lines in the CNS of healthy mice, only IL4- and IL13-expressing MEF induced a clear anti-inflammatory M2a-polarised activation phenotype in MEF graft-associated inflammatory cells. For specific reasons further explained in section 1.4.5, we decided to continue our studies with IL13 as our preferential immunomodulating cytokine.

*These results are described in detail in **chapter 4** of this doctoral thesis.*

In the third and final part of this doctoral thesis, we investigated whether targeted transplantation of MSC genetically engineered to secrete IL13 in the CNS is able to modulate pathology-associated immune response and able to reduce neuropathology in the cuprizone mouse model of CNS inflammation and demyelination[39, 40]. In this experimental setup, we transplanted control MSC and IL13-producing MSC in in the splenium of the corpus callosum and compared neuro-inflammatory and demyelinating events with non-grafted mice after 4 weeks receiving a cuprizone (CPZ)-supplemented diet, as well as to a healthy coltrol group of

mice. In our experimental approach, all mice were analyzed by T2-weigthed magnetic resonance imaging (MRI)[41, 42] and profound post-mortem immunofluorescence analysis[43, 44]. This multimodal imaging approach allowed us to clearly demonstrate using two independent analysis tools the beneficial effect of grafting IL13-producing MSC on neuroinflammatory en demyelinating events. Moreover, one of the repeat experiments was performed in the $CX_3CR1^{eGFP/+}CCR2^{RFP/+}$ transgenic mouse model[45] in order to distinguish microglia and macrophage populations without the need of performing a BMT procedure. Consequently, we here propose a novel hypothesis, as further explained in this doctoral thesis, in which the neuroprotective role of M2a-polarised macrophages is brought forward as a novel research strategy to counteract pathological microglia responses in the CNS.

*These results, as described in detail in **chapter 5** of this doctoral thesis, were summarized in a research manuscript currently submitted for publication. While the presented results clearly create new pathways for the development of novel advanced cellular therapies for both the first line treatment of acute neuroinflammatory insults, like traumatic brain and spinal cord injury or stroke for which currently no therapeutic options exist[46, 47], and the secondary treatment of chronic neuroinflammatory insults, like multiple sclerosis for which current treatment options are still far from optimal[48], it is clear that further research will be needed to further enhance our understanding of IL13-mediated modulation of neuroinflammatory responses. A final summarization of the data presented in this doctoral thesis, as well as our future research perspectives, are provided in* ***chapter 5*** of this doctoral thesis.

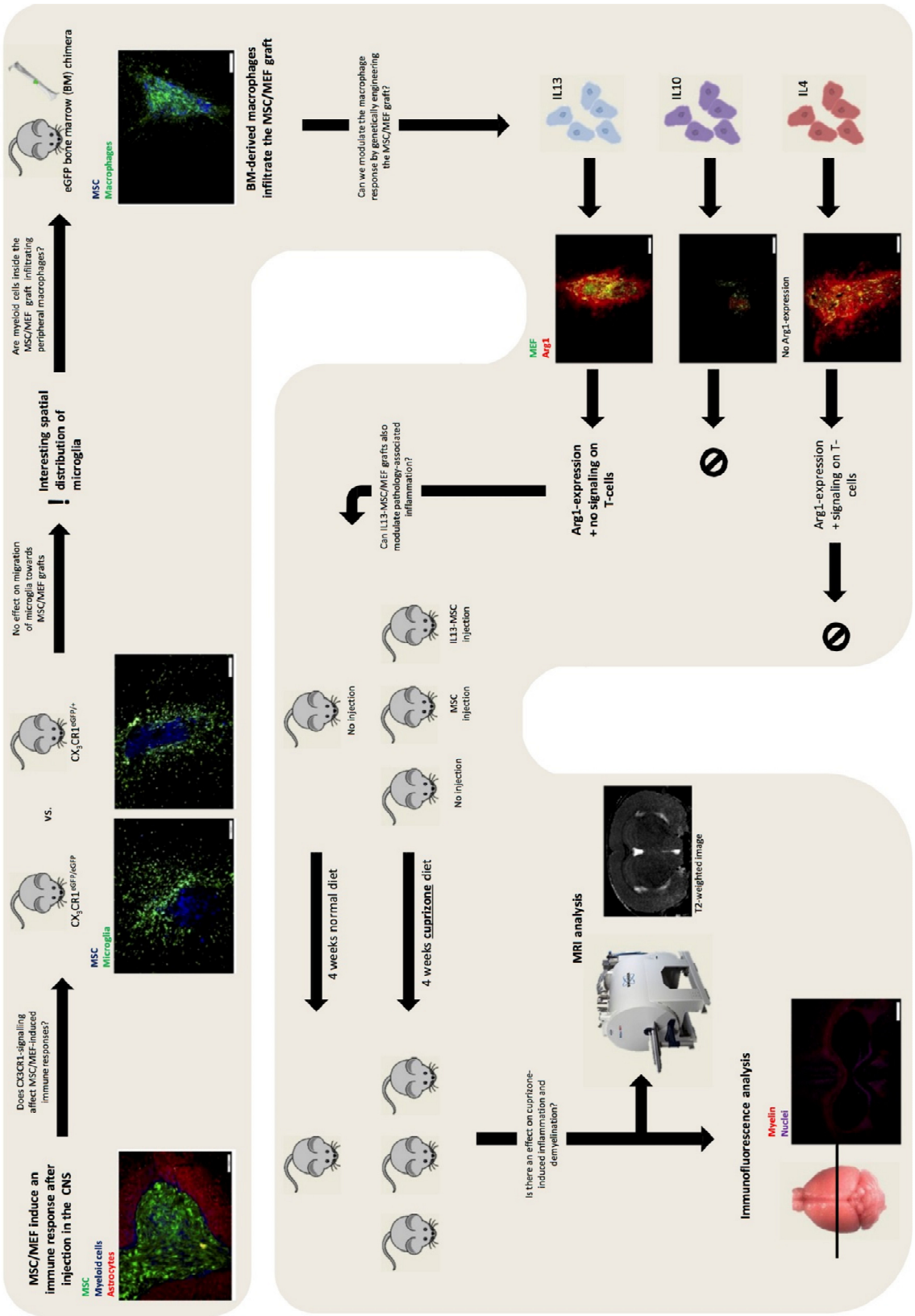

Figure 1. Outline of the study

An overview of the study, showing the investigated hypotheses and the experimental workflow.

1.4. EXPERIMENTAL CHOICES IN COURSE OF THIS DOCTORAL THESIS

1.4.1. Why use MSC and not NSC for cell grafting in the CNS?

Although previous studies within the laboratory focused on elucidating the cellular events following both MSC and NSC grafting in the CNS, within this doctoral thesis our choice to use MSC, but not NSC, was made based on the following reasoning: (i) Looking forward to potential clinical applications, autologous MSC can easily be isolated from bone marrow or – more recently – from other tissues, such as adipose tissue, dental pulp, placenta and Wharton's jelly[2]. As opposed to isolation of adult NSC, MSC thus have a clear practical and ethical advantage[49, 50]. (ii) Recent literature reports strongly elaborate on the intrinsic potential of MSC to modulate immune cells and secrete tissue-protective and repair-inducing factors, at least *in vitro*[17, 51, 52]. Given these properties, MSC might have an advantage over NSC to develop into an effective therapy for a variety of CNS injuries and/or diseases. Moreover, our previous studies demonstrated that grafted MSC display a higher survival capacity, related to new blood vessel formation *in vivo*[25, 53], as compared to grafted NSC in the CNS[14].

1.4.2. Why perform intracerebral injection of MSC and not intravenous administration?

Reviewing current literature regarding MSC transplantation, it is clearly noticeable that most pre-clinical and clinical studies apply MSC therapy by means of intravenous administration. This method of administration is based on the (mistaken) assumption that MSC are able to home to the lesion site in the CNS[54]. However, previous research within our laboratory[55], and confirmed by other research groups[56-58], demonstrated that after intravenous administration MSC become rapidly captured in the lung and the spleen. Therefore, we believe that maximizing the therapeutic potential of MSC transplantation will require an administration approach allowing MSC biodistribution to be directly targeted to the lesion site via intracerebral injection. Although this approach is more invasive than intravenous administration, we should keep in mind that in case of severe brain damage, eg. spinal cord injury, stroke, progressive multiple sclerosis, the impact of direct intracerebral injection will most likely not outweigh the impact of injury or disease.

1.4.3. Why use CX_3CR1-eGFP mice for investigating MSC graft-induced immune responses?

$CX_3CR1^{eGFP/eGFP}$ transgenic mice have both CX_3CR1 alleles replaced by the eGFP reporter gene, leading to dysfunctional CX_3CR1 signaling in $eGFP^+$ microglial cells[34]. CX_3CR1 is a receptor found exclusively on microglia in the CNS, where it can bind its ligand CX_3CL1, a chemokine also known as fractalkine. Fractalkine is mainly expressed by neurons in the CNS, therefore it acts as an important ligand for signaling neuronal damage[35]. Whenever damage occurs in the CNS, microglia will be attracted to the lesion site by CX_3CR1 signaling. Since fractalkine signaling appeared to be an important trigger for microglia migration, we wanted to investigate whether this pathway is also involved in the initiation of microglia migration towards an MSC graft in the CNS. A recent publication by Giunti et al.[59] further suggested that MSC were able to secrete fractalkine and modulate microglia responses through this signaling pathway. However, in our hands we could not detect fractalkine secretion by our MSC cultures. Moreover, no effects on microglia migration or activation were observed in the absence of the CX_3CR1 signal after transplantation of MSC in the CNS. Nevertheless, as no clear differences were found in this and other studies[23, 34, 60] with regard to microglial functioning in heterozygous $CX_3CR1^{eGFP/+}$ mice, this transgenic mouse model is highly suitable for microglial cell tracking and phenotyping studies, as further used in course of this doctoral thesis.

1.4.4. Why use $eGFP^+$ BM chimeric mice and $CX_3CR1^{eGFP/+}CCR2^{RFP/+}$ transgenic mice to distinguish microglia and macrophages in the CNS ?

In course of our experiments, we came across the hypothesis that BM-derived macrophages may play an important role during the recognition of MSC grafts in the CNS. As the CX3CR1-eGFP model described above allows for identification of microglia[34], in first instance we chose to create $eGFP^+$ BM chimeric mice[23]. The main advantage of this technique is that microglia in the CNS are relatively resistant to the irradiation procedure[36], allowing after BMT to distinguish them from infiltrating eGFP+ peripheral macrophages. Although electron microscopy[61] and flow cytometry[62] techniques have been described to distinguish microglia from macrophages, these techniques are not applicable on a large-scale level or in

situ, respectively. Table 1 provided an overview of the specific characteristics of these methodologies and their specific advantages and disadvantages.

Method	Discrimination		Advantages	Disadvantages
	Microglia	Macrophage		
Electron microscopy	Spine-bearing surface	No spines on surface	Does not change when activated	Invasive Time-consuming Not suitable for in situ research
Flow cytometry	$CD11b^{hi}$ $CD45^{lo/int}$	$CD11b^{hi}$ $CD45^{hi}$	Easy and fast Does not change when activated	Not suitable for in situ research
$eGFP^{+}$ bone marrow transplantation	$eGFP^{-}$	$eGFP^{+}$	In situ research is possible Does not change when activated	Irradiation can cause disturbance of BBB, damage of endothelial cells, induction of pro-inflammatory cytokines Time-consuming
$CX_3CR1^{eGFP/+}$ $CCR2^{RFP/+}$ transgenic mouse	$eGFP^{+}$ RFP^{-}	$eGFP^{-/lo}$ RFP^{+}	In situ research is possible No irradiation Does not change when activated	Lower expression of transgenes

Table 1. Advantages and disadvantages of the different methods of discrimination between microglia and macrophages

In the second part of this study we changed toward the use of CX3CR1-eGFP x CCR2-RFP transgenic mice[45] to discriminate between microglia and macrophages in the CNS upon cell grafting and upon therapeutic intervention. $CX_3CR1^{eGFP/+}$ $CCR2^{RFP/+}$ transgenic mice were generated by cross-breeding $CX_3CR1^{eGFP/eGFP}$ mice[34] and $CCR2^{RFP/RFP}$ mice[63]. The crossed transgenic mice have one allele of the CX_3CR1 gene replaced by eGFP and one allele of the CCR2 gene replaced by RFP. CX_3CR1, as explained above, is a chemokine receptor exclusively expressed on brain-resident microglia in the CNS[35]. CCR2 is a chemokine receptor for the chemotactic ligand CCL2, also known as monocyte chemotactic protein-1 (MCP-1)[63]. As the name already implies, its receptor is expressed on blood-borne monocytes and macrophages. To visualize microglia and infiltrating macrophages separately in situ, this transgenic mouse model is preferred over the eGFP BM chimeric mouse model, since no irradiation of the mouse is needed (Table 1). The latter became of high importance especially when performing cuprizone experiments, as this model of neuroinflammation and demyelination is best performed with mice at the age of 8-10 weeks[40], which is due to the recovery period more complex, although not impossible, in the setup of BMT experiments.

1.4.5. Why use IL-13 for immunomodulation in the CNS?

The main goal within this doctoral thesis was to alter pathology-induced neuroinflammation by transplantation of MSC genetically engineered to secrete an immune modulating factor. Since the key players in neuroinflammation are microglia and peripheral macrophages, we aimed to modulate the activation of these immune cells. It is known that brain-resident microglia and blood-borne macrophages are difficult to distinguish, since these two cell types are very much alike and display similar activation phenotypes. *In vitro* studies have demonstrated pro-inflammatory activation phenotypes, called M1 activation, and anti-inflammatory activation phenotypes, called M2 activation, of microglia and macrophages (Figure 2)[37, 64]. In most cases, M1 activation is seen as the bad and M2 activation as the good phenotype, however, this mainly depends on the type of pathogen and the time point within the course of inflammation. For instance during viral and bacterial infections, an M1 activation is preferred, while in an allergic reaction and parasitic infection, an M2 activation is required. In the case of brain damage, in the most ideal situation M1-activated macrophages/microglia would clear up all necrotic tissue followed by M2-activated macrophages/microglia limiting the destructive and cytotoxic inflammatory response, while promoting repair and regeneration. However, many CNS diseases and severe brain injuries become chronic pro-inflammatory due to an inadequate switch from M1 towards M2 activation[65, 66]. Therefore, we hypothesized that grafting of MSC genetically engineered to secrete an M2-inducing factor might have a beneficial effect on chronic CNS inflammation and pathology. At the start of this doctoral thesis, we chose to investigate three known M2-inducing cytokines: IL4, IL10 and IL13. *In vitro* results demonstrated that when IL4-, IL10- and IL13-expressing MSC were co-cultured with BV2-cells, after LPS activation, all transgenic cell lines were able to suppress TNFα secretion to a higher extent than control MSC. *In vivo* results showed that IL4- and IL13-expressing grafts induced high expression of Arginase 1 (Arg1), an M2a marker[37], while this was not observed upon grafting of IL10-expressing MSC most likely corresponding to the induction of an M2c phenotype[64]. Moreover, it is stated in literature that IL10 induces deactivation of macrophages and microglia, while our hypothesis is based on the diversion of a type I immune response towards a type II immune response. The reason we chose to continue the study with IL13 can be explained by the lack of an IL13-receptor on

T-cells[67]. Since the IL4-receptor is found on T-cells, we believe that in certain CNS pathologies, e.g. MS, an additional T-cell stimulus is not preferred.

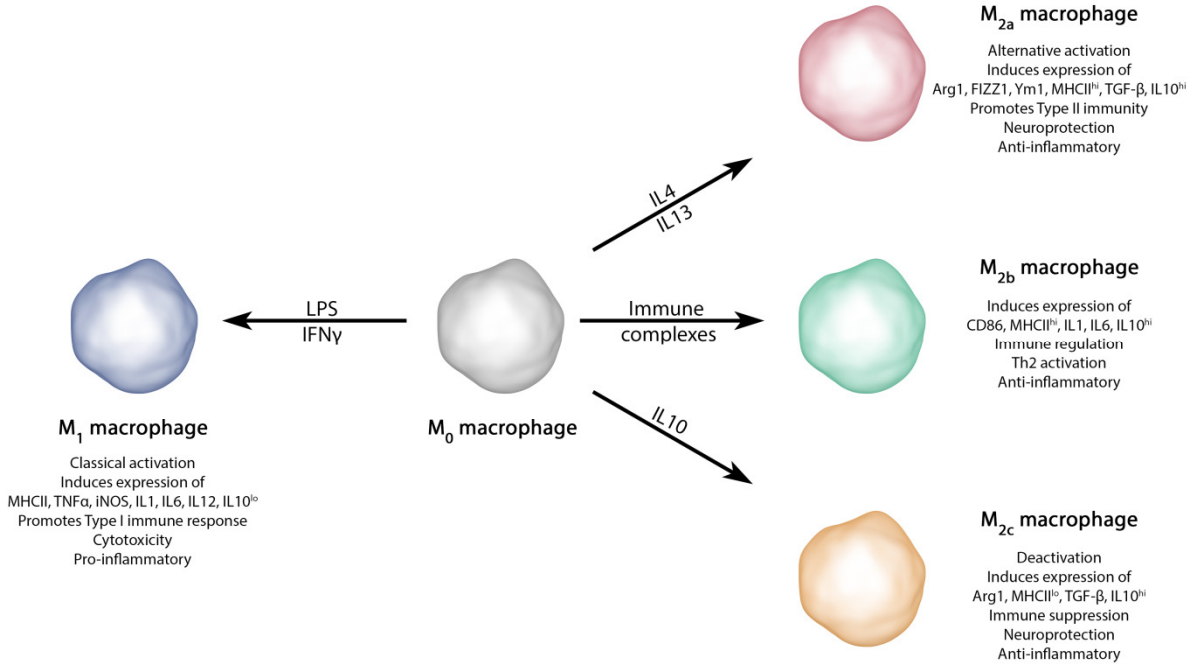

Figure 2. M1 and M2 activation phenotypes of macrophages
An overview of different activation stimuli and the activation phenotypes they induce, the various expression patterns that are induced and the effect on inflammation and tissue damage in macrophages.

1.4.6. Why use the cuprizone mouse model for investigating immunomodulation by IL13?

CPZ is a copper chelator able to induce severe oxidative stress in metabolically highly active oligodendrocytes in the CNS. At the same time microglia and astrocytes become highly active, leading to severe oligodendrocyte death and demyelination[40]. Experimentally, it is well-established that the toxic effects of CPZ are most prominent in brain regions with high myelin content, e.g. the corpus callosum, the external capsule, etc. The CPZ mouse model is specifically used for the investigation of de- and remyelination processes and its associated chronic neuroinflammation[39, 40]. The CPZ model is easily and reproducibly established by adding 0.2% w/w CPZ to the normal rodent diet. Previous studies have shown that the copper chelator reaches its maximum toxic effect after 4 weeks of administration as inflammation and demyelination reach their highest level[40]. At this point a large part of the

oligodendrocytes have died and microglia completely invaded the necrotic and demyelinated regions. Since it is known that these chronically activated microglia add to the neurotoxicity in the CPZ mouse model, it would be interesting to investigate whether modulation of microglia activation, by means of IL13, could have a beneficial effect on the chronic inflammation and demyelination in the CPZ mouse model. Currently, the CPZ model is the second most widely used demyelination model following the EAE mouse model for human MS[39, 40].Although the EAE model might mimic MS pathology more correctly in terms of T-cell activation[68], although this also can be debated[69], in this study we wanted to examine the immune modulating effect of genetically engineered MSC on neuro-inflammation without contribution of an auto-immune T-cell response, which also resembles certain types of MS lesions[40]. Another advantage of the CPZ model over the EAE model is the easy read-out of results through magnetic resonance imaging (MRI). Since demyelination and inflammation are always localized at the same brain regions[70], a feature not being observed in the EAE model where lesions are randomly spread throughout the CNS[55]. Moreover, as an important read-out for the CPZ model is based on MRI analyses[41, 42], as performed in this doctoral thesis, it allows for a more objective evaluation as compared to the EAE model where the functional read-out is usually done by scoring of symptoms, which is a more subjective and variable method[55].

1.4.7. Why use MRI analysis to evaluate neuroinflammation and demyelination?

MRI is a technique widely used for both clinical and research purposes to evaluate structural and functional alteration in the brain. MRI can generate high-resolution images of the CNS as it is based on the magnetic properties of protons that are subjected to a strong oscillating magnetic field. In most cases of MRI, these protons are hydrogen atoms, since these are the most abundant in the CNS and allow for visualization of different brain structures. With regard to the CPZ mouse model, MRI is highly suitable to evaluate a combination of inflammation and demyelination[41, 42]. When analyzing the brain of CPZ-treated mice, T_2-weighted MRI is mostly used as it easily assessed regions with high water content, corresponding to a hyper-intense signal (i.e. bright signal e.g. in the ventricles). Since sites of inflammation and demyelination undergo major changes, including edema formation, lesion sites in corpus callosum of CPZ-treated mice can easily recognized from healthy brain tissue by the

appearance of a hyper-intense signal (Figure 3). Therefore, this technique is a valuable tool for analyzing possible therapeutic effects on inflammation and demyelination and in the CPZ mouse model[41, 42].

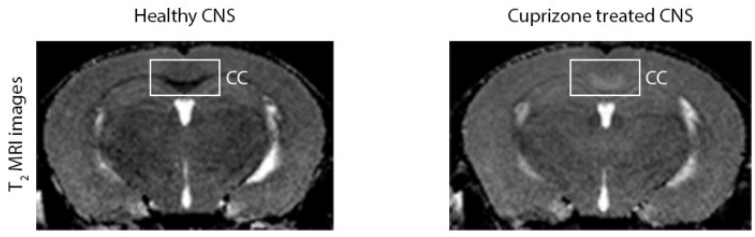

Figure 3. T2-weighted MRI analysis of brains of healthy and cuprizone-treated mice.
T2-weighted images showing the change at the corpus callosum (CC) after a 4-week cuprizone diet. A dark signal corresponds to high fat content (myelin), while a bright signal corresponds to a high water content (edema and inflammatory cells).

1.4.8. Why use quantitative histological analysis?

Post-mortem immunofluorescent staining of tissue sections is undoubtedly the highest sensitive technique to evaluate cellular grafts and their interaction with surrounding tissue in more detail[43, 44]. Using this method specific cell types and/or tissue architecture can be visualized by staining with fluorescently labelled antibodies or – as also used throughout this doctoral thesis – directly by one or more endogenously expressed fluorescent proteins. For instance with regard to transplanted MSC, cellular grafts can be genetically engineerd to express fluorescent proteins such as eGFP, blue fluorescent protein (BFP), etc. (Figure 4). Following histological tissue processing, grafted MSC can be easily located by immunofluorescence microscopy in brain tissue. Other endogenous fluorescent signals can be obtained by using transgenic mouse models, created to express certain fluorescent proteins in specific cell types. For instance, the transgenic $CX_3CR1^{eGFP/+}$ $CCR2^{RFP/+}$ mice were in this doctoral thesis used to to discriminate between brain-resident microglia ($eGFP^+$) and infiltrating monocytes/macrophages (red fluorescent protein; RFP^+) in brain tissue (Figure 4A). The main advantage of direct fluorescence imaging, eventually in combination with immunofluorescent labeling, is that several cell types or tissue components can be visualized in situ on the same image (Figure 4). Furthermore, in this doctoral thesis we have put a large effort in quantification of (immune)fluorescent images, more specifically using ImageJ and

TissueQuest software[23, 43, 44]. Consequently this approach allows for more accurate estimation of cellular events following cell grafting and its influence on inflammation and demyelination in the CNS, which undoubtedly increases the validity of the obtained results as compared to the for decades accepted research approach to provide only visually selected representative images.

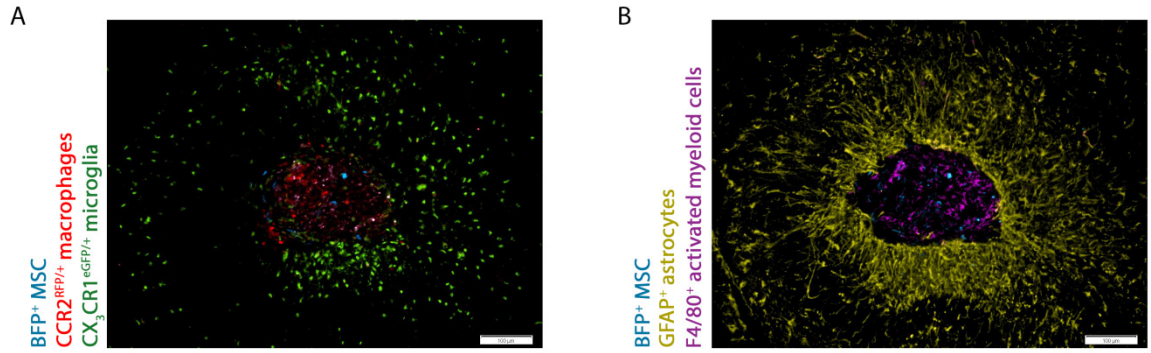

Figure 4. Immunofluorescent images of an MSC graft in healthy CNS tissue.
(A) Endogenous BFP expression by genetically engineered MSC (blue), endogenous eGFP expression by CX3CR1eGFP/+ microglia (green), and endogenous RFP expression by CCR2RFP/+ infiltrated macrophages.
(B) Endogenous BFP expression by genetically engineered MSC (blue), stained for GFAP expression on astrocytes (yellow, pseudocolor), and stained for F4/80 expression on activated myeloid cells (purple, pseudocolor).

Image processing

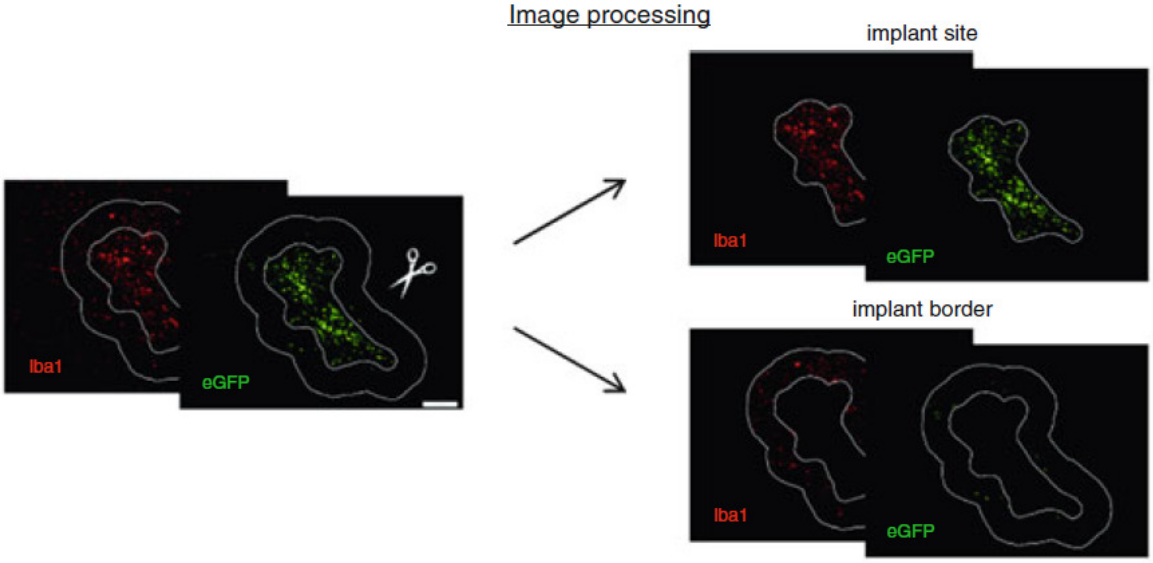

TissueQuest analysis of implant site

1. Defining the master channel (TOPRO3 staining)

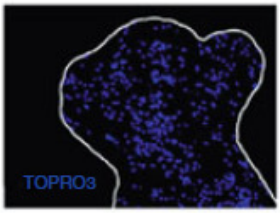

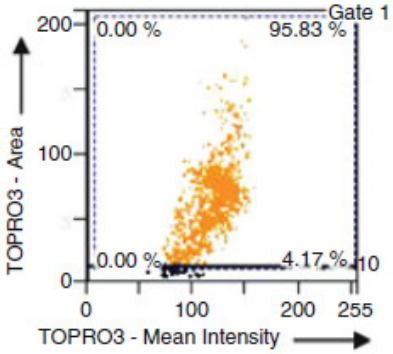

2. Defining positivity for a first marker (eGFP staining)

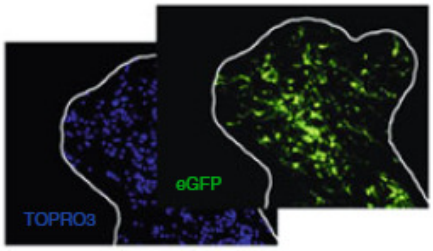

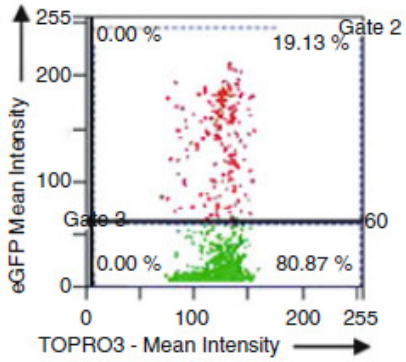

3. Defining positivity for a second marker (Iba1 staining)

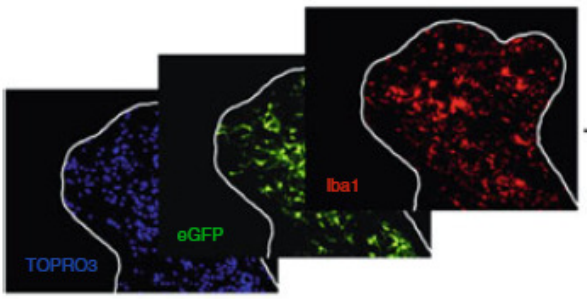

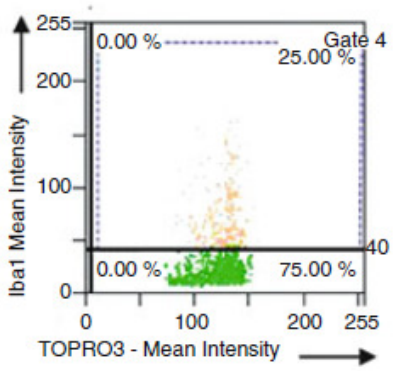

Figure 5. Advanced multi-color immunofluorescence analysis and cellular quantification of cell grafts on brain tissue sections.
Work flow representation of a quantitative analysis of immunofluorescently labeled CNS tissue sections. First, image processing is done, by which the graft site and the graft border are selected. Next the graft site or the graft border is analyzed using TissueQuest analysis software. For this, nuclear staining is needed to define the number of cells present at the graft site or graft border. Next, a first marker can be analyzed, e.g. determining the number of $eGFP^+$ cells. Then, a second marker can be analyzed and co-localization with the first marker can be defined, e.g. the number of $eGFP^+Iba1^+$ cells. The analysis is displayed as a dot plot, showing the percentage of positive cells and negative cells present at the graft site or graft border.

1.5. GENERAL CONCLUSIONS

In this thesis we will address using the currently important research aim whether the conversion of M1 to M2 can lead to a beneficial outcome, by means of transplantation of MSC genetically engineered to secrete IL13, for this we applied a highly multidisciplinary approach, including:

- genetic engineering of MSC using lentiviral vector;
- cell grafting in the central nervous system of mice;
- magnetic resonance imaging to monitor inflammatory CNS lesions and therapeutic effect;
- bone marrow transplantation and transgenic mouse models to distinguish microglia and macrophages;
- advanced multi-color immunofluorescence analysis and cellular quantification of neuroinflammation and cell grafts on brain tissue sections.

1.6. REFERENCES

1. Mitalipov S, Wolf D. Totipotency, pluripotency and nuclear reprogramming. Advances in biochemical engineering/biotechnology. 2009;114:185-99. doi:10.1007/10_2008_45.
2. Stoltz JF, de Isla N, Li YP, Bensoussan D, Zhang L, Huselstein C et al. Stem Cells and Regenerative Medicine: Myth or Reality of the 21th Century. Stem cells international. 2015;2015:734731. doi:10.1155/2015/734731.
3. Yu BD, Mukhopadhyay A, Wong C. Skin and hair: models for exploring organ regeneration. Human molecular genetics. 2008;17(R1):R54-9. doi:10.1093/hmg/ddn086.
4. Pachter HL. Prometheus bound: evolution in the management of hepatic trauma--from myth to reality. The journal of trauma and acute care surgery. 2012;72(2):321-9. doi:10.1097/TA.0b013e31824b15a7.
5. Temple S. Division and differentiation of isolated CNS blast cells in microculture. Nature. 1989;340(6233):471-3. doi:10.1038/340471a0.
6. Kohman RA, Rhodes JS. Neurogenesis, inflammation and behavior. Brain, behavior, and immunity. 2013;27(1):22-32. doi:10.1016/j.bbi.2012.09.003.
7. Tepavcevic V, Lazarini F, Alfaro-Cervello C, Kerninon C, Yoshikawa K, Garcia-Verdugo JM et al. Inflammation-induced subventricular zone dysfunction leads to olfactory deficits in a targeted mouse model of multiple sclerosis. The Journal of clinical investigation. 2011;121(12):4722-34. doi:10.1172/JCI59145.
8. Goldberg NR, Caesar J, Park A, Sedgh S, Finogenov G, Masliah E et al. Neural Stem Cells Rescue Cognitive and Motor Dysfunction in a Transgenic Model of Dementia with Lewy Bodies through a BDNF-Dependent Mechanism. Stem cell reports. 2015. doi:10.1016/j.stemcr.2015.09.008.
9. Ma H, Yu B, Kong L, Zhang Y, Shi Y. Transplantation of neural stem cells enhances expression of synaptic protein and promotes functional recovery in a rat model of traumatic brain injury. Molecular medicine reports. 2011;4(5):849-56. doi:10.3892/mmr.2011.510.
10. Ma J, Gao J, Hou B, Liu J, Chen S, Yan G et al. Neural stem cell transplantation promotes behavioral recovery in a photothrombosis stroke model. International journal of clinical and experimental pathology. 2015;8(7):7838-48.
11. Marei HE, Lashen S, Farag A, Althani A, Afifi N, A AE et al. Human olfactory bulb neural stem cells mitigate movement disorders in a rat model of Parkinson's disease. Journal of cellular physiology. 2015;230(7):1614-29. doi:10.1002/jcp.24909.
12. Martino G, Pluchino S. The therapeutic potential of neural stem cells. Nature reviews Neuroscience. 2006;7(5):395-406. doi:10.1038/nrn1908.
13. Reekmans K, De Vocht N, Praet J, Fransen E, Le Blon D, Hoornaert C et al. Spatiotemporal evolution of early innate immune responses triggered by neural stem cell grafting. Stem cell research & therapy. 2012;3(6):56. doi:10.1186/scrt147.
14. Praet J, Reekmans K, Lin D, De Vocht N, Bergwerf I, Tambuyzer B et al. Cell type-associated differences in migration, survival, and immunogenicity following grafting in CNS tissue. Cell transplantation. 2012;21(9):1867-81. doi:10.3727/096368912X636920.
15. Murray IR, West CC, Hardy WR, James AW, Park TS, Nguyen A et al. Natural history of mesenchymal stem cells, from vessel walls to culture vessels. Cellular and molecular life sciences : CMLS. 2014;71(8):1353-74. doi:10.1007/s00018-013-1462-6.
16. Duffy MM, Ritter T, Ceredig R, Griffin MD. Mesenchymal stem cell effects on T-cell effector pathways. Stem cell research & therapy. 2011;2(4):34. doi:10.1186/scrt75.
17. Nauta AJ, Fibbe WE. Immunomodulatory properties of mesenchymal stromal cells. Blood. 2007;110(10):3499-506. doi:10.1182/blood-2007-02-069716.
18. Kovach TK, Dighe AS, Lobo PI, Cui Q. Interactions between MSCs and immune cells: implications for bone healing. Journal of immunology research. 2015;2015:752510. doi:10.1155/2015/752510.

19. Maitra B, Szekely E, Gjini K, Laughlin MJ, Dennis J, Haynesworth SE et al. Human mesenchymal stem cells support unrelated donor hematopoietic stem cells and suppress T-cell activation. Bone marrow transplantation. 2004;33(6):597-604. doi:10.1038/sj.bmt.1704400.
20. Guo K, Ikehara S, Meng X. Mesenchymal stem cells for inducing tolerance in organ transplantation. Frontiers in cell and developmental biology. 2014;2:8. doi:10.3389/fcell.2014.00008.
21. Dulamea AO. The potential use of mesenchymal stem cells in stroke therapy--From bench to bedside. Journal of the neurological sciences. 2015;352(1-2):1-11. doi:10.1016/j.jns.2015.03.014.
22. Rivera FJ, Aigner L. Adult mesenchymal stem cell therapy for myelin repair in multiple sclerosis. Biological research. 2012;45(3):257-68. doi:10.4067/S0716-97602012000300007.
23. Le Blon D, Hoornaert C, Daans J, Santermans E, Hens N, Goossens H et al. Distinct spatial distribution of microglia and macrophages following mesenchymal stem cell implantation in mouse brain. Immunology and cell biology. 2014;92(8):650-8. doi:10.1038/icb.2014.49.
24. De Vocht N, Lin D, Praet J, Hoornaert C, Reekmans K, Le Blon D et al. Quantitative and phenotypic analysis of mesenchymal stromal cell graft survival and recognition by microglia and astrocytes in mouse brain. Immunobiology. 2013;218(5):696-705. doi:10.1016/j.imbio.2012.08.266.
25. Praet J, Santermans E, Daans J, Le Blon D, Hoornaert C, Goossens H et al. Early inflammatory responses following cell grafting in the CNS trigger activation of the sub-ventricular zone: a proposed model of sequential cellular events. Cell transplantation. 2014. doi:10.3727/096368914X682800.
26. Reus GZ, Fries GR, Stertz L, Badawy M, Passos IC, Barichello T et al. The role of inflammation and microglial activation in the pathophysiology of psychiatric disorders. Neuroscience. 2015;300:141-54. doi:10.1016/j.neuroscience.2015.05.018.
27. Ward RJ, Dexter DT, Crichton RR. Ageing, neuroinflammation and neurodegeneration. Frontiers in bioscience. 2015;7:189-204.
28. Lozano D, Gonzales-Portillo GS, Acosta S, de la Pena I, Tajiri N, Kaneko Y et al. Neuroinflammatory responses to traumatic brain injury: etiology, clinical consequences, and therapeutic opportunities. Neuropsychiatric disease and treatment. 2015;11:97-106. doi:10.2147/NDT.S65815.
29. Kriz J, Lalancette-Hebert M. Inflammation, plasticity and real-time imaging after cerebral ischemia. Acta neuropathologica. 2009;117(5):497-509. doi:10.1007/s00401-009-0496-1.
30. Zhou X, He X, Ren Y. Function of microglia and macrophages in secondary damage after spinal cord injury. Neural regeneration research. 2014;9(20):1787-95. doi:10.4103/1673-5374.143423.
31. Benveniste EN. Role of macrophages/microglia in multiple sclerosis and experimental allergic encephalomyelitis. Journal of molecular medicine. 1997;75(3):165-73.
32. Durafourt BA, Moore CS, Zammit DA, Johnson TA, Zaguia F, Guiot MC et al. Comparison of polarization properties of human adult microglia and blood-derived macrophages. Glia. 2012;60(5):717-27. doi:10.1002/glia.22298.
33. Hickman SE, Kingery ND, Ohsumi TK, Borowsky ML, Wang LC, Means TK et al. The microglial sensome revealed by direct RNA sequencing. Nature neuroscience. 2013;16(12):1896-905. doi:10.1038/nn.3554.
34. Jung S, Aliberti J, Graemmel P, Sunshine MJ, Kreutzberg GW, Sher A et al. Analysis of fractalkine receptor CX(3)CR1 function by targeted deletion and green fluorescent protein reporter gene insertion. Molecular and cellular biology. 2000;20(11):4106-14.
35. Maciejewski-Lenoir D, Chen S, Feng L, Maki R, Bacon KB. Characterization of fractalkine in rat brain cells: migratory and activation signals for CX3CR-1-expressing microglia. Journal of immunology. 1999;163(3):1628-35.
36. Larochelle A, Bellavance MA, Michaud JP, Rivest S. Bone marrow-derived macrophages and the CNS: An update on the use of experimental chimeric mouse models and bone marrow transplantation in neurological disorders. Biochimica et biophysica acta. 2015. doi:10.1016/j.bbadis.2015.09.017.
37. Van Dyken SJ, Locksley RM. Interleukin-4- and interleukin-13-mediated alternatively activated macrophages: roles in homeostasis and disease. Annual review of immunology. 2013;31:317-43. doi:10.1146/annurev-immunol-032712-095906.

38. Moore KW, de Waal Malefyt R, Coffman RL, O'Garra A. Interleukin-10 and the interleukin-10 receptor. Annual review of immunology. 2001;19:683-765. doi:10.1146/annurev.immunol.19.1.683.
39. Torkildsen O, Brunborg LA, Myhr KM, Bo L. The cuprizone model for demyelination. Acta neurologica Scandinavica Supplementum. 2008;188:72-6. doi:10.1111/j.1600-0404.2008.01036.x.
40. Praet J, Guglielmetti C, Berneman Z, Van der Linden A, Ponsaerts P. Cellular and molecular neuropathology of the cuprizone mouse model: clinical relevance for multiple sclerosis. Neuroscience and biobehavioral reviews. 2014;47:485-505. doi:10.1016/j.neubiorev.2014.10.004.
41. Guglielmetti C, Praet J, Rangarajan JR, Vreys R, De Vocht N, Maes F et al. Multimodal imaging of subventricular zone neural stem/progenitor cells in the cuprizone mouse model reveals increased neurogenic potential for the olfactory bulb pathway, but no contribution to remyelination of the corpus callosum. NeuroImage. 2014;86:99-110. doi:10.1016/j.neuroimage.2013.07.080.
42. Wu QZ, Yang Q, Cate HS, Kemper D, Binder M, Wang HX et al. MRI identification of the rostral-caudal pattern of pathology within the corpus callosum in the cuprizone mouse model. Journal of magnetic resonance imaging : JMRI. 2008;27(3):446-53. doi:10.1002/jmri.21111.
43. Praet J, Santermans E, Reekmans K, de Vocht N, Le Blon D, Hoornaert C et al. Histological characterization and quantification of cellular events following neural and fibroblast(-like) stem cell grafting in healthy and demyelinated CNS tissue. Methods in molecular biology. 2014;1213:265-83. doi:10.1007/978-1-4939-1453-1_22.
44. Reekmans K, De Vocht N, Praet J, Le Blon D, Hoornaert C, Daans J et al. Quantitative evaluation of stem cell grafting in the central nervous system of mice by in vivo bioluminescence imaging and postmortem multicolor histological analysis. Methods in molecular biology. 2013;1052:125-41. doi:10.1007/7651_2013_17.
45. Mizutani M, Pino PA, Saederup N, Charo IF, Ransohoff RM, Cardona AE. The fractalkine receptor but not CCR2 is present on microglia from embryonic development throughout adulthood. Journal of immunology. 2012;188(1):29-36. doi:10.4049/jimmunol.1100421.
46. Kwon BK, Tetzlaff W, Grauer JN, Beiner J, Vaccaro AR. Pathophysiology and pharmacologic treatment of acute spinal cord injury. The spine journal : official journal of the North American Spine Society. 2004;4(4):451-64. doi:10.1016/j.spinee.2003.07.007.
47. Mikulik R, Wahlgren N. Treatment of acute stroke: an update. Journal of internal medicine. 2015;278(2):145-65. doi:10.1111/joim.12387.
48. Farjam M, Zhang GX, Ciric B, Rostami A. Emerging immunopharmacological targets in multiple sclerosis. Journal of the neurological sciences. 2015. doi:10.1016/j.jns.2015.09.346.
49. Peister A, Mellad JA, Larson BL, Hall BM, Gibson LF, Prockop DJ. Adult stem cells from bone marrow (MSCs) isolated from different strains of inbred mice vary in surface epitopes, rates of proliferation, and differentiation potential. Blood. 2004;103(5):1662-8. doi:10.1182/blood-2003-09-3070.
50. Conti L, Pollard SM, Gorba T, Reitano E, Toselli M, Biella G et al. Niche-independent symmetrical self-renewal of a mammalian tissue stem cell. PLoS biology. 2005;3(9):e283. doi:10.1371/journal.pbio.0030283.
51. Kinnaird T, Stabile E, Burnett MS, Shou M, Lee CW, Barr S et al. Local delivery of marrow-derived stromal cells augments collateral perfusion through paracrine mechanisms. Circulation. 2004;109(12):1543-9. doi:10.1161/01.CIR.0000124062.31102.57.
52. Crigler L, Robey RC, Asawachaicharn A, Gaupp D, Phinney DG. Human mesenchymal stem cell subpopulations express a variety of neuro-regulatory molecules and promote neuronal cell survival and neuritogenesis. Experimental neurology. 2006;198(1):54-64. doi:10.1016/j.expneurol.2005.10.029.
53. Costa R, Bergwerf I, Santermans E, De Vocht N, Praet J, Daans J et al. Distinct in vitro properties of embryonic and extraembryonic fibroblast-like cells are reflected in their in vivo behavior following grafting in the adult mouse brain. Cell transplantation. 2015;24(2):223-33. doi:10.3727/096368913X676196.
54. Eggenhofer E, Luk F, Dahlke MH, Hoogduijn MJ. The life and fate of mesenchymal stem cells. Frontiers in immunology. 2014;5:148. doi:10.3389/fimmu.2014.00148.

55. Reekmans KP, Praet J, De Vocht N, Tambuyzer BR, Bergwerf I, Daans J et al. Clinical potential of intravenous neural stem cell delivery for treatment of neuroinflammatory disease in mice? Cell transplantation. 2011;20(6):851-69. doi:10.3727/096368910X543411.
56. Boeykens N, Ponsaerts P, Van der Linden A, Berneman Z, Ysebaert D, De Greef K. Injury-dependent retention of intraportally administered mesenchymal stromal cells following partial hepatectomy of steatotic liver does not lead to improved liver recovery. PloS one. 2013;8(7):e69092. doi:10.1371/journal.pone.0069092.
57. Acosta SA, Tajiri N, Hoover J, Kaneko Y, Borlongan CV. Intravenous Bone Marrow Stem Cell Grafts Preferentially Migrate to Spleen and Abrogate Chronic Inflammation in Stroke. Stroke; a journal of cerebral circulation. 2015;46(9):2616-27. doi:10.1161/STROKEAHA.115.009854.
58. Schrepfer S, Deuse T, Reichenspurner H, Fischbein MP, Robbins RC, Pelletier MP. Stem cell transplantation: the lung barrier. Transplantation proceedings. 2007;39(2):573-6. doi:10.1016/j.transproceed.2006.12.019.
59. Giunti D, Parodi B, Usai C, Vergani L, Casazza S, Bruzzone S et al. Mesenchymal stem cells shape microglia effector functions through the release of CX3CL1. Stem cells. 2012;30(9):2044-53. doi:10.1002/stem.1174.
60. Praet J, Orije J, Kara F, Guglielmetti C, Santermans E, Daans J et al. Cuprizone-induced demyelination and demyelination-associated inflammation result in different proton magnetic resonance metabolite spectra. NMR in biomedicine. 2015;28(4):505-13. doi:10.1002/nbm.3277.
61. Giulian D, Li J, Bartel S, Broker J, Li X, Kirkpatrick JB. Cell surface morphology identifies microglia as a distinct class of mononuclear phagocyte. The Journal of neuroscience : the official journal of the Society for Neuroscience. 1995;15(11):7712-26.
62. Zhang GX, Li J, Ventura E, Rostami A. Parenchymal microglia of naive adult C57BL/6J mice express high levels of B7.1, B7.2, and MHC class II. Experimental and molecular pathology. 2002;73(1):35-45.
63. Charo IF. CCR2: from cloning to the creation of knockout mice. Chemical immunology. 1999;72:30-41.
64. Murray PJ, Allen JE, Biswas SK, Fisher EA, Gilroy DW, Goerdt S et al. Macrophage activation and polarization: nomenclature and experimental guidelines. Immunity. 2014;41(1):14-20. doi:10.1016/j.immuni.2014.06.008.
65. Hu X, Leak RK, Shi Y, Suenaga J, Gao Y, Zheng P et al. Microglial and macrophage polarization-new prospects for brain repair. Nature reviews Neurology. 2015;11(1):56-64. doi:10.1038/nrneurol.2014.207.
66. Shechter R, Schwartz M. Harnessing monocyte-derived macrophages to control central nervous system pathologies: no longer 'if' but 'how'. The Journal of pathology. 2013;229(2):332-46. doi:10.1002/path.4106.
67. Zurawski G, de Vries JE. Interleukin 13, an interleukin 4-like cytokine that acts on monocytes and B cells, but not on T cells. Immunology today. 1994;15(1):19-26. doi:10.1016/0167-5699(94)90021-3.
68. Rangachari M, Kuchroo VK. Using EAE to better understand principles of immune function and autoimmune pathology. Journal of autoimmunity. 2013;45:31-9. doi:10.1016/j.jaut.2013.06.008.
69. Gold R, Linington C, Lassmann H. Understanding pathogenesis and therapy of multiple sclerosis via animal models: 70 years of merits and culprits in experimental autoimmune encephalomyelitis research. Brain : a journal of neurology. 2006;129(Pt 8):1953-71. doi:10.1093/brain/awl075.
70. Gudi V, Moharregh-Khiabani D, Skripuletz T, Koutsoudaki PN, Kotsiari A, Skuljec J et al. Regional differences between grey and white matter in cuprizone induced demyelination. Brain research. 2009;1283:127-38. doi:10.1016/j.brainres.2009.06.005.

Chapter II

Distinct spatial distribution of microglia and macrophages following mesenchymal stem cell implantation in mouse brain

2.1. ABSTRACT

Although implantation of cellular material in the central nervous system (CNS) is a key-direction in CNS regenerative medicine, this approach is currently limited by the occurrence of strong endogenous immune cell responses. In a model of mesenchymal stem cell (MSC) grafting in the CNS of immune competent mice, we previously described that MSC grafts become highly surrounded and invaded by $Iba1^+$ myeloid cells (microglia and/or macrophages). Here, following grafting of blue fluorescent protein (BFP)-expressing MSC in the CNS of $CX_3CR1^{+/-}$ and $CX_3CR1^{-/-}$ mice, our results indicate: (i) that the observed inflammatory response is independent of the fractalkine signalling axis, and (ii) that a significant spatial distribution of $Iba1^+$ inflammatory cells occurs, in which $Iba1^+$ CX_3CR1^+ myeloid cells mainly surround the MSC graft and $Iba1^+$ CX_3CR1^- myeloid cells mainly invade the graft at 10 days post-transplantation. While $Iba1^+$ CX_3CR1^+ myeloid cells are considered to be of resident microglial origin, $Iba1^+$ CX_3CR1^- myeloid cells are most likely of peripheral monocyte/macrophage origin. In order to confirm the latter, we performed MSC-BFP grafting experiments in the CNS of $eGFP^+$ bone marrow chimeric C57BL/6 mice. Analysis of MSC-BFP grafts in the CNS of these mice confirmed our observation that peripheral monocytes/macrophages invade the MSC graft and that resident microglia surround the MSC graft site. Furthermore, analysis of MHCII expression revealed that mainly macrophages, but not microglia, express this M1 pro-inflammatory marker in the context of MSC grafting in the CNS. These results again highlight the complexity of cell implantation immunology in the CNS.

2.2. INTRODUCTION

Although mesenchymal stem cell (MSC) transplantation in the central nervous system (CNS) is widely suggested as a potential cell-based therapeutic intervention following injury or disease of the central nervous system (CNS), such intervention coincides with strong immune cell responses towards grafted MSC [1-4]. In this context, we previously described that pro-inflammatory $CD11b^+$ $MHCII^+$ $NOS2^+$ $Iba1^+$ inflammatory cells (commonly suggested as being M1-activated microglia) invade and surround grafted MSC, while activated $GFAP^+$ astrocytes form an isolating glial scar surrounding grafted MSC [5-7]. However, it is currently unclear which signalling pathways underlie these - to date poorly understood - beneficial or detrimental processes potentially involved in MSC transplantation-guided CNS repair. In order

to further investigate the observed Iba1^{+} inflammatory cell response following MSC transplantation in the CNS, in this study we performed MSC grafting experiments in transgenic $CX_3CR1^{+/-}$ mice [8], in which one copy of the CX_3CR1 gene is replaced by the eGFP reporter gene, thereby resulting in the expression of eGFP in $CX_3CR1^{+/-}$ Iba1^{+} microglia in the CNS. As in healthy brain tissue nearly all Iba1^{+} inflammatory cells are of microglial origin [9-13], thus expressing CX_3CR1, the $CX_3CR1^{+/-}$ transgenic mouse model is therefore suitable for the direct imaging of fully functional microglial cell responses. These MSC grafting experiments were also performed in transgenic $CX_3CR1^{-/-}$ mice [8], in which both copies of the CX_3CR1 gene are replaced by the eGFP reporter gene, thereby resulting in the expression of eGFP in $CX_3CR1^{-/-}$ Iba1^{+} microglia in the CNS. The $CX_3CR1^{-/-}$ transgenic mouse is thus a suitable model for the direct imaging of microglia unresponsive to fractalkine (CX_3CL1) signalling. Given the involvement of fractalkine signalling in many CNS inflammatory responses, which can either be beneficial [14-16] or detrimental [17-19] under certain conditions, we here additionally aimed to investigate whether or not this signalling pathway is involved during the establishment of the Iba1^{+} inflammatory cell response observed after MSC grafting in the CNS. During the course of these experiments, we identified a CX_3CR1^{-} Iba1^{+} immune cell population which was involved in the observed inflammatory response. Following MSC grafting in the CNS of eGFP^{+} bone marrow (BM) chimeras, we here provide the first evidence that the *in vivo* remodelling of MSC grafts following implantation in the CNS is a complex process in which both CX_3CR1^{+} Iba1^{+} microglia and CX_3CR1^{-} Iba1^{+} macrophages have a specific spatial distribution and phenotype.

2.3. MATERIALS AND METHODS

2.3.1. Mice

Transgenic C57BL/6 $CX_3CR1^{-/-}$ (strain code 005582) and C57BL/6-eGFP (strain code 003291) mice were obtained via Jackson Laboratories and further bred in the animalarium of the University of Antwerp. C57BL/6 $CX_3CR1^{+/-}$ mice were obtained by crossing $CX_3CR1^{-/-}$ mice with wild type C57BL/6 mice (Charles River Laboratories, strain code 027). For generation of BM chimeras, wild type C57BL/6 mice were used. During the entire study, mice were kept under normal day-night cycle (12/12) with free access to food and water. All animal experimental

procedures were approved by the Ethics Committee for Animal Experiments of the UA (Approval No 2011-13 and 2012-39).

2.3.2. Generation of eGFP$^+$ BM chimeras

For BM transplantation experiments (n=8), mice received 10Gy total body irradiation using an XRAD320 small animal irradiation device (Precision X-Ray). For this, groups of five non-anesthetised mice were placed in a single cage within the whole irradiation field (without head protection). Next, a single intravenous (iv) injection of total BM cells ($1.5x10^6$ cells in 100µl PBS) was administered via the tail vein 6 hours post-irradiation. Total BM was isolated from 8-week old C57BL/6-eGFP mice by flushing the dissected femurs and tibias with sterile PBS. Before administration, total BM cells were filtered over a 70µm sterile mesh (Becton Dickinson), centrifuged and suspended in PBS. As internal control for the irradiation procedure, one mouse per group did not receive a BM transplant, resulting in death approximately 2 weeks after irradiation. During recovery, mice were treated with enrofloxacin (1µl/mL; Baytril 10%; Bayer) added to the drinking water for 8 weeks post-irradiation.

2.3.3. Flow cytometric analysis

Immunophenotyping of splenocytes derived from eGFP$^+$ BM chimeras was performed using the following monoclonal antibodies: phycoerythrin (PE)-labelled anti-mouse CD45 (eBioscience, 12-0451), PE-labelled anti-mouse CD3 (eBioscience, 12-0031), PE-labelled anti-mouse CD11b (eBioscience, 12-0112) and PE-labelled anti-mouse CD11c (eBioscience, 12-0114). Before staining, harvested cells were washed twice with PBS and resuspended in PBS at a concentration of 5×10^5 cells/ml. For antibody staining, 1µg of antibody was added to 100µl of cell suspension for 30 min at 4°C. Following incubation, cells were washed once with PBS, resuspended in 1mL PBS, and analysed using an Epics XL-MCL analytical flow cytometer (Beckman Coulter). Determination of eGFP transgene expression was performed directly during flow cytometric analysis. Cell viability was assessed through addition of GelRed (1× final concentration, Biotum) to the cell suspension immediately before flow cytometric analysis. At least 1×10^4 cells were analysed per sample and flow cytometry data were analysed using FlowJo software.

2.3.4. BFP lentiviral vector construction and production

The following DNA plasmids were used in this study: (i) the commercially available TagBFP plasmid encoding the blue fluorescent protein (BFP) (Evrogen) and (ii) the pCHMWS-eGFP-IRES-Pac plasmid (provided by the Leuven viral vector core, Molmed, KULeuven, Belgium). The pCHMWS-BFP-IRES-Pac plasmid was constructed by replacing the eGFP cDNA insert (SpeI/XbaI digest) from the pCHMWS-eGFP-IRES-Pac plasmid with the BFP cDNA (SmaI/XbaI digest) from the TagBFP plasmid. Blunt-end ligation was performed following Klenow reaction on both insert and receptor plasmid and CIAP treatment of the receptor plasmid. After selection of successfully ligated pCHMWS-BFP-IRES-Pac clones, correct orientation of the insert was confirmed by sequence analysis. All plasmids were propagated in E.coli supercompetent cells (Stratagene) and purified using plasmid midi or maxiprep columns (Qiagen). Before proceeding to Lentiviral vector (LVv) production, the pCHMWS-BFP-IRES-Pac plasmid was electroporated in K562 cells followed by stable selection under addition of puromycin to the culture medium. Expression of the BFP was confirmed by direct flow cytometric analysis of stably transfected puromycin-resistant K562 cells on a FACS AriaII cell sorter (BD Biosciences). Following confirmation of BFP expression and Pac functionality, LVv production was outsourced to the Leuven viral vector core (Molmed, KULeuven, Belgium) [35, 36].

2.3.5. Genetic modification of MSC

In this study, we used a previously established and characterised C57BL/6 mouse bone marrow-derived MSC line [12]. For cell expansion, MSC were cultured in standard cell culture plasticware (well plates and/or culture flasks) in 'complete expansion medium' (CEM) consisting of Iscove's modified Dulbecco's medium (IMDM; Lonza) supplemented with 8% fetal bovine serum (FBS; Invitrogen), 8% horse serum (HS; Invitrogen), 200U/mL penicillin + 100µg/mL streptomycin (Invitrogen) and 1µg/mL amphotericin B (Invitrogen). MSC cultures were split 1:5 twice a week following cell detachment after 0.05% trypsin-EDTA (Invitrogen) treatment. For histological analysis following cell implantation *in vivo*, MSC cultures were transduced with the pCHMWS-BFP-IRES-Pac LVv. For this, MSC were seeded in 24-well plates at a concentration of $1x10^4$ cells/well in 750µl CEM and 10µl ($3.1x10^7$ pg/mL p24) of the LVv

was added to the MSC culture. 24 hours after transduction, medium was replaced with fresh CEM. Upon confluence, transduced cells were selected by adding 10µg/mL puromycin (Invivogen) to the medium. Following selection of transduced cells, MSC-BFP were further cultured in CEM supplemented with 1µg/mL puromycin.

2.3.6. Cell implantation experiments

All surgical interventions were performed under sterile conditions, as previously described by us [5, 7, 37, 38]. In brief, mice were anesthetised by an intraperitoneal injection of a ketamine (80 mg/kg, Pfizer) + xylazine (16 mg/kg, Bayer Health care) mixture in phosphate buffered saline (PBS) and placed in a stereotactic frame (Stoelting). Next, a midline scalp incision was made and a hole was drilled in the skull using a dental drill burr (Stoelting) at the level of bregma and 2.5mm to the right side of the midline. Next, an automatic microinjector pump (kdScientific) with a 10µl Hamilton Syringe was positioned above the exposed dura. A 30-gauge needle (Hamilton), attached to the syringe, was stereotactically placed through the intact dura to a depth of 2.3 mm, thereby targeting the injected cell population directly below the right capsula externa. After 2 minutes of pressure equilibration, a suspension of $1.25x10^5$ MSC-BFP in a volume of 2µl PBS (or an equal volume of PBS as sham control) was injected at a speed of 0.7µl/min. The needle was retracted after another 4 min to allow pressure equilibration and to prevent backflow of the injected cell suspension. Next, the skin was sutured (Vicryl, Ethicon) and a 0.9% NaCl solution (Baxter) was administered subcutaneously in order to prevent dehydration while mice were placed under a heating lamp to recover.

2.3.7. Histological analysis

At day 10 post-cell grafting, mice were deeply anaesthetised via an intraperitoneal injection of 60 mg/kg/BW pentobarbital (Nembutal, Ceva Sante Animale), transcardially perfused with ice cold 0,9% NaCl and perfused-fixed with 4% paraformaldehyde. Whole brains were then surgically removed and post-fixed in 4% paraformaldehyde for 2 hours. Fixed brains were freeze-protected via a sucrose gradient (2 hours at 5%, 2 hours at 10% and overnight at 20%), snap frozen in liquid nitrogen and stored at -80°C until further processing. Histological analysis was then performed according to optimised procedures previously described by us [5, 37, 38].

In brief, consecutive 10 µm-thick cryosections were prepared using a microm HM500 cryostat for all cell-grafted brains starting before the graft site until beyond the graft site. Slides were observed by direct fluorescence microscopy in order to locate BFP-expressing cell grafts. Further immunofluorescence analyses were performed using the following primary + secondary antibody combinations: a rabbit anti-mouse Iba1 antibody (1/500 dilution, Wako, 019-19741) in combination with an Alexa Fluor 555-labelled donkey anti-rabbit secondary antibody (1/500 dilution, Invitrogen, A31572) or an Alexa Fluor 350-labelled donkey anti-rabbit secondary antibody (1/100 dilution, Invitrogen, A310039), a rabbit anti-S100β antibody (1/800 dilution, Abcam, ab52642) and a rabbit anti-GFAP antibody (1/1000 dilution, Abcam, ab7779) in combination with an Alexa Fluor-labelled 555-labelled donkey anti-rabbit secondary antibody, a rat anti-MHCII antibody (1/200 dilution, eBioscience, 14-5321-82) in combination with an Alexa Fluor 555-labelled goat anti-rat secondary antibody (1/200 dilution, Invitrogen, A21434). Briefly, tissue sections were permeabilised with 0.1% triton-X (Merck) in TBS for 30 min and then blocked by adding donkey serum (20% in TBS; Jackson ImmunoResearch) for minimum 1h at room temperature (RT). Subsequently, primary antibody was added and incubated overnight at 4°C. Next, brain slices were rinsed with TBS and secondary antibody was added, which was incubated at RT on a shaker for 1h. Next, tissue slices were rinsed with TBS and TOPRO-3 (1/200 dilution, Invitrogen, 3605) was added and incubated for 20 min at RT. Finally, slides were rinsed with water and mounted with Prolong Gold anti-fade reagent (Invitrogen). Immunofluorescence images were acquired using an Olympus BX51 fluorescence microscope equipped with an Olympus DP71 digital camera. Olympus cellSens Dimension software was used for image acquisition and processing.

2.3.8. Histological quantification

Quantitative analysis of glial cell responses was performed using NIH ImageJ analysis software (v1.47) and TissueQuest immunofluorescence analysis software (TissueGnostics GmbH, v3.0), as previously described by us [5, 37, 38]. For each of the slides analysed, the graft site was manually delineated based on BFP-fluorescence of MSC-BFP grafts. The graft site border was then determined as a region extending 85µm from the MSC graft site. According to previously established procedures, the following parameters were then determined for the MSC graft

site and the MSC graft site border: (i) the total cellular density (1 slide per cell graft analysed), (ii) the cellular density of $Iba1^+$ myeloid cells (1 slide per cell graft analysed), (ii) the cellular density of grafted MSC-BFP cells (1 slide per cell graft analysed), (iii) the cellular density of $S100\beta^+$ astrocytes (1 slide per cell graft analysed), (iv) the optical density (% OD) $GFAP^+$ astrogliosis (1 slide per cell graft analysed), (v) the percentage of $eGFP^+$ $Iba1^+$ and $eGFP^-$ $Iba1^+$ cells in $CX_3CR1^{-/-}$ and $CX_3CR1^{+/-}$ mice (1 slide per cell graft analysed), (vi) percentage of $eGFP^+$ $Iba1^+$ and $eGFP^-$ $Iba1^+$ cells in $eGFP^+$ BM chimeras (2 or 3 slides per cell graft analysed) and (vii) the percentage of $MHCII^+$ cells in $eGFP^+$ BM chimeras (1 slide per cell graft analysed).

2.3.9. Statistical analysis

All data sets were tested for normality. Comparison of the cell density of BFP^+, $Iba1^+$ and $S100\beta^+$ cells, as well as the degree of GFAP expression in the graft site and the graft site border between cell implants in $CX_3CR1^{+/-}$ and $CX_3CR1^{-/-}$ transgenic mice were done using the Wilcoxon Rank-Sum test with false-discovery rate correction for multiple testing. Comparisons of the percentage of $eGFP^+$ CX_3CR1^+ cells in $CX_3CR1^{-/-}$ and $CX_3CR1^{+/-}$ transgenic mice and the percentage of $eGFP^+$ Iba^+ cells in $eGFP^+$ BM chimeras within the graft site and the graft site border were done using respectively the Wilcoxon Signed-Rank test and the Wilcoxon Signed-Rank test for clustered observations. Comparisons of the percentage of $MHCII^+$ cells within the graft site and the graft site border, and of $MHCII^+$ macrophages and $MHCII^+$ microglia in the graft site or in the graft site border were done using the Wilcoxon Signed-Rank test. Data are represented as mean ± standard deviation (SD) and a p-value < 0.05 was considered statistically significant. All significant p-values are stated in the result section.

2.4. RESULTS

2.4.1. Transgenic impairment of fractalkine signalling does not lead to altered Iba1^{+} myeloid cell responses

In order to investigate the role of fractalkine signalling on microglia recruitment during MSC graft remodelling in the CNS, we grafted blue fluorescent protein (BFP)-expressing MSC (MSC-BFP) in the CNS of $CX_3CR1^{+/-}$ (n=6) and $CX_3CR1^{-/-}$ (n=6) mice. At day 10 post-grafting, as shown by the representative immunofluorescence images in figure 1A and the provided quantitative histological analysis, no significant differences were observed in the cellular density of graft-infiltrating and graft-surrounding Iba1^{+} myeloid cells (figures 1B and 1C respectively), grafted MSC-BFP (figure 1B) and graft-surrounding S100β^{+} astrocytes (figure 1C), and in the degree of graft-surrounding GFAP^{+} astrogliosis (figure 1D), when comparing MSC-BFP grafts in $CX_3CR1^{+/-}$ and $CX_3CR1^{-/-}$ mice. Based on the data from this comparative experiment, we here suggest that interference with microglial fractalkine signalling does not lead to alterations in MSC graft remodelling in the CNS. Hence, fractalkine signalling is not involved during the establishment of the Iba1+ inflammatory cell response observed after MSC grafting in the CNS.

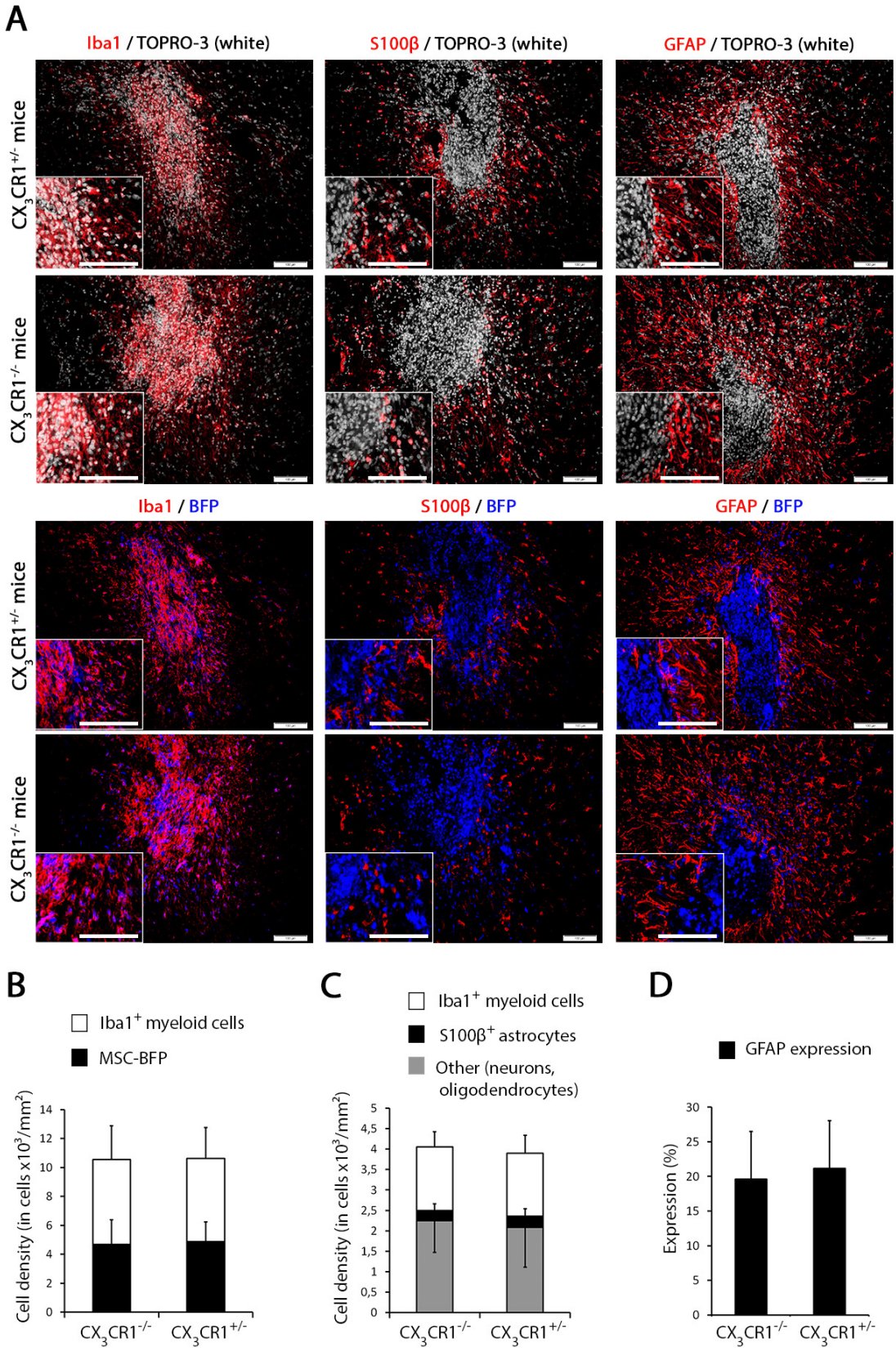

Figure 1. Characterisation of MSC-BFP implants in $CX_3CR1^{+/-}$ and $CX_3CR1^{-/-}$ mice.

(A) Representative immunofluorescence images of TOPRO-3$^+$ nuclei (in white) and grafted MSC-BFP (in blue) in the striatum of $CX_3CR1^{+/-}$ mice and $CX_3CR1^{-/-}$ mice at day 10 post-grafting. The images show Iba1$^+$ microglia/macrophages (in red), S100β$^+$ astrocytes (in red) and GFAP$^+$ astrocytes/astrogliosis (in red). The scale

bars of the main images and the insets indicate 100µm. (B) Graph showing the cell density (in cells x 10^3/mm^2) of grafted MSC-BFP and $Iba1^+$ microglia/macrophages within the MSC-BFP graft site in $CX_3CR1^{+/-}$ mice and in $CX_3CR1^{-/-}$ mice. (C) Graph showing the cell density (in cells x 10^3/mm^2) of $Iba1^+$ microglia/macrophages and $S100\beta^+$ astrocytes in the MSC-BFP graft site border in $CX_3CR1^{+/-}$ mice and in $CX_3CR1^{-/-}$ mice. (D) Graph showing the degree (in percentage area coverage) of $GFAP^+$ astrogliosis in the MSC-BFP graft site border in $CX_3CR1^{+/-}$ mice and in $CX_3CR1^{-/-}$ mice. For all graphs, data are presented as mean ± standard deviation (n=6 for both $CX_3CR1^{+/-}$ mice and $CX_3CR1^{-/-}$ mice).

2.4.2. MSC graft-infiltrating $Iba1^+$ myeloid cells do not express the fractalkine receptor

From the representative immunofluorescence images in figures 2A and 2D and the provided quantitative histological analyses in figures 2B and 2E, we noted that eGFP expression, which is linked to the absence of one or both copies of the fractalkine receptor on brain microglia in $CX_3CR1^{+/-}$ and $CX_3CR1^{-/-}$ mice, is spatially distributed on MSC-BFP graft-surrounding and graft-infiltrating $Iba1^+$ myeloid cells. In MSC-BFP grafted $CX_3CR1^{+/-}$ mice, 80% ± 13% of $Iba1^+$ myeloid cells within the MSC-BFP graft site border are $eGFP^+$, while only 26% ± 12% of $Iba1^+$ myeloid cells within the MSC-BFP graft site are $eGFP^+$. In MSC-BFP grafted $CX_3CR1^{-/-}$ mice, 80% ± 14% of $Iba1^+$ myeloid cells within the MSC-BFP graft site border are $eGFP^+$, while only 20% ± 7% of $Iba1^+$ myeloid cells within the MSC-BFP implant site are $eGFP^+$. Further statistical analysis confirmed that eGFP expression (or CX_3CR1 promoter activity indicating $eGFP^+$ cells being of microglial origin) is significantly different between $Iba1^+$ myeloid cells within the MSC-BFP graft site and $Iba1^+$ myeloid cells surrounding the graft site ($p=0.031$ for cell grafts in both $CX_3CR1^{+/-}$ and $CX_3CR1^{-/-}$ mice). Based on the presented data, we conclude that the MSC-BFP graft site border is mainly populated by $CX_3CR1^{+/-}$ $eGFP^{+/-}$ $Iba1^+$ microglia or $CX_3CR1^{-/-}$ $eGFP^{+/+}$ $Iba1^+$ microglia in respectively $CX_3CR1^{+/-}$ and $CX_3CR1^{-/-}$ mice, and we might suggest that $Iba1^+$ microglia within the MSC-BFP implant site either suppress CX_3CR1 (or eGFP) gene expression due to interaction with the MSC graft, or - alternatively - are a different cell population. Furthermore, in agreement with our preceding results [5], graft-infiltrating immune cells display a higher degree of MHCII expression as compared to graft-surrounding immune cells in both $CX_3CR1^{+/-}$ and $CX_3CR1^{-/-}$ mice (figures 2C and 2F). Hence, besides this differential expression of MHCII, fractalkine signalling on graft-surrounding $CX_3CR1^{+/-}$ $Iba1^+$ microglia or $CX_3CR1^{-/-}$ $Iba1^+$ microglia in respectively $CX_3CR1^{+/-}$ and $CX_3CR1^{-/-}$ mice is not involved in regulating MHCII expression on graft-infiltrating $Iba1^+$ immune cells.

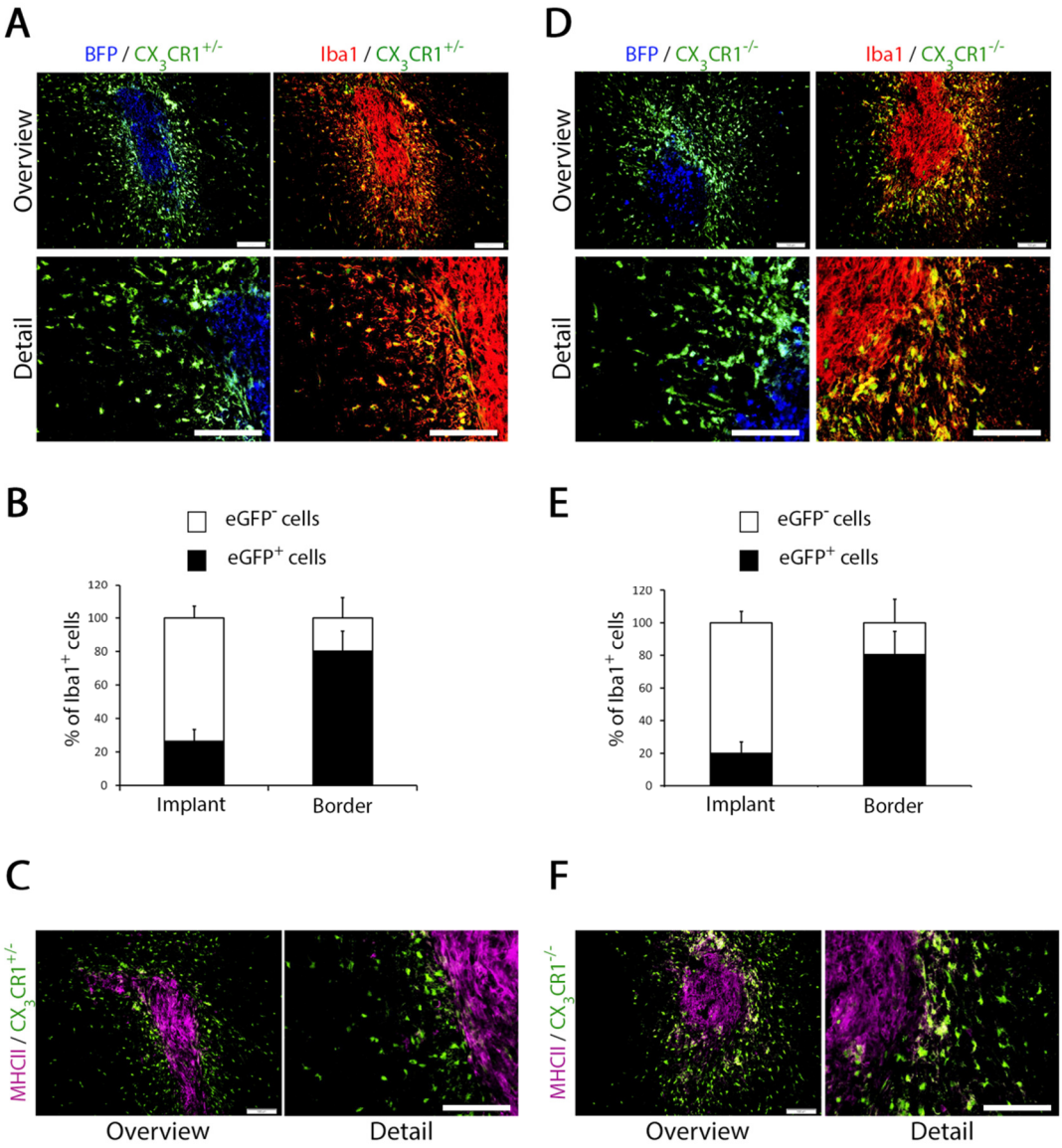

Figure 2. Quantification of eGFP-CX₃CR1 cells in MSC-BFP grafted CX₃CR1$^{+/-}$ mice.

Upper panel: representative immunofluorescence images of grafted MSC-BFP (in blue) in the striatum of CX₃CR1$^{+/-}$ mice (A) and CX₃CR1$^{-/-}$ mice (D) at day 10 post-grafting. The images show Iba1^{+} microglia/macrophages (in red) and, respectively, CX₃CR1$^{+/-}$ eGFP-expressing microglia (in green) and CX₃CR1$^{-/-}$ eGFP-expressing microglia (in green). Note the predominant co-localisation of Iba1 and eGFP in the MSC-BFP graft site border (in yellow), but not within the MSC-BFP graft site. The scale bars indicate 100µm. Middle panel: graphs showing the percentages of eGFP^{+} Iba1^{+} and eGFP^{-} Iba1^{+} microglia/macrophages in the MSC-BFP graft site and graft site border in CX₃CR1$^{+/-}$ mice (B) and in CX₃CR1$^{-/-}$ mice (E). Data are presented as mean ± standard deviation (n=6). Lower panel: representative immunofluorescence images of grafted MSC-BFP in the striatum of CX₃CR1$^{+/-}$ mice (C) and CX₃CR1$^{-/-}$ mice (F) at day 10 post-grafting. The images show MHCII expression (in purple) and, respectively, CX₃CR1$^{+/-}$ eGFP-expressing microglia (in green) and CX₃CR1$^{-/-}$ eGFP-expressing microglia (in green). Note the predominant localisation of MHCII expression in the MSC-BFP graft site, but not in the MSC-BFP graft site border. The scale bars indicate 100µm.

2.4.3. MSC graft infiltrating CX_3CR1^- $Iba1^+$ myeloid cells are of peripheral origin

In order to investigate the hypothesis that CX_3CR1^- $Iba1^+$ inflammatory cells within the MSC graft site are peripheral macrophages and not brain-derived microglia (which are CX_3CR1^+ $Iba1^+$), we performed MSC-BFP grafting experiments in $eGFP^+$ bone marrow chimeras. For the latter, 8-week old C57BL/6 mice were irradiated and total BM derived from C57BL/6-eGFP transgenic mice was administered intravenously, as described in the methods section. Following 8 weeks of recovery, $eGFP^+$ BM chimeras underwent MSC-BFP grafting in the CNS followed by brain and spleen dissection at day 10 post-grafting. Flow cytometric analysis of splenocyte subsets, among which $CD45^+$ myeloid cells, $CD3^+$ T-cells, $CD11b^+$ monocytes/macrophages and $CD11c^+$ dendritic cells, indicated successful generation of $eGFP^+$ bone marrow chimeras as eGFP expression was detected in the majority of the peripheral monocyte/macrophage population (> 95%, figure 3A). From the representative immunofluorescence images of MSC-BFP grafted brains in figure 3B and the provided quantitative histological analysis in figure 3C, we noted that eGFP expression, which is here restricted to immune cells of peripheral origin, is spatially distributed on MSC-BFP graft-surrounding and graft-infiltrating $Iba1^+$ myeloid cells. In MSC-BFP grafted $eGFP^+$ BM chimeras, 81% ± 9% of $Iba1^+$ myeloid cells within the MSC-BFP graft site are $eGFP^+$, while only 31% ± 9% of $Iba1^+$ myeloid cells within the MSC-BFP graft site border are $eGFP^+$. Further statistical analysis confirmed that eGFP expression is significantly different between $Iba1^+$ myeloid cells within the MSC-BFP graft site and $Iba1^+$ myeloid cells surrounding the graft site ($p=0.018$). Based on these results, we here conclude that the MSC-BFP graft site is - in contrast to the graft site border - mainly populated by invading (CX_3CR1^-) $Iba1^+$ peripheral macrophages.

2.4.4. Graft-infiltrating bone marrow-derived macrophages display MHCII expression

As already shown above in figures 2C and 2F, MHCII is predominantly expressed by immune cells within the MSC-BFP implant site. Here we further investigated the expression of MHCII by $Iba1^+$ $eGFP^-$ microglia and $Iba1^+$ $eGFP^+$ macrophages within and surrounding the MSC-BFP graft site in $eGFP^+$ BM chimeras (figure 3D). Within the implant site the following distribution was quantified: 58% ± 24% $Iba1^+$ $eGFP^+$ $MHCII^+$ macrophages, 32% ± 26% $Iba1^+$ $eGFP^+$ $MHCII^-$ macrophages, 3% ± 3% $Iba1^+$ $eGFP^-$ $MHCII^+$ microglia and 8% ± 5% $Iba1^+$ $eGFP^-$ $MHCII^-$ microglia

(figure 3E, implant). Within the implant border the following distribution was quantified: 13% ± 9% Iba1$^+$ eGFP$^+$ MHCII$^+$ macrophages, 22% ± 13% Iba1$^+$ eGFP$^+$ MHCII$^-$ macrophages, 8% ± 4% Iba1$^+$ eGFP$^-$ MHCII$^+$ microglia and 57% ± 14% Iba1$^+$ eGFP$^-$ MHCII$^-$ microglia (figure 3E, border). Further statistical analysis revealed that the percentage of MHCII$^+$ cells is significantly higher in the graft site than in the graft site border ($p=0.016$) and the percentage of MHCII$^+$ macrophages is significantly higher than the percentage of MHCII$^+$ microglia in the graft site ($p=0.016$). Of note, the appearance of Iba1$^+$ eGFP$^+$ MHCII$^+$ macrophages within the MSC graft site seems to be highly specific for immune recognition/remodelling of MSC grafts in the CNS as a control sham injection-induced immune response in eGFP$^+$ BM chimeras consists mainly of Iba1$^+$ eGFP$^-$ microglia and only a limited number of Iba1$^+$ eGFP$^+$ macrophages and MHCII$^+$ microglia/macrophages (figure 3F).

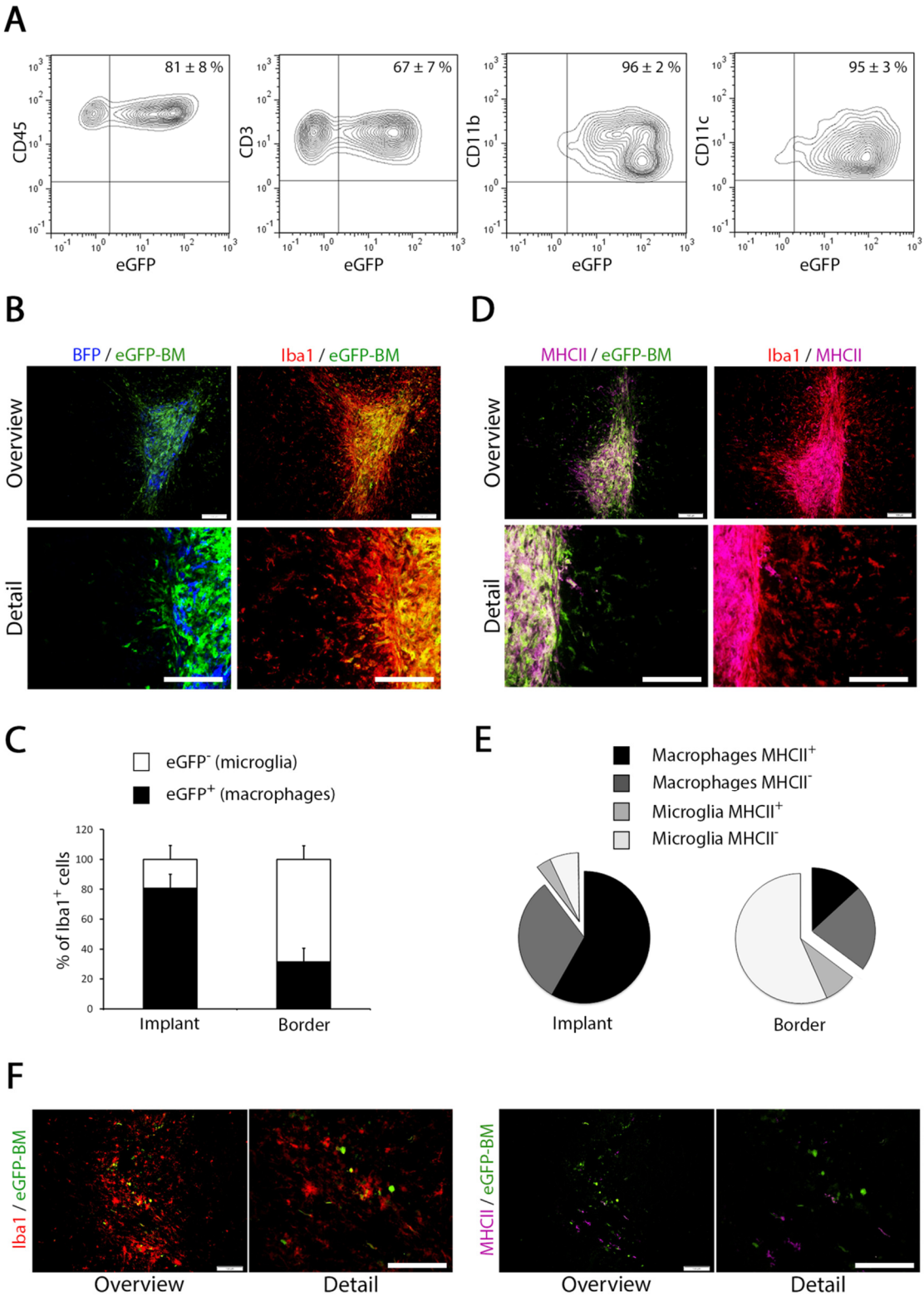

Figure 3. Quantification and characterisation of eGFP⁺ blood-derived macrophages in MSC-BFP grafted eGFP⁺ bone marrow chimeras.

(A) Representative flow cytometric contour plots demonstrating eGFP expression (X-axis) fraction within all hematopoietic cells (CD45, Y-axis), T-cells (CD3, Y-axis), monocytes/macrophages (CD11b, Y-axis) and dendritic cells (CD11c, Y-axis) isolated from the spleen of MSC-BFP grafted eGFP⁺ BM chimeras, indicating successful

hematopoietic reconstitution. Percentages indicated are mean ± standard deviation (n=5). (B) Representative immunofluorescence images of grafted MSC-BFP (in blue) in the striatum of eGFP$^+$ BM chimeras at day 10 post-grafting. The images show Iba1$^+$ microglia/macrophages (in red) and eGFP-expressing peripheral macrophages (in green). Note the predominant co-localisation of Iba1 and eGFP in the MSC-BFP graft site (in yellow), but not in the MSC-BFP graft site border. The scale bars indicate 100µm. (C) Graph showing the percentages of eGFP$^+$ Iba1$^+$ macrophages and eGFP$^-$ Iba1$^+$ microglia in the MSC-BFP graft site and graft site border. Data are presented as mean ± standard deviation (n=7). (D) Representative immunofluorescence images of the MSC-BFP graft site in the striatum of eGFP$^+$ BM chimeras at day 10 post-grafting. The images show MHCII expression (in purple), Iba1$^+$ microglia/macrophages (in red) and eGFP-expressing peripheral macrophages (in green). Note the predominant co-localisation of Iba1 and MHCII (resulting in pink colour) and of eGFP and MHCII (resulting in white colour) in the MSC-BFP graft site, but not in the MSC-BFP graft site border. The scale bars indicate 100µm. (E) Pie charts showing the percentages of Iba1$^+$ eGFP$^+$ MHCII$^+$ macrophages, Iba1$^+$ eGFP$^+$ MHCII$^-$ macrophages, Iba1$^+$ eGFP$^-$ MHCII$^+$ microglia and Iba1$^+$ eGFP$^-$ MHCII$^-$ microglia in the MSC-BFP graft site and graft site border. Microglia (outside) and macrophages (inside) are presented as separate pieces of the pie charts. Data are represented as mean (n=7). (F) Representative immunofluorescence images of a sham injection with PBS in the striatum of eGFP$^+$ BM chimeras at day 10 post-grafting. The images show Iba1$^+$ microglia/macrophages (in red), MHCII$^+$ microglia/macrophages (in purple) and eGFP$^+$ peripheral macrophages (in green). The scale bars indicate 100µm.

2.5. DISCUSSION

Although in our preceding work with regard to cell implantation into the CNS, Iba1$^+$ myeloid cells were designated as microglia and/or macrophages, we did not yet investigate the nature of the inflammatory cell response in depth, as both cell types - despite their ability to act in different ways - appear to be difficult to distinguish in the CNS [12, 20, 21]. To our knowledge, we here report for the first time that the *in vivo* remodelling of MSC grafts following implantation in the CNS is a complex process in which both CX_3CR1^+ Iba1$^+$ microglia and CX_3CR1^- Iba1$^+$ macrophages have a specific spatial distribution and phenotype in the process of cell graft-induced neuro-inflammation. We here provide evidence that upon MSC grafting in the CNS, the MSC graft itself becomes invaded by peripheral macrophages, while both the MSC graft and the invading macrophages become encapsulated by microglia and astroglial scar tissue. Although initially not expected, the influx of peripheral macrophages into MSC grafts in the CNS is not very surprising as: (i) the procedure of cell grafting into the CNS inevitably causes a (temporary) disruption of the blood brain barrier due to needle-related injury, and (ii) we previously described the process of neo-angiogenesis within cellular grafts of mesenchymal origin [22], thereby allowing direct contact between the MSC graft and the peripheral immune system. These suggestions are fully in line with established observations that in healthy CNS BM-derived macrophages are restricted to regions lacking the blood-brain-

barrier (BBB), i.e. the leptomeninges, ventricles, choroid plexus and blood vessels, while resident microglia are only found within the brain parenchyma [23-25]. In case of brain injury/disease accompanied with BBB disruption, macrophages will enter the brain parenchyma and together with the resident microglia contribute to neuroinflammation [26-28]. However, in contrast to trauma or disease, MSC grafting in the CNS, after creating an initial small injury by needle injection, results in a specific distribution of macrophages and microglia, suggesting an unknown mechanism by which MSC differentially signal to microglia and macrophages. Nevertheless, whereas the influx of peripheral macrophages into the CNS may seem to be a rather dramatic outcome, it remains unclear whether this macrophage influx into CNS-grafted MSC implants is beneficial or detrimental for graft survival, a feature undoubtedly difficult to investigate.

On the other hand, within the context of pathology-inducing neuroinflammation it is becoming understood that brain-infiltrating macrophages and brain-resident microglia might play different roles in neuroinflammatory processes. For example, upon ablation of blood-derived monocytes in mouse models for Alzheimer Disease [29] and Multiple Sclerosis [27, 30], respectively β-amyloid clearance was impaired and autoimmunity was strongly reduced. In addition, significant differences in the proliferation profile of brain-resident microglia and infiltrating macrophages have been described [31], thereby suggesting a stronger contribution of infiltrating BM-derived macrophages to neuroinflammation as compared to brain-resident microglia. This hypothesis fits within our presented results with regard to MHCII expression being predominantly on BM-derived macrophages within the MSC implant. Therefore, we might argue, based on the distinct spatial distribution of at one side microglia and on the other side macrophages, a more important role for MSC graft-infiltrating macrophages during the process of MSC graft remodelling. As far as our data support for now, it appears that microglia - together with astrocytes - seem to prevent grafted MSC from infiltrating the brain parenchyma, while infiltrating pro-inflammatory MHCII-expressing macrophages seem to control survival (or death) of the MSC graft from within the graft site itself.

In our experimental setup using $eGFP^{+}$ BM chimeras to distinguish brain-resident microglia from infiltrating macrophages, one might argue that the irradiation procedure might have displayed some influence on the functional properties of both populations during the process of MSC graft-induced neuroinflammation due to irradiation-induced alterations of the CNS

micromilieu, including disturbances of the BBB, damage of endothelial cells and local induction of proinflammatory cytokines [32]. Although we cannot neglect a potential influence of the BM transplantation event, it should however be noted that the results obtained following MSC grafting in $CX_3CR1^{+/-}$ and $CX_3CR1^{-/-}$ mice are - in quantitative numbers of histological analysis - nearly equal to the results obtained following MSC grafting in $eGFP^+$ BM chimeras. Nevertheless, in future experiments it would be highly interesting to further investigate the cross-talk between grafted stem cell populations and the CNS/peripheral innate immune system in the established CX_3CR1-eGFP x CCR2-Red mouse model for efficient discrimination between respectively brain-resident microglia and infiltrating macrophages, without the need for a BM transplantation procedure [25].

Although the major outcome of this manuscript lies in the discrimination between microglia and macrophages in the context of cell grafting in the CNS, the original aim of this manuscript was to investigate the role of fractalkine signalling in the occurrence of microglial cell responses following cell implantation in the CNS. The CX_3CL1/CX_3CR1 signalling axis is a major regulator of microglial activation and neurotoxicity in the CNS. Under normal conditions within the CNS, CX_3CL1 is mainly expressed by neurons as an extracellular membrane-bound chemokine. Hereby it is proposed to play a major role in neuron-microglia communication via its receptor CX_3CR1 on microglia. However, upon neuronal injury, CX_3CL1 can be cleaved from the membrane, after which soluble CX_3CL1 then acts as a chemokine responsible for the recruitment of microglia to sites of CNS injury [10, 13, 14, 33]. However, within the context of cell transplantation into the CNS, it was recently suggested by *in vitro* experiments that microglial function can be switched from a detrimental phenotype to a neuroprotective phenotype due to the release of CX_3CL1 by MSC [34]. Therefore, in the first part of this study we aimed to investigate the contribution of fractalkine signalling, either released by damaged neurons or by grafted MSC, during the recruitment of Iba1+ myeloid cells (microglia and macrophages) towards MSC implants in the CNS. Based on our results, we here demonstrate that CX_3CL1/CX_3CR1 signalling is not involved - or at least not the main trigger - in this process as equal numbers of $Iba1^+$ $eGFP^+$ microglia and $Iba1^+$ $eGFP^-$ macrophages were, respectively, found surrounding or within the MSC graft site in both $CX_3CR1^{+/-}$ and $CX_3CR1^{-/-}$ mice. In addition, the presence or absence of functional CX_3CL1/CX_3CR1 signalling on $eGFP^+$ graft-surrounding microglia in both $CX_3CR1^{+/-}$ and $CX_3CR1^{-/-}$ mice did not influence the appearance

of MHCII expression on MSC graft-infiltrating macrophages. Given the unresponsiveness of the CX_3CL1/CX_3CR1 signalling axis following MSC implantation into the CNS, we might suggest with precaution that despite the $Iba1^+$ inflammatory response associated with this intervention, the process of cell grafting in the CNS might not lead to major neuronal injury. Nevertheless, strong immune cell responses do occur, suggesting an important role of other signalling pathways involved in this process. Despite previous suggestions that CX_3CL1 released by MSC can modulate microglia function *in vitro*, this seems to be rather complicated *in vivo* as grafted MSC are in direct contact with CX_3CR1^- macrophages, but not with CX_3CR1^+ microglia, upon grafting into the CNS [34]. Nevertheless, it cannot be excluded that MSC-derived CX_3CL1 *in vivo* can induce subtle differences in microglia phenotype and function *in vivo*. Further research will thus be needed to unravel the early post-transplantation events (<10 days post-grafting) in order to fully understand - and eventually modulate – cell graft-induced inflammatory responses both on the molecular and cellular level.

In conclusion, following a series of preceding reports from our group describing the occurrence of inflammatory responses following cell grafting into the CNS, with this study we aimed to further unravel part of this complex series of events. As such, we now are aware of the fact that the observed inflammatory response directed against grafted MSC is orchestrated by both brain-resident microglia and peripheral macrophages. Although neglected in many studies, we believe that a thorough understanding of the cellular events, including a proper phenotyping of those cells involved, will lead to a better understanding of the potential beneficial effects of cell grafting in the CNS, and – ultimately – will lead to the design of safe and functional cell implantation strategies in injured or diseased CNS tissue.

2.6. REFERENCES

1. Ronsyn MW, Berneman ZN, Van Tendeloo VF, Jorens PG, Ponsaerts P. Can cell therapy heal a spinal cord injury? *Spinal Cord* 2008; **46**: 532-539.
2. Bergwerf I, Tambuyzer B, De Vocht N, Reekmans K, Praet J, Daans J *et al.* Recognition of cellular implants by the brain's innate immune system. *Immunol Cell Biol* 2011; **89**: 511-516.
3. De Vocht N, Praet J, Reekmans K, Le Blon D, Hoornaert C, Daans J *et al.* Tackling the physiological barriers for successful mesenchymal stem cell transplantation into the central nervous system. *Stem Cell Res Ther* 2013; **4**: 101.
4. Reekmans K, Praet J, De Vocht N, Daans J, Van der Linden A, Berneman Z *et al.* Stem cell therapy for multiple sclerosis: preclinical evidence beyond all doubt? *Regen Med* 2012; **7**: 245-259.
5. De Vocht N, Lin D, Praet J, Hoornaert C, Reekmans K, Le Blon D *et al.* Quantitative and phenotypic analysis of mesenchymal stromal cell graft survival and recognition by microglia and astrocytes in mouse brain. *Immunobiology* 2013; **218**: 696-705.
6. De Vocht N, Bergwerf I, Vanhoutte G, Daans J, De Visscher G, Chatterjee S *et al.* Labeling of Luciferase/eGFP-expressing bone marrow-derived stromal cells with fluorescent micron-sized iron oxide particles improves quantitative and qualitative multimodal imaging of cellular grafts in vivo. *Mol Imaging Biol* 2011; **13**: 1133-1145.
7. Praet J, Reekmans K, Lin D, De Vocht N, Bergwerf I, Tambuyzer B *et al.* Cell type-associated differences in migration, survival, and immunogenicity following grafting in CNS tissue. *Cell Transplant* 2012; **21**: 1867-1881.
8. Jung S, Aliberti J, Graemmel P, Sunshine MJ, Kreutzberg GW, Sher A *et al.* Analysis of fractalkine receptor CX(3)CR1 function by targeted deletion and green fluorescent protein reporter gene insertion. *Mol Cell Biol* 2000; **20**: 4106-4114.
9. Tarozzo G, Bortolazzi S, Crochemore C, Chen SC, Lira AS, Abrams JS *et al.* Fractalkine protein localization and gene expression in mouse brain. *J Neurosci Res* 2003; **73**: 81-88.
10. Hughes PM, Botham MS, Frentzel S, Mir A, Perry VH. Expression of fractalkine (CX3CL1) and its receptor, CX3CR1, during acute and chronic inflammation in the rodent CNS. *Glia* 2002; **37**: 314-327.
11. Nishiyori A, Minami M, Ohtani Y, Takami S, Yamamoto J, Kawaguchi N *et al.* Localization of fractalkine and CX3CR1 mRNAs in rat brain: does fractalkine play a role in signaling from neuron to microglia? *FEBS Lett* 1998; **429**: 167-172.
12. Tambuyzer BR, Ponsaerts P, Nouwen EJ. Microglia: gatekeepers of central nervous system immunology. *J Leukoc Biol* 2009; **85**: 352-370.
13. Kim KW, Vallon-Eberhard A, Zigmond E, Farache J, Shezen E, Shakhar G *et al.* In vivo structure/function and expression analysis of the CX3C chemokine fractalkine. *Blood* 2011; **118**: e156-167.
14. Cardona AE, Pioro EP, Sasse ME, Kostenko V, Cardona SM, Dijkstra IM *et al.* Control of microglial neurotoxicity by the fractalkine receptor. *Nat Neurosci* 2006; **9**: 917-924.
1. 15. Cho SH, Sun B, Zhou Y, Kauppinen TM, Halabisky B, Wes P *et al.* CX3CR1 protein signaling modulates microglial activation and protects against plaque-independent cognitive deficits in a mouse model of Alzheimer disease. *J Biol Chem* 2011; **286**: 32713-32722.
15. Huang D, Shi FD, Jung S, Pien GC, Wang J, Salazar-Mather TP *et al.* The neuronal chemokine CX3CL1/fractalkine selectively recruits NK cells that modify experimental autoimmune encephalomyelitis within the central nervous system. *FASEB J* 2006; **20**: 896-905.
16. Fumagalli S, Perego C, Ortolano F, De Simoni MG. CX3CR1 deficiency induces an early protective inflammatory environment in ischemic mice. *Glia* 2013; **61**: 827-842.
17. Donnelly DJ, Longbrake EE, Shawler TM, Kigerl KA, Lai W, Tovar CA *et al.* Deficient CX3CR1 signaling promotes recovery after mouse spinal cord injury by limiting the recruitment and activation of Ly6Clo/iNOS+ macrophages. *J Neurosci* 2011; **31**: 9910-9922.
18. Clark AK, Grist J, Al-Kashi A, Perretti M, Malcangio M. Spinal cathepsin S and fractalkine contribute to chronic pain in the collagen-induced arthritis model. *Arthritis Rheum* 2012; **64**: 2038-2047.

19. Prinz M, Priller J, Sisodia SS, Ransohoff RM. Heterogeneity of CNS myeloid cells and their roles in neurodegeneration. *Nat Neurosci* 2011; **14**: 1227-1235.
20. Ransohoff RM, Cardona AE. The myeloid cells of the central nervous system parenchyma. *Nature* 2010; **468**: 253-262.
21. Costa R, Bergwerf I, Santermans E, De Vocht N, Praet J, Daans J *et al.* Distinct in vitro properties of embryonic and extra?embryonic fibroblast?like cells are reflected in their in vivo behaviour following grafting in the adult mouse brain. *Cell Transplant* 2013.
22. Perry VH, Hume DA, Gordon S. Immunohistochemical localization of macrophages and microglia in the adult and developing mouse brain. *Neuroscience* 1985; **15**: 313-326.
23. Vallieres L, Sawchenko PE. Bone marrow-derived cells that populate the adult mouse brain preserve their hematopoietic identity. *J Neurosci* 2003; **23**: 5197-5207.
24. Mizutani M, Pino PA, Saederup N, Charo IF, Ransohoff RM, Cardona AE. The fractalkine receptor but not CCR2 is present on microglia from embryonic development throughout adulthood. *J Immunol* 2012; **188**: 29-36.
25. Shechter R, London A, Varol C, Raposo C, Cusimano M, Yovel G *et al.* Infiltrating blood-derived macrophages are vital cells playing an anti-inflammatory role in recovery from spinal cord injury in mice. *PLoS Med* 2009; **6**: e1000113.
26. Ajami B, Bennett JL, Krieger C, McNagny KM, Rossi FM. Infiltrating monocytes trigger EAE progression, but do not contribute to the resident microglia pool. *Nat Neurosci* 2011; **14**: 1142-1149.
27. Schilling M, Besselmann M, Leonhard C, Mueller M, Ringelstein EB, Kiefer R. Microglial activation precedes and predominates over macrophage infiltration in transient focal cerebral ischemia: a study in green fluorescent protein transgenic bone marrow chimeric mice. *Exp Neurol* 2003; **183**: 25-33.
28. Mildner A, Schlevogt B, Kierdorf K, Bottcher C, Erny D, Kummer MP *et al.* Distinct and non-redundant roles of microglia and myeloid subsets in mouse models of Alzheimer's disease. *J Neurosci* 2011; **31**: 11159-11171.
29. Mildner A, Mack M, Schmidt H, Bruck W, Djukic M, Zabel MD *et al.* CCR2+Ly-6Chi monocytes are crucial for the effector phase of autoimmunity in the central nervous system. *Brain* 2009; **132**: 2487-2500.
30. Davies LC, Rosas M, Jenkins SJ, Liao CT, Scurr MJ, Brombacher F *et al.* Distinct bone marrow-derived and tissue-resident macrophage lineages proliferate at key stages during inflammation. *Nat Commun* 2013; **4**: 1886.
31. Kierdorf K, Katzmarski N, Haas CA, Prinz M. Bone marrow cell recruitment to the brain in the absence of irradiation or parabiosis bias. *PLoS One* 2013; **8**: e58544.
32. Wolf Y, Yona S, Kim KW, Jung S. Microglia, seen from the CX3CR1 angle. *Front Cell Neurosci* 2013; **7**: 26.
33. Giunti D, Parodi B, Usai C, Vergani L, Casazza S, Bruzzone S *et al.* Mesenchymal stem cells shape microglia effector functions through the release of CX3CL1. *Stem Cells* 2012; **30**: 2044-2053.
34. Baekelandt V, Eggermont K, Michiels M, Nuttin B, Debyser Z. Optimized lentiviral vector production and purification procedure prevents immune response after transduction of mouse brain. *Gene Ther* 2003; **10**: 1933-1940.
35. Geraerts M, Michiels M, Baekelandt V, Debyser Z, Gijsbers R. Upscaling of lentiviral vector production by tangential flow filtration. *J Gene Med* 2005; **7**: 1299-1310.
36. Reekmans K, De Vocht N, Praet J, Le Blon D, Hoornaert C, Daans J *et al.* Quantitative evaluation of stem cell grafting in the central nervous system of mice by in vivo bioluminescence imaging and postmortem multicolor histological analysis. *Methods Mol Biol* 2013; **1052**: 1-17
37. Reekmans K, De Vocht N, Praet J, Fransen E, Le Blon D, Hoornaert C *et al.* Spatiotemporal evolution of early innate immune responses triggered by neural stem cell grafting. *Stem Cell Res Ther* 2012; **3**: 56.

Chapter III

Immune remodelling of stromal cell grafts in the central nervous system: therapeutic inflammation or (harmless) side effect?

3.1. ABSTRACT

Over the past two decades, several cell types with fibroblast-like morphology, including mesenchymal stem/stromal cells, but also other adult, embryonic and extra-embryonic fibroblast-like cells, have been brought forward in the search for cellular therapies to treat severe brain injuries and/or diseases. Although current views in regenerative medicine are highly focused on the immune modulating and regenerative properties of stromal cell transplantation *in vivo*, many open questions remain regarding their true mode of action. In this perspective, we integrate insights gathered over the past 10 years to formulate a unifying model of the cellular events that accompany fibroblast-like cell grafting in the rodent brain. Cellular interactions are discussed step-by-step, starting from the day of implantation up to 10 days after transplantation. During the short period that precedes stable settlement of autologous/syngeneic stromal cell grafts, there is a complex interplay between hypoxia-mediated cell death of grafted cells, neutrophil invasion, microglia and macrophage recruitment, astrocyte activation and neo-angiogenesis within the stromal cell graft site. Consequently, we speculate that regenerative processes following cell therapeutic intervention in the CNS are not only modulated by soluble factors secreted by grafted stromal cells (bystander hypothesis), but also by *in vivo* inflammatory processes following stromal cell grafting.

3.2. INTRODUCTION

During the past two decades, pre-clinical research aiming to cure severe neurological injuries has witnessed a spectacular increase of highly promising experimental therapeutic interventions, jointly referred to as “stem cell therapy” [1]. Various multipotent cell types, including adult mesenchymal stem/stromal cells (MSC) and adult/embryonic/extra-embryonic fibroblast-like cells, are investigated in experimental cellular therapies to overcome the nearly irreversible nature of brain injuries [2, 3]. As *ex vivo* culture-expanded MSC and other fibroblast-like cells (independent of their origin) are phenotypically and functionally indistinguishable they will be referred to as stromal cells further on in this perspective [4-7]. While numerous studies provide evidence for the beneficial effects on neuropathology by stromal cell grafting in the CNS [8-11], to date the true mode of action remains unknown. To shed light on the underlying mechanisms, it is not only necessary to investigate the effects exerted by grafted cells on CNS function/physiology, but it is equally important to focus on the response of the host niche to the cell graft [6, 12-15]. In this perspective, we try to create a new model focusing on the bidirectional interplay of cellular events following stromal cell grafting in the CNS of mice, integrating current literature with our own efforts over the past 10 years.

3.3. IMMUNE REMODELING OF STROMAL CELL GRAFTS IN THE CENTRAL NERVOUS SYSTEM

Although neglected for many years, it is now well established that direct grafting of both autologous (syngeneic) and allogeneic/xenogeneic stromal cells, including MSC and embryonic/extra-embryonic fibroblast-like cells, in brain tissue induces a severe immunological response. While xenogeneic and allogeneic stromal cell grafts become rapidly rejected upon grafting in immune competent hosts [16-18], grafting of syngeneic stromal cells seems to be well tolerated [12, 19, 20] despite complex immune remodeling within and surrounding the graft site [14, 15]. Here, we will provide a step-by-step overview of cellular events that occur following syngeneic stromal cell grafting into brain tissue starting from the day of implantation until 10 days after implantation. We consider this 10-day period to be the most critical time frame for stromal cell grafts to settle in - for them - the non-natural brain environment.

3.3.1. Entry routes to the CNS: stromal cell administration

Several routes of administration can be applied for stromal cell delivery to the (injured) CNS. Although for practical reasons intravenous (iv) injection would be preferred in current clinical settings, this route strongly relies on the original assumption that stromal cells can migrate to the site of injury in the CNS via intrinsic expression of multiple homing receptors [21, 22]. However, various studies have demonstrated that iv administered stromal cells are unable to reach the CNS in sufficient numbers to be of clinical relevance, due to cell retention in lung capillaries, the spleen or lymph nodes [23-25]. Although iv administered stromal cells may exert immune-modulating effects on peripheral immune cells in those retention tissues, only to migrate to the lesion sites in the CNS at a later time point and induce an indirect beneficial effect on neuropathology [26, 27], current clinical trials for multiple sclerosis and amyotrophic lateral sclerosis have not yet provided a proof-of-principle for successful iv administered stromal cell therapy in human pathology. So far, only safety and tolerability of stromal cell injection have been validated by these clinical trials [28-31]. However, several studies comparing various administration routes of stromal cells have observed a superior effect when cells were injected at the targeted location [32-34]. Therefore, potential alternative routes for cell delivery to the injured CNS are intrathecal, intraventricular, intracerebral (comprising multiple regions) or intraspinal injection. Based on our own experience, we will here further discuss the cellular remodeling events following intracerebral implantation of stromal cells (see Figure 1) [35, 12, 36, 15].

3.3.2. The day of intracerebral stromal cell grafting: hypoxic stress

Conceptually, intracerebral injection of a stromal cell suspension consists of a precise slowly timed mechanical injection of minute volumes of cells into the CNS, thereby subtly pushing and possibly damaging the surrounding tissue. Immediately following injection, the stromal cell graft will present itself as a bolus of viable cells entrapped within the host's tissue (Figure 1A) [14]. Due to the absence of blood vessels within the cell graft, the core of the stromal cell graft will be subjected to severe hypoxic stress within the first hours post-grafting (Figure 1B) [14, 13]. Although detrimental for the stromal cell graft itself, this natural feature is not necessarily negative in terms of therapeutic potential, as stromal cells under hypoxic

conditions are known to alter their gene expression and the secretion of paracrine factors [37, 38]. For instance, expression of vascular endothelial growth factor (VEGF) is upregulated, which is involved in the induction of angiogenesis, while secretion of monocyte chemotactic protein-1 (MCP-1), which is involved in the chemotaxis of monocytes towards the site of injury/disease, and matrix metalloproteinase-2 (MMP-2), which is involved in the breakdown of extracellular matrix, is decreased [38]. These hypoxia-induced alterations in gene/protein expression by cellular grafts might possibly act as pro-survival and/or neuro-protective signals for the injured brain [39, 40], although this hypothesis will need further confirmation *in vivo*.

3.3.3. Day 1: Early infiltration of neutrophils

Despite grafted stromal cells reside under hypoxic conditions for the first 24 hours, which may generate a beneficial effect on neuro-repair, it is also well-known that severe oxidative stress on cells will lead to caspase-dependent apoptosis [37]. As a consequence of this hypoxic and most likely also nutrient-deprived environment, 24 hours after cell implantation the core of a stromal cell graft will be highly apoptotic and necrotic, leading to a very early influx of neutrophils (Figure 1C). The influx of neutrophils is by no way surprising as the direct injection of a stromal cell graft in the CNS will inevitably cause a disruption of the blood-brain-barrier in proximity of the graft-site and needle tract, a feature also observed following sham-injection [14]. Whether this disruption is only temporary still needs to be defined. Furthermore, as at this stage a large portion of grafted cells will be apoptotic and necrotic, cell debris in the core of the implant will give rise to a large amount of damage-associated molecular patterns (DAMPs), e.g. heat shock proteins (HSP), ATP, nucleic acids, consequently being an additional driving force for attracting neutrophils [41, 42].

3.3.4. Day 3: Second phase of immune cell invasion and first sign of neo-angiogenesis

By day three post-implantation, neutrophils will have cleared most of the cell debris present within the core of the stromal cell graft. This is also the stage where several major changes will occur within the stromal cell graft in the CNS (Figure 1D). First, the size of the cellular graft will strongly decrease as all necrotic tissue will be cleared, with less than an average of 20% of the initial grafted cell number remaining [12]. Second, once neutrophils have exerted their

phagocytic function, they will start expressing several soluble mediators. These include so-called 'find-me'-signals, which serve as a tracking signal for phagocytic leukocytes, such as microglia and macrophages [42, 43]. Next, neutrophils may be killed via death receptor-induced apoptosis, as both infiltrating macrophages and brain-resident microglia are able to release death receptor ligands, e.g. TNFα and Fas-ligand [44, 43]. In line with this, at day three post-implantation phagocytic leukocytes, microglia and/or macrophages, are abundantly present at the graft site, most likely in order to phagocytose apoptotic neutrophils and/or remaining cellular debris [45, 46]. Note that it is extremely difficult to distinguish between both phagocytic cell populations, especially in wild type mice [47, 48]. Third, while stromal cells can produce VEGF under hypoxic conditions [38], they also produce high levels of VEGF in the presence of pro-inflammatory microglia [6]. Moreover, several other stromal cell-derived factors, including basic fibroblast growth factor (bFGF), angiopoietin-1, MCP-1 may support this process [49, 50]. As a result, the first signs of neo-angiogenesis can be appreciated at this stage by the appearance of endothelial cell structures within the stromal cell graft [6, 14]. Fourth, at this time point a significant increase in GFAP-expression can be noticed around the graft, which implicates the start of astroglial scarring [14]. The process of reactive astrogliosis is known to be triggered by several factors, of which in the case of stromal cell implantation the most important ones are hypoxia, ATP release by damaged cells, ROS and NO production, and cytokines such as IL6, IL10, IL1, TNFα and IFNγ [51]. Altogether, our data demonstrate that the initial remodeling of stromal cell grafts in the CNS is triggered by hypoxia-mediated cell death of grafted cells, which subsequently activates neutrophils, microglia, macrophages, endothelial cells and astrocytes.

3.3.5. Day 7: Astroglial barrier formation

During the following 3-4 days, no major changes can be observed within and surrounding the stromal cell graft, apart from an increasing number of endothelial cells, microglia and/or macrophages [14]. However, at this stage, astroglial scarring around the stromal cell graft becomes stronger (Figure 1E). Plausibly, this is induced through a STAT3-dependent mechanism by the surviving stromal cells as well as the ongoing inflammatory processes, as a comparable situation is observed in spinal cord injury lesions where the astroglial scar surrounds inflammatory and fibrotic cells in a STAT3-dependent manner [52]. We may assume

that the observed astroglial scarring will create an effective barrier to avoid stromal cell migration on the one hand and peripheral inflammatory cell migration into the surrounding brain tissue on the other hand. From a physiological point of view, both suggestions are reasonable as stromal cells and peripheral immune cells are non-natural cells in the healthy CNS, at least in the amount present at the stromal cell graft site.

3.3.6. Day 10: Stabilization of the stromal cell graft

By day 10 post-implantation, the remnant stromal cells become stabilized within their new micro-environment (Figure 1F and Figure 2a). At this stage, neutrophils are no longer present and a clear distinction can be made between blood-derived macrophages mainly within the stromal cell implant and brain-resident microglia mainly surrounding the stromal cell implant, both being separated by an astroglial scar. However, we cannot rule out that a migration of microglia or macrophages through the astroglial scar occurs, since a small percentage of macrophages can be found around the astrocyte barrier. Our study demonstrating this separation, was performed in an eGFP bone marrow transplantation mouse model, in which the origin of 96 ± 2% of $eGFP^+$ macrophages can be claimed as bone-marrow-derived, although we cannot exclude a minority of macrophages being derived from microglia. Nevertheless, our findings demonstrate a clear distinction between both cell types, with the astroglial scar as the visual border [15]. Currently we do not yet know how and why exactly this separation of at one end grafted stromal cells and peripheral macrophages and on the other end brain-resident microglia is established by reactive astrocytes. However, clear parallels can be drawn with natural lesion site remodeling in the CNS. For example, in a mouse model of spinal cord injury, macrophages and microglia are similarly separated by an astroglial scar, with macrophages residing within the astroglial scar and microglia surrounding the lesion site [53]. Another study in a mouse model for TBI demonstrated that there is a temporal difference in the appearance of brain-resident microglia and infiltrating macrophages [54]. These findings indicate that CNS resident microglia and infiltrating blood-borne macrophages contribute differently to neuro-inflammation [55, 56]. Further analysis of macrophages and microglia phenotypes following stromal cell graft remodeling revealed a differential expression pattern of activation markers, like F4/80 and MHCII, on both microglia and macrophages. While graft-infiltrating macrophages express high levels of these activation markers, its expression on

graft-surrounding microglia is highly reduced (Figure 2b). Consequently, this suggests that both cell types are differently activated after stromal cell grafting in the CNS. And certainly their three-dimensional separation (Figure 2c) promotes further investigation of associations between microglia and macrophage phenotype and function during stromal cell graft remodeling and furthermore the influence on, or contribution to, neuroprotection following cell grafting in the CNS.

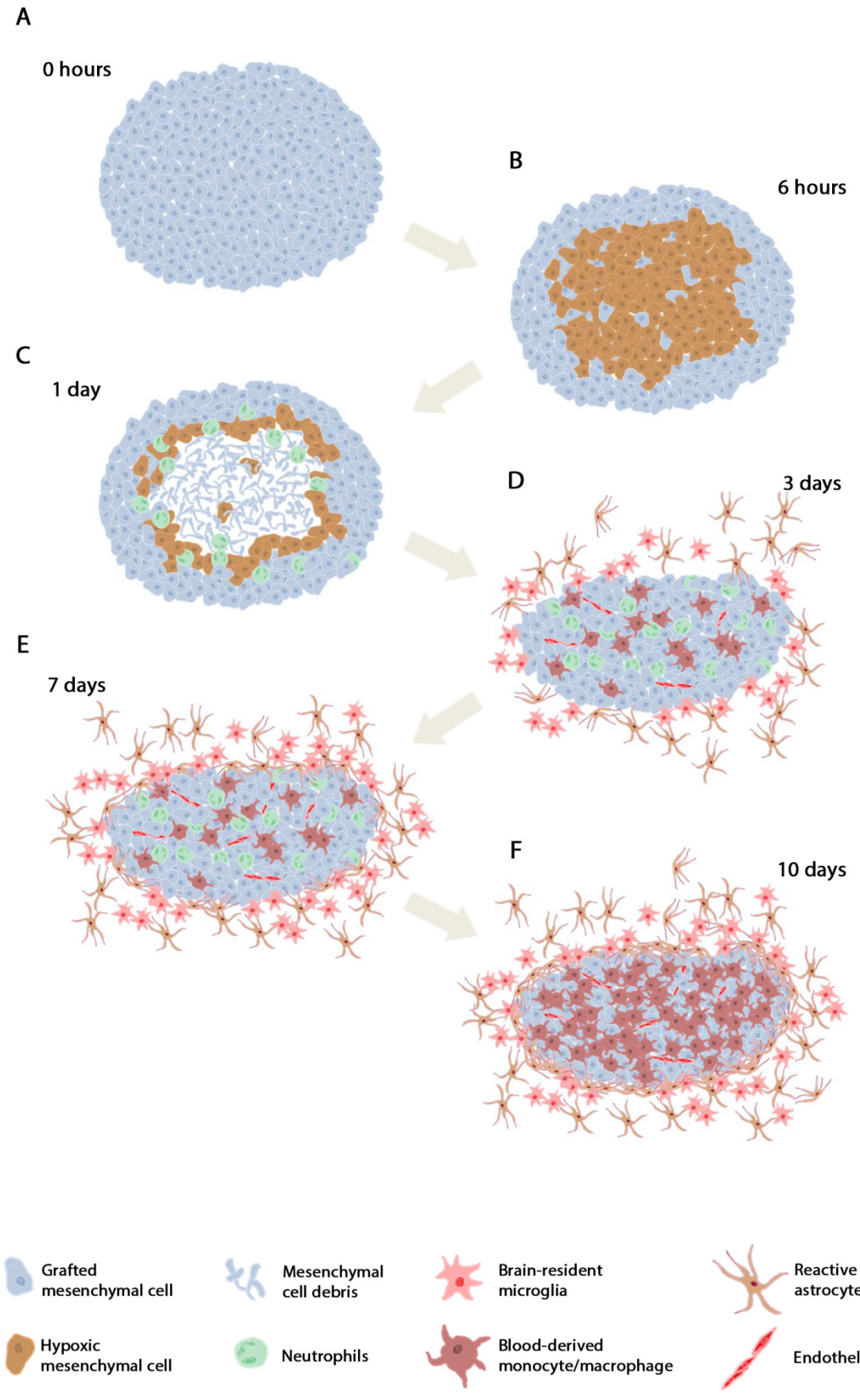
A
0 hours
B
6 hours
C
1 day
D
3 days
E
7 days
F
10 days
Grafted mesenchymal cell
Mesenchymal cell debris
Brain-resident microglia
Reactive astrocytes
Hypoxic mesenchymal cell
Neutrophils
Blood-derived monocyte/macrophage
Endothelial cells

Figure 1. Stromal cell graft-remodeling from day 0 until day 10 after transplantation in the central nervous system.

(A) Representative image of the stromal cell graft site at the moment of transplantation. A bolus of viable stromal cells is present at the site of injection. (B) Representative image of the stromal cell graft site at 6 hours after transplantation. All stromal cells in the dense core have become hypoxic. (C) Representative image of the stromal cell graft site at 24 hours after transplantation. Nearly all hypoxic stromal cells in the core underwent apoptosis or necrosis, leaving a high concentration of stromal cell debris at the core. At this time point the graft is also infiltrated by neutrophils. (D) Representative image of the stromal cell graft site at day 3 after transplantation. The graft has become smaller with only viable stromal cells to remain. At this time point the graft becomes infiltrated by macrophages and surrounded by microglia. Furthermore, astrocytes are surrounding the implant and the first endothelial cells are appearing within the graft. (E) Representative image of the stromal cell graft site at day 7 after transplantation. At this time point more macrophages and microglia accumulate in and around the graft. Furthermore, the astroglial scar surrounding the stromal cell graft has become stronger and blood vessels are in full development. (F) Representative image of the stromal cell graft site at day 10 after transplantation. The implant is completely infiltrated by macrophages and surrounded by microglia. Meanwhile, a very strong barrier is formed around the graft by the astroglial scar. Note that at this stage, neutrophils are no longer present at the stromal cell graft site.

3.4. TOWARDS A UNIFYING THEORY

In the past few years, it has become clear that stromal cell implantation into the (injured) CNS is not trivial. Indeed, assuming that soluble factors secreted by injected stromal cells and/or endogenous cell types invading the graft site will be strong enough to create a bystander effect that positively influences neuro-inflammatory and/or degenerative processes, is overly simplistic. As discussed in this manuscript, the process of stromal cell grafting, but also for other cell types like neural stem/progenitor cells [36, 57], relies on a complex interplay between hypoxia-mediated cell death of grafted cells, neutrophil invasion, microglia and macrophage recruitment, astrocyte activation and neo-angiogenesis at the graft site, ultimately leading to the survival of a limited number of grafted cells. Although the notion that only a small fraction of the initial cell graft is able to survive is well accepted, the immune-remodeling processes occurring after hypoxia-mediated apoptotic death of grafted stromal cells have been largely ignored by most studies. Comprehensibly, reports of inflammatory processes following stromal cell grafting *in vivo*, especially in the CNS, are not in favor of the current assumption that stromal cell grafting is a safe and well-tolerated procedure. However, we believe that it are exactly these inflammatory processes induced by stromal cell grafting that are of substantial importance to the overall observed neuroprotection in animal models of CNS injury. This view is supported by strong evidence in past studies demonstrating that macrophages, key players in the stromal cell graft-induced inflammatory environment, can

contribute to improved disease outcome in animal models of neuropathology when activated in a 'correct'-anti-inflammatory/neuroprotective- way [58, 59]. Therefore, it is certainly worthwhile to study not only the *in vivo* function of stromal cells, but also to reorient interest towards functional properties of stromal cell graft-associated microglia and macrophage responses. This way, stromal cell graft-induced inflammatory responses, currently considered as a harmless side effect, may turn out to be therapeutic inflammation.

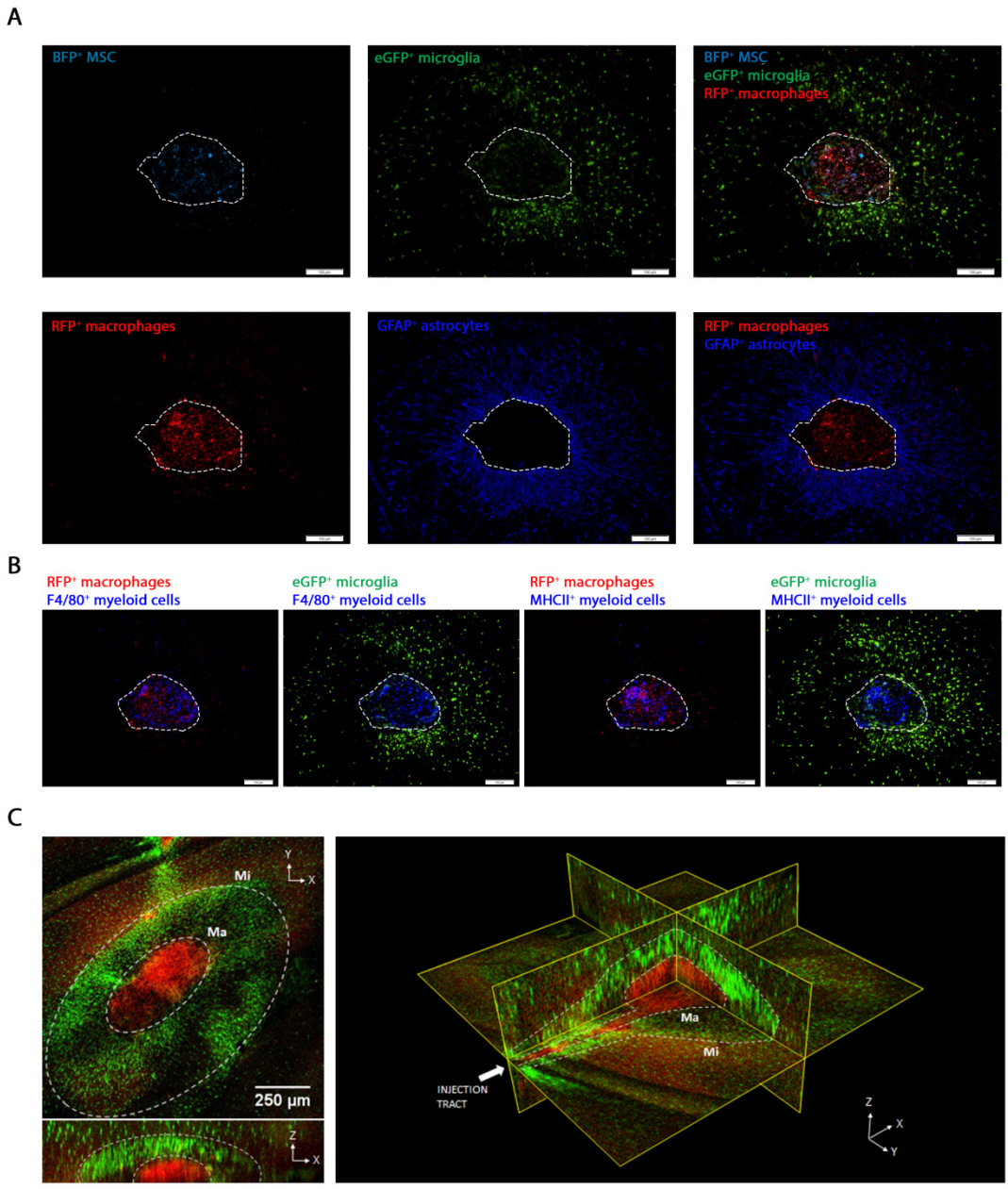

Figure 2. Immunofluorescent images demonstrating important cellular events during stromal cell graft-remodelling.

(A) Representative immunofluorescent images showing the stromal cell graft (light blue), the surrounding microglia (green), the infiltrating macrophages (red) and the astroglial scar (blue) at day 10 after transplantation in the CNS. (B) Representative immunofluorescent images showing the activation of infiltrated macrophages (red) and surrounding microglia (green). The two left images demonstrate F4/80 expression (blue) on macrophages and microglia, signifying a general activation state. The two right images demonstrate MHCII expression (blue) on macrophages and microglia, signifying a more specific activation phenotype. The graft site is delineated by a dotted line in all images. All scale bars indicate 100µm. (C) 3D recording of a cleared CX3CR1-CCR2 brain tissue block (1273 μm^2 x 500 µm) illustrates the invasion of macrophages (Ma) in the centre of the graft site, while microglia (Mi) are only observed surrounding the graft. The injection-tract shows a similar invasion pattern, with macrophages inside the tract, and microglia encapsulating it. A 2D (XY-XZ, left) and 3D (right) orthogonal view are shown.

3.5. REFERENCES

1. Stoltz JF, de Isla N, Li YP, Bensoussan D, Zhang L, Huselstein C et al. Stem Cells and Regenerative Medicine: Myth or Reality of the 21th Century. Stem cells international. 2015;2015:734731. doi:10.1155/2015/734731.
2. Rivera FJ, Aigner L. Adult mesenchymal stem cell therapy for myelin repair in multiple sclerosis. Biological research. 2012;45(3):257-68. doi:10.4067/S0716-97602012000300007.
3. Dulamea AO. The potential use of mesenchymal stem cells in stroke therapy--From bench to bedside. Journal of the neurological sciences. 2015;352(1-2):1-11. doi:10.1016/j.jns.2015.03.014.
4. Hematti P. Mesenchymal stromal cells and fibroblasts: a case of mistaken identity? Cytotherapy. 2012;14(5):516-21. doi:10.3109/14653249.2012.677822.
5. Mueller CG, Coles MC. Emerging immune functions of non-hematopoietic stromal cells. Frontiers in immunology. 2014;5:437. doi:10.3389/fimmu.2014.00437.
6. Costa R, Bergwerf I, Santermans E, De Vocht N, Praet J, Daans J et al. Distinct in vitro properties of embryonic and extraembryonic fibroblast-like cells are reflected in their in vivo behavior following grafting in the adult mouse brain. Cell transplantation. 2015;24(2):223-33. doi:10.3727/096368913X676196.
7. Jones S, Horwood N, Cope A, Dazzi F. The antiproliferative effect of mesenchymal stem cells is a fundamental property shared by all stromal cells. Journal of immunology. 2007;179(5):2824-31.
8. Jaramillo-Merchan J, Jones J, Ivorra JL, Pastor D, Viso-Leon MC, Armengol JA et al. Mesenchymal stromal-cell transplants induce oligodendrocyte progenitor migration and remyelination in a chronic demyelination model. Cell death & disease. 2013;4:e779. doi:10.1038/cddis.2013.304.
9. Yoo SW, Chang DY, Lee HS, Kim GH, Park JS, Ryu BY et al. Immune following suppression mesenchymal stem cell transplantation in the ischemic brain is mediated by TGF-beta. Neurobiology of disease. 2013;58:249-57. doi:10.1016/j.nbd.2013.06.001.
10. Zanier ER, Pischiutta F, Riganti L, Marchesi F, Turola E, Fumagalli S et al. Bone marrow mesenchymal stromal cells drive protective M2 microglia polarization after brain trauma. Neurotherapeutics : the journal of the American Society for Experimental NeuroTherapeutics. 2014;11(3):679-95. doi:10.1007/s13311-014-0277-y.
11. Lee JK, Jin HK, Endo S, Schuchman EH, Carter JE, Bae JS. Intracerebral transplantation of bone marrow-derived mesenchymal stem cells reduces amyloid-beta deposition and rescues memory deficits in Alzheimer's disease mice by modulation of immune responses. Stem cells. 2010;28(2):329-43. doi:10.1002/stem.277.
12. De Vocht N, Lin D, Praet J, Hoornaert C, Reekmans K, Le Blon D et al. Quantitative and phenotypic analysis of mesenchymal stromal cell graft survival and recognition by microglia and astrocytes in mouse brain. Immunobiology. 2013;218(5):696-705. doi:10.1016/j.imbio.2012.08.266.
13. De Vocht N, Praet J, Reekmans K, Le Blon D, Hoornaert C, Daans J et al. Tackling the physiological barriers for successful mesenchymal stem cell transplantation into the central nervous system. Stem cell research & therapy. 2013;4(4):101. doi:10.1186/scrt312.
14. Praet J, Santermans E, Daans J, Le Blon D, Hoornaert C, Goossens H et al. Early inflammatory responses following cell grafting in the CNS trigger activation of the sub-ventricular zone: a proposed model of sequential cellular events. Cell transplantation. 2014. doi:10.3727/096368914X682800.
15. Le Blon D, Hoornaert C, Daans J, Santermans E, Hens N, Goossens H et al. Distinct spatial distribution of microglia and macrophages following mesenchymal stem cell implantation in mouse brain. Immunology and cell biology. 2014;92(8):650-8. doi:10.1038/icb.2014.49.
16. Tambuyzer BR, Bergwerf I, De Vocht N, Reekmans K, Daans J, Jorens PG et al. Allogeneic stromal cell implantation in brain tissue leads to robust microglial activation. Immunology and cell biology. 2009;87(4):267-73. doi:10.1038/icb.2009.12.
17. Ronsyn MW, Daans J, Spaepen G, Chatterjee S, Vermeulen K, D'Haese P et al. Plasmid-based genetic modification of human bone marrow-derived stromal cells: analysis of cell survival and transgene expression after transplantation in rat spinal cord. BMC biotechnology. 2007;7:90. doi:10.1186/1472-6750-7-90.

18. Camp DM, Loeffler DA, Farrah DM, Borneman JN, LeWitt PA. Cellular immune response to intrastriatally implanted allogeneic bone marrow stromal cells in a rat model of Parkinson's disease. Journal of neuroinflammation. 2009;6:17. doi:10.1186/1742-2094-6-17.
19. Praet J, Reekmans K, Lin D, De Vocht N, Bergwerf I, Tambuyzer B et al. Cell type-associated differences in migration, survival, and immunogenicity following grafting in CNS tissue. Cell transplantation. 2012;21(9):1867-81. doi:10.3727/096368912X636920.
20. Coyne TM, Marcus AJ, Reynolds K, Black IB, Woodbury D. Disparate host response and donor survival after the transplantation of mesenchymal or neuroectodermal cells to the intact rodent brain. Transplantation. 2007;84(11):1507-16. doi:10.1097/01.tp.0000288185.09601.4d.
21. Cornelissen AS, Maijenburg MW, Nolte MA, Voermans C. Organ-specific migration of mesenchymal stromal cells: Who, when, where and why? Immunology letters. 2015. doi:10.1016/j.imlet.2015.06.019.
22. Eggenhofer E, Luk F, Dahlke MH, Hoogduijn MJ. The life and fate of mesenchymal stem cells. Frontiers in immunology. 2014;5:148. doi:10.3389/fimmu.2014.00148.
23. Acosta SA, Tajiri N, Hoover J, Kaneko Y, Borlongan CV. Intravenous Bone Marrow Stem Cell Grafts Preferentially Migrate to Spleen and Abrogate Chronic Inflammation in Stroke. Stroke; a journal of cerebral circulation. 2015;46(9):2616-27. doi:10.1161/STROKEAHA.115.009854.
24. Reekmans KP, Praet J, De Vocht N, Tambuyzer BR, Bergwerf I, Daans J et al. Clinical potential of intravenous neural stem cell delivery for treatment of neuroinflammatory disease in mice? Cell transplantation. 2011;20(6):851-69. doi:10.3727/096368910X543411.
25. Jackson JS, Golding JP, Chapon C, Jones WA, Bhakoo KK. Homing of stem cells to sites of inflammatory brain injury after intracerebral and intravenous administration: a longitudinal imaging study. Stem cell research & therapy. 2010;1(2):17. doi:10.1186/scrt17.
26. Morando S, Vigo T, Esposito M, Casazza S, Novi G, Principato MC et al. The therapeutic effect of mesenchymal stem cell transplantation in experimental autoimmune encephalomyelitis is mediated by peripheral and central mechanisms. Stem cell research & therapy. 2012;3(1):3. doi:10.1186/scrt94.
27. Salinas Tejedor L, Berner G, Jacobsen K, Gudi V, Jungwirth N, Hansmann F et al. Mesenchymal stem cells do not exert direct beneficial effects on CNS remyelination in the absence of the peripheral immune system. Brain, behavior, and immunity. 2015. doi:10.1016/j.bbi.2015.06.024.
28. Oh KW, Moon C, Kim HY, Oh SI, Park J, Lee JH et al. Phase I trial of repeated intrathecal autologous bone marrow-derived mesenchymal stromal cells in amyotrophic lateral sclerosis. Stem cells translational medicine. 2015;4(6):590-7. doi:10.5966/sctm.2014-0212.
29. Lublin FD, Bowen JD, Huddlestone J, Kremenchutzky M, Carpenter A, Corboy JR et al. Human placenta-derived cells (PDA-001) for the treatment of adults with multiple sclerosis: a randomized, placebo-controlled, multiple-dose study. Multiple sclerosis and related disorders. 2014;3(6):696-704. doi:10.1016/j.msard.2014.08.002.
30. Martinez HR, Molina-Lopez JF, Gonzalez-Garza MT, Moreno-Cuevas JE, Caro-Osorio E, Gil-Valadez A et al. Stem cell transplantation in amyotrophic lateral sclerosis patients: methodological approach, safety, and feasibility. Cell transplantation. 2012;21(9):1899-907. doi:10.3727/096368911X582769.
31. Prockop DJ, Prockop SE, Bertoncello I. Are clinical trials with mesenchymal stem/progenitor cells too far ahead of the science? Lessons from experimental hematology. Stem cells. 2014;32(12):3055-61. doi:10.1002/stem.1806.
32. Seo SH, Kim KS, Park SH, Suh YS, Kim SJ, Jeun SS et al. The effects of mesenchymal stem cells injected via different routes on modified IL-12-mediated antitumor activity. Gene therapy. 2011;18(5):488-95. doi:10.1038/gt.2010.170.
33. Paul C, Samdani AF, Betz RR, Fischer I, Neuhuber B. Grafting of human bone marrow stromal cells into spinal cord injury: a comparison of delivery methods. Spine. 2009;34(4):328-34. doi:10.1097/BRS.0b013e31819403ce.
34. Moscoso I, Barallobre J, de Ilarduya OM, Anon P, Fraga M, Calvino R et al. Analysis of different routes of administration of heterologous 5-azacytidine-treated mesenchymal stem cells in a porcine model of

myocardial infarction. Transplantation proceedings. 2009;41(6):2273-5. doi:10.1016/j.transproceed.2009.06.011.
35. Bergwerf I, De Vocht N, Tambuyzer B, Verschueren J, Reekmans K, Daans J et al. Reporter gene-expressing bone marrow-derived stromal cells are immune-tolerated following implantation in the central nervous system of syngeneic immunocompetent mice. BMC biotechnology. 2009;9:1. doi:10.1186/1472-6750-9-1.
36. Reekmans K, De Vocht N, Praet J, Fransen E, Le Blon D, Hoornaert C et al. Spatiotemporal evolution of early innate immune responses triggered by neural stem cell grafting. Stem cell research & therapy. 2012;3(6):56. doi:10.1186/scrt147.
37. Zhu W, Chen J, Cong X, Hu S, Chen X. Hypoxia and serum deprivation-induced apoptosis in mesenchymal stem cells. Stem cells. 2006;24(2):416-25. doi:10.1634/stemcells.2005-0121.
38. Page P, DeJong J, Bandstra A, Boomsma RA. Effect of serum and oxygen concentration on gene expression and secretion of paracrine factors by mesenchymal stem cells. International journal of cell biology. 2014;2014:601063. doi:10.1155/2014/601063.
39. Plotnikov EY, Pulkova NV, Pevzner IB, Zorova LD, Silachev DN, Morosanova MA et al. Inflammatory pre-conditioning of mesenchymal multipotent stromal cells improves their immunomodulatory potency in acute pyelonephritis in rats. Cytotherapy. 2013;15(6):679-89. doi:10.1016/j.jcyt.2013.02.003.
40. Tong C, Hao H, Xia L, Liu J, Ti D, Dong L et al. Hypoxia pretreatment of bone marrow-derived mesenchymal stem cells seeded in a collagen-chitosan sponge scaffold promotes skin wound healing in diabetic rats with hindlimb ischemia. Wound repair and regeneration : official publication of the Wound Healing Society [and] the European Tissue Repair Society. 2015. doi:10.1111/wrr.12369.
41. Caielli S, Banchereau J, Pascual V. Neutrophils come of age in chronic inflammation. Current opinion in immunology. 2012;24(6):671-7. doi:10.1016/j.coi.2012.09.008.
42. Vernon PJ, Tang D. Eat-me: autophagy, phagocytosis, and reactive oxygen species signaling. Antioxidants & redox signaling. 2013;18(6):677-91. doi:10.1089/ars.2012.4810.
43. Martin KR, Ohayon D, Witko-Sarsat V. Promoting apoptosis of neutrophils and phagocytosis by macrophages: novel strategies in the resolution of inflammation. Swiss medical weekly. 2015;145:w14056. doi:10.4414/smw.2015.14056.
44. Geering B, Simon HU. Peculiarities of cell death mechanisms in neutrophils. Cell death and differentiation. 2011;18(9):1457-69. doi:10.1038/cdd.2011.75.
45. Denes A, Vidyasagar R, Feng J, Narvainen J, McColl BW, Kauppinen RA et al. Proliferating resident microglia after focal cerebral ischaemia in mice. Journal of cerebral blood flow and metabolism : official journal of the International Society of Cerebral Blood Flow and Metabolism. 2007;27(12):1941-53. doi:10.1038/sj.jcbfm.9600495.
46. Neumann J, Sauerzweig S, Ronicke R, Gunzer F, Dinkel K, Ullrich O et al. Microglia cells protect neurons by direct engulfment of invading neutrophil granulocytes: a new mechanism of CNS immune privilege. The Journal of neuroscience : the official journal of the Society for Neuroscience. 2008;28(23):5965-75. doi:10.1523/JNEUROSCI.0060-08.2008.
47. Durafourt BA, Moore CS, Zammit DA, Johnson TA, Zaguia F, Guiot MC et al. Comparison of polarization properties of human adult microglia and blood-derived macrophages. Glia. 2012;60(5):717-27. doi:10.1002/glia.22298.
48. Hickman SE, Kingery ND, Ohsumi TK, Borowsky ML, Wang LC, Means TK et al. The microglial sensome revealed by direct RNA sequencing. Nature neuroscience. 2013;16(12):1896-905. doi:10.1038/nn.3554.
49. Kinnaird T, Stabile E, Burnett MS, Shou M, Lee CW, Barr S et al. Local delivery of marrow-derived stromal cells augments collateral perfusion through paracrine mechanisms. Circulation. 2004;109(12):1543-9. doi:10.1161/01.CIR.0000124062.31102.57.
50. Watt SM, Gullo F, van der Garde M, Markeson D, Camicia R, Khoo CP et al. The angiogenic properties of mesenchymal stem/stromal cells and their therapeutic potential. British medical bulletin. 2013;108:25-53. doi:10.1093/bmb/ldt031.
51. Sofroniew MV. Molecular dissection of reactive astrogliosis and glial scar formation. Trends in neurosciences. 2009;32(12):638-47. doi:10.1016/j.tins.2009.08.002.

52. Wanner IB, Anderson MA, Song B, Levine J, Fernandez A, Gray-Thompson Z et al. Glial scar borders are formed by newly proliferated, elongated astrocytes that interact to corral inflammatory and fibrotic cells via STAT3-dependent mechanisms after spinal cord injury. The Journal of neuroscience : the official journal of the Society for Neuroscience. 2013;33(31):12870-86. doi:10.1523/JNEUROSCI.2121-13.2013.
53. Zhou X, He X, Ren Y. Function of microglia and macrophages in secondary damage after spinal cord injury. Neural regeneration research. 2014;9(20):1787-95. doi:10.4103/1673-5374.143423.
54. Morganti JM, Jopson TD, Liu S, Riparip LK, Guandique CK, Gupta N et al. CCR2 antagonism alters brain macrophage polarization and ameliorates cognitive dysfunction induced by traumatic brain injury. The Journal of neuroscience : the official journal of the Society for Neuroscience. 2015;35(2):748-60. doi:10.1523/JNEUROSCI.2405-14.2015.
55. Shechter R, Schwartz M. Harnessing monocyte-derived macrophages to control central nervous system pathologies: no longer 'if' but 'how'. The Journal of pathology. 2013;229(2):332-46. doi:10.1002/path.4106.
56. Jung S, Schwartz M. Non-identical twins - microglia and monocyte-derived macrophages in acute injury and autoimmune inflammation. Frontiers in immunology. 2012;3:89. doi:10.3389/fimmu.2012.00089.
57. De Waele J, Reekmans K, Daans J, Goossens H, Berneman Z, Ponsaerts P. 3D culture of murine neural stem cells on decellularized mouse brain sections. Biomaterials. 2015;41:122-31. doi:10.1016/j.biomaterials.2014.11.025.
58. Hu X, Leak RK, Shi Y, Suenaga J, Gao Y, Zheng P et al. Microglial and macrophage polarization-new prospects for brain repair. Nature reviews Neurology. 2015;11(1):56-64. doi:10.1038/nrneurol.2014.207.
59. Corraliza I. Recruiting specialized macrophages across the borders to restore brain functions. Frontiers in cellular neuroscience. 2014;8:262. doi:10.3389/fncel.2014.00262.

Chapter IV

Mouse embryonic fibroblasts genetically engineered to produce interleukin (IL)4/13 or IL10 differentially modulate graft-remodeling in the central nervous system of healthy mice

4.1. ABSTRACT

Neuroinflammation is an important factor involved in nearly all central nervous system (CNS) diseases and traumata, with peripheral macrophages and brain-resident microglia of the adaptive immune response as major key players. Consequently, new therapeutic strategies consist of a forced modulation of classically - pro-inflammatory activated - towards alternatively - anti-inflammatory activated - macrophages/microglia. In the present study, our aim was to investigate whether transplantation of cellular grafts genetically engineered to secrete IL4, IL10 or IL13, are able to modulate the activation state of macrophages/microglia involved in cell graft-remodeling in healthy CNS tissue. For this, enhanced green fluorescent protein (eGFP)-expressing mouse embryonic fibroblasts (MEF) were isolated from C57BL/6-eGFP transgenic mice and transduced with lentiviral vectors encoding IL4, IL10 or IL13. After validation of the transgenic interleukin secretion *in vitro*, MEFs were grafted in healthy CNS of C57BL/6 mice. Results demonstrate: (i) that significant levels of IL4, IL10 and IL13 are secreted by genetically engineered MEF *in vitro*, and (ii) that IL4/13 MEF, but not IL10 MEF, induce high expression of the alternative activation-marker Arginase-1 on MEF graft-infiltrating macrophages following transplantation in the CNS. Based on our own results and those obtained from literature, we suggest IL4 and/or IL13 to be further investigated as a potential new therapeutic approach to counteract pro-inflammatory responses following CNS injury or disease.

4.2. INTRODUCTION

Since neuro-inflammation is an important factor contributing to nearly all central nervous system (CNS) diseases and traumata, a lot of research has been focusing on the modulation of immune responses in the CNS[1-3]. As the infiltration of immune cells involving adaptive immunity, including T- and B-cells, is rather limited in the CNS, macrophages and brain-resident microglia of the innate immune response are often the key players neuropathologies[4-10]. Modulation of the latter has been investigated extensively the last years, leading to the determination of different activation phenotypes in macrophages and microglia. Both cell types can either be classically activated or alternatively activated, depending on the stimulus. Classical, or M1 polarized activation of macrophages, which can be stimulated *in vitro* by adding LPS and/or IFNγ, leads to a pro-inflammatory immune

response. *In vivo*, such M1-activated macrophages create a more cytotoxic and destructive immune environment. The interleukins (IL)4, 10 and 13 are known to induce alternative, or M2 polarized activation of macrophages *in vitro*, leading to anti-inflammatory responses which are able to promote tissue repair and regeneration *in vivo*[11, 12]. In many CNS pathologies, both classically and alternatively activated macrophages/microglia have been described at the lesion sites. However, mainly M1-activated macrophages/microglia tend to have the upper hand in case of neural damage, while the number of M2-activated macrophages/microglia is limited and unable to switch neuro-inflammatory response from a pro-inflammatory towards an anti-inflammatory response[2]. Therefore, a number of new therapeutic strategies aim to force an M1-to-M2 switch in CNS immune responses. In the present study, our aim was to investigate whether: (i) the transplantation of cell grafts, genetically engineered to secrete IL4, IL10 or IL13, is able to modulate the activation state of macrophages/microglia involved in cell graft-remodeling in healthy CNS tissue, and (ii) select the most potent cytokine for further research.

4.3. MATERIALS AND METHODS

4.3.1. Mice

Wild type C57BL/6 mice were obtained via Charles River Laboratories (strain code 027). Transgenic C57BL/6-eGFP mice were obtained via Jackson Laboratories (strain code 003291). During the entire study, mice were kept in the animalarium of the University of Antwerp (UA) under normal day-night cycle (12/12) with free access to food and water. All animal experimental procedures were approved by the Ethics Committee for Animal Experiments of the UA (Approval No 2011–13 and 2012–39).

4.3.2. Lentiviral vector production

The pCHMWS-IL13-IRES-Pac and the pCHMWS-IL4-IRES-Pac LVv plasmids were constructed by replacing the eGFP cDNA insert (SpeI/XbaI digest) from the pCHMWS-eGFP-IRES-Pac plasmid (provided by the Leuven viral vector core, Molmed, KULeuven, Belgium) with the IL13 cDNA or IL4 cDNA (for both NcoI/NheI digest) from the pORF-mIL13 or pORF-mIL4 plasmids (both

from InvivoGen) using standard subcloning techniques. The pCHMWS-IL10-IRES-Pac LVv plasmid was constructed by replacing the eGFP cDNA insert (SpeI/XbaI digest) from the pCHMWS-eGFP-IRES-Pac plasmid with the IL10 cDNA (Sal1/BamH1 digest) from the pNGVL3-mIL10 plasmid (kindly provided by Prof. Roland Tisch, University of North Carolina at Chapel Hill, Chapel Hill, NC, USA) using standard subcloning techniques. Before proceeding to LVv production, the pCHMWS-IL13-IRES-Pac, the pCHMWS-IL4-IRES-Pac and the pCHMWS-IL10-IRES-Pac plasmid were electroporated in K562 cells followed by stable selection by addition of puromycin to the culture medium. Following confirmation of IL13, IL4 or IL10 expression and Pac functionality, LVv production was outsourced to the Leuven viral vector core[13, 14].

4.3.3. Isolation, culture and genetic engineering of MEF

For culture of enhanced green fluorescent protein (eGFP)-MEF, embryos (E14.5) of C57BL/6-eGFP transgenic mice were isolated and liver, spleen and brain were removed. Next, the embryo is dissociated by mechanical trituration until a homogenous cell suspension is achieved. This suspension is then further enzymatically digested by means of trypsin-EDTA (Invitrogen)/ DNAse-1 (1000 Kunitz units/50 ml, Sigma) incubation until a single cell suspension is obtained. The total cell population obtained was plated in a T25 culture flask in 10 ml MEF medium, consisting of DMEM containing L-glutamine (Invitrogen) supplemented with 10% fetal calf serum (FCS, Hyclone), 100 U/ml penicillin (Invitrogen), and 100 mg/ml streptomycin (Invitrogen). For lentiviral transduction of eGFP-MEF, the cells were transduced with the pCHMWS-IL13-IRES-Pac, the pCHMWS-IL4-IRES-Pac or the pCHMWS-IL10-IRES-Pac LV vectors according to previously established procedures[15, 16]. Following puromycin selection, the resulting engineered MEF lines were further named as IL4-, IL10- and IL13-MEF. For normal eGFP-MEF culture, cells were split 1:3 every 4-5 days until passage 7. All cultured MEF were incubated at 37°C and 5% CO_2.

4.3.4. In vitro validation of cytokine secretion by MEF

In order to validate the production of cytokine levels by genetically engineered MEF cell lines, the medium of control MEF, IL4-, IL10- and IL13-MEF cultures was replaced by 15ml of fresh MEF medium 24h prior to injection experiments. When cells were harvested for injections, all

medium was collected and cells were counted. Viability of cells was also measured by flow cytometry before injections, making it possible to calculate interleukin secretion per cell in 24 hours. IL4 (Peprotech), IL10 (eBioScience) and IL13 ELISAs (Peprotech) were performed according to manufacturer's protocols.

4.3.5. Cell implantation experiments

All surgical experiments were performed under sterile conditions, as previously described[17-19]. Briefly, mice were anesthetized by an intraperitoneal injection of a ketamine (80 mg/kg, Pfizer) + xylazine (16 mg/kg, Bayer Health Care) mixture in PBS and placed in a stereotactic frame (Stoelting). A midline scalp incision was made and a hole was drilled in the skull using a dental burr drill (Stoelting) at 2.3mm *dextra* relative to *bregma.* Next, an automatic microinjector pump (kdScientific) with a 10µl Hamilton Syringe was positioned above the exposed *dura*. A 30-gauge needle (Hamilton), attached to the syringe, was placed through the intact *dura* to a depth of 2.3mm. After 2 minutes of pressure equilibration, a suspension of $2x10^5$ MEF in a volume of 2µl was injected. The needle was retracted after another 4 min to allow pressure equilibration and to prevent backflow of the injected cell suspension. Next, the skin was sutured (Vicryl, Ethicon) and 100 µl of a 0.9% NaCl solution (Baxter) was administered subcutaneously in order to prevent dehydration while mice were placed under a heating lamp to recover.

4.3.6. Immunofluorescence analysis

All immunofluorescence analyses were performed according to previously described procedures[17, 19]. Mice were transcardially perfused with 0.9% NaCl solution followed by 4% paraformaldehyde (PFA) solution. Next, brains were isolated and further fixed in 4% PFA for 3h, then dehydrated through a sucrose gradient of 5%, 10% and 20%. Afterwards, brain tissue was snap-frozen in liquid nitrogen and kept at -80°C until further processing. Ten µm-thick cryosections were made using a microm HM500 cryostat. Immunofluorescence staining was performed on brain slides using the following antibody combinations: a primary rabbit anti-Iba1 antibody (1/200; Wako) with a secondary donkey anti-rabbit Alexa Fluor 350 antibody (1/100; Invitrogen). A primary chicken anti-GFAP antibody (1/100; Abcam) with a

secondary donkey anti-chicken DyLight 549 antibody (1/200; Jackson). A primary rat anti-MHCII antibody (1/200; eBioscience) and a secondary goat anti-rat Alexa Fluor 555 antibody (1/200; Invitrogen). A primary goat anti-Arginase 1 antibody (1/50; Santa Cruz) with a secondary donkey anti-goat Alexa Fluor 568 antibody (1/200; Invitrogen).

4.4. RESULTS

4.4.1. Genetically engineered MEF produce high levels of transgenic cytokine in vitro

Before implantation of IL4-, IL10- and IL13-MEF in the CNS of mice, we estimated the secreted level of each cytokine. The produced cytokines were measured in medium collected from the IL4-, IL10-, IL13- and control eGFP-MEF cultures 24h following medium refreshement. Figure 1 shows that IL4-transduced MEF secrete up to 1784 ± 365 ng/ml/2.10^5 cells (figure 1a), IL10-transduced MEF produce 164 ± 5 ng/ml/2.10^5 cells (figure 1b) and IL13-MEF secrete 32 ± 14 ng/ml/2.10^5 cells within 24h (figure 1c). No secretion of IL4, IL10 or IL13 could be detected in control eGFP-MEF (figure 1). These results indicate that genetically engineered MEF provide a substantial source of transgenic interleukin.

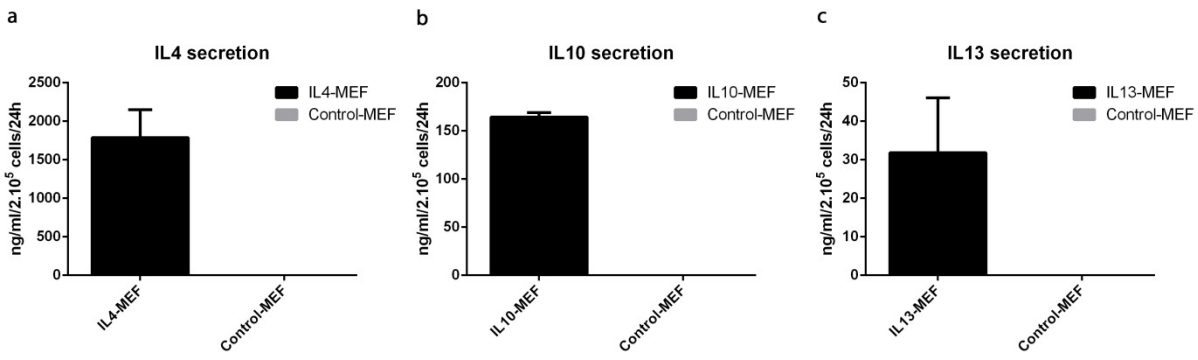

Figure 1. Secretion of IL4, IL10 and IL13 by control, IL4-, IL10- and IL13-MEF *in vitro*.
(a) Graph showing secretion of IL4 by IL4-transduced MEF and control-MEF. (b) Graph showing secretion of IL10 by IL10-transduced MEF and control-MEF. (c) Graph showing secretion of IL13 by IL13-transduced MEF and control-MEF. Error bars indicate standard deviations.

4.4.2. IL4- and IL13-MEF, but not IL10-MEF, induce high levels of M2-marker expression following transplantation in the CNS

Since all genetically engineered MEF lines produced significant levels of the transduced interleukins, the following step was to investigate whether transplantation of IL4- (n=4), IL10- (n=4) or IL13-MEF (n=4) induces changes in graft-remodeling after transplantation in healthy CNS tissue compared to transplantation of control eGFP-MEF (n=4). Ten days post-transplantation, grafts were examined by means of immunofluorescence analysis. In figure 2 representative immunofluorescence images show that all MEF grafts become infiltrated and surrounded by $Iba1^+$ macrophages/microglia, and encapsulated by $GFAP^+$ astrocytes (figure 2, first row). No changes were observed in interleukin-producing MEF compared to control eGFP-MEF. Next, the activation state of macrophages/microglia was examined and mainly showed overall expression of MHCII within the graft site of control and IL10-MEF grafts, while lower expression of MHCII could be observed within the IL4- and IL13-MEF grafts (figure 2, second row). However, more $MHCII^+$ macrophages/microglia were detected surrounding the IL4- and IL13-producing MEF grafts. In order to evaluate whether IL4, IL10 and IL13 are able to induce alternatively activated macrophages/microglia *in vivo*, we stained for M2-marker Arginase1 (arg1). Representative images show that $Arg1^+$ immune cells are abundantly found in and around IL4- and IL13-MEF grafts, while low or no Arg1-expression was observed in IL10- and control MEF grafts (figure 2, third row). These results indicate that differentially activated macrophages/microglia are induced by control, IL10-MEF and IL4/IL13-MEF in healthy CNS.

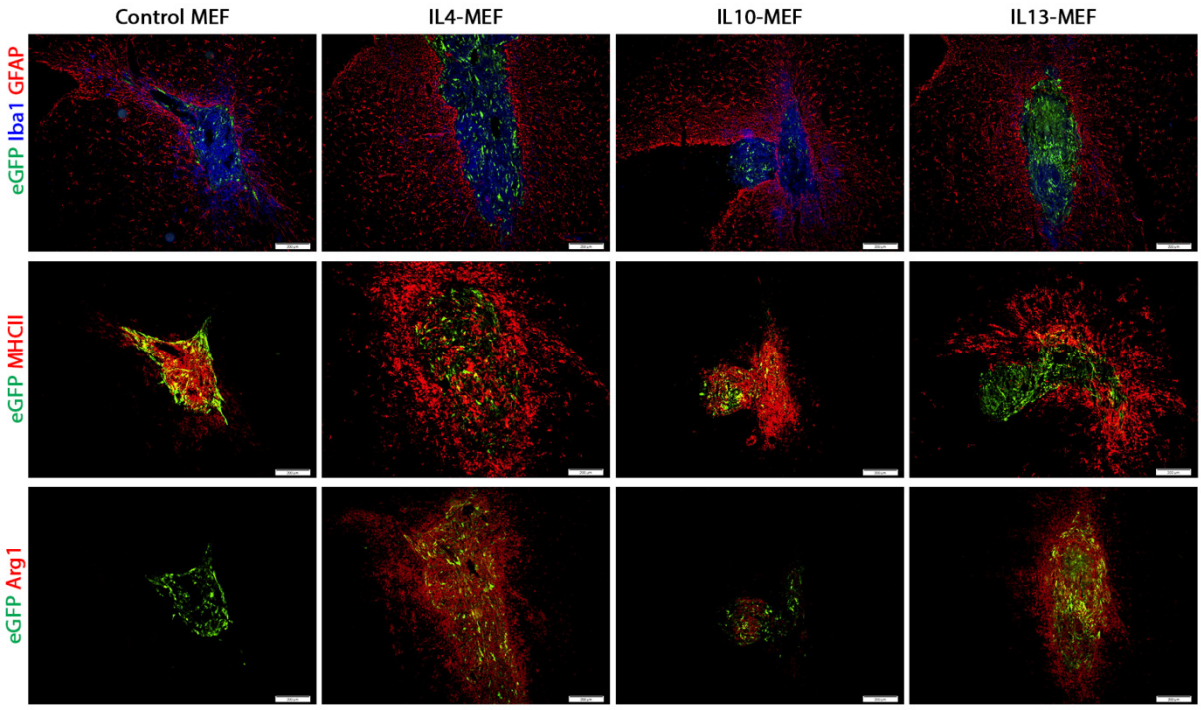

Figure 2. Immunofluorescence analysis reveals differences in M2 activation state of macrophage/microglia in IL4-, IL10- and IL13-MEf grafts in healthy CNS.
Immunofluorescent images of IL4-, IL10- and IL13-producing MEF grafts (green) in healthy CNS tissue. First row: infiltrating and surrounding Iba^+ macrophage/microglia (blue) and surrounding $GFAP^+$ astrogliosis (red). Second row: infiltrating and surrounding $MHCII^+$ activated macrophages/microglia (red). Third row: infiltrating and surrounding Arg^+ M2-activated macrophages/microglia (red). All scale bars indicate 200 µm.

4.5. DISCUSSION

The aim of this intermediate study was to validate the potential of MEF grafts, genetically modified in order to secrete IL4, IL10 or IL13, to induce alternatively activated macrophages and/or microglia in healthy CNS. Results have indicated that both IL4- and IL13-producing MEF grafts are able to induce high expression of the known M2-marker, Arg1, in macrophages and microglia *in vivo*, which is not observed in the case of control or IL10-producing MEF grafts. The appearance of numerous M2-activated macrophages and microglia suggests that an anti-inflammatory environment is created at the graft site of IL4- and IL13-MEF, which might serve as a potential therapeutic approach in neuro-inflammatory diseases. Both IL4 and IL13 induce M2-activated macrophages and microglia *in vivo*, which could be expected when investigating literature on the action of these interleukins on macrophages in vitro[11, 12]. Research has

revealed that the two cytokines are very similar and are closely related members of the short-chain four-helix bundle cytokine family. However, despite similarities between IL4 and IL13, these two interleukins can act differentially on several immune cells. As such, signaling of these cytokines differs according to the type of receptor, i.e. type 1 IL4 receptor (IL4R), binding only IL4, or type 2 IL4R, binding both IL4 and IL13[20]. With regard to immune cells, T-cells express the type 1, but not the type 2 receptor being exclusively responsive to IL4 and not IL13, while macrophages and microglia express both types of the IL4R[20, 21]. For this reason, we suggest that IL13 is more attractive as a therapeutic cytokine in neurologic diseases, more specifically in CNS pathologies with an intrinsic modulatory capacity for innate immunity, without potential influence on the adaptive immune system, as it is unable to influence T-cell responses.

Next to the induction of alternative activation in macrophages and microglia by IL4 and IL13, a prolonged exposure of microglia to IL4 or IL13 can cause death of activated microglia *in vitro*[22, 23]. This effect may be an additional reason to choose IL4 or IL13 over IL10, as chronic microgliosis is often seen as a detrimental feature in many CNS diseases, including Alzheimer's disease, Parkinson's disease, chronic pain, …[24, 25].

4.6. CONCLUSION

Based on our own results and those described by literature, we suggest IL13 should be further investigated as a potential new therapeutic, since it (i) induces alternative activation in macrophages/microglia as shown in this study, (ii) does not signal T-cells as shown by a parallel study in the laboratory, and (iii) is –- able to induce cell death in activated microglia according to literature.

4.7. REFERENCES

1. Cherry JD, Olschowka JA, O'Banion MK. Neuroinflammation and M2 microglia: the good, the bad, and the inflamed. Journal of neuroinflammation. 2014;11:98. doi:10.1186/1742-2094-11-98.
2. Hu X, Leak RK, Shi Y, Suenaga J, Gao Y, Zheng P et al. Microglial and macrophage polarization-new prospects for brain repair. Nature reviews Neurology. 2015;11(1):56-64. doi:10.1038/nrneurol.2014.207.
3. Shechter R, Schwartz M. Harnessing monocyte-derived macrophages to control central nervous system pathologies: no longer 'if' but 'how'. The Journal of pathology. 2013;229(2):332-46. doi:10.1002/path.4106.
4. Benakis C, Garcia-Bonilla L, Iadecola C, Anrather J. The role of microglia and myeloid immune cells in acute cerebral ischemia. Frontiers in cellular neuroscience. 2014;8:461. doi:10.3389/fncel.2014.00461.
5. Yamasaki R, Lu H, Butovsky O, Ohno N, Rietsch AM, Cialic R et al. Differential roles of microglia and monocytes in the inflamed central nervous system. The Journal of experimental medicine. 2014;211(8):1533-49. doi:10.1084/jem.20132477.
6. Morganti JM, Jopson TD, Liu S, Riparip LK, Guandique CK, Gupta N et al. CCR2 antagonism alters brain macrophage polarization and ameliorates cognitive dysfunction induced by traumatic brain injury. The Journal of neuroscience : the official journal of the Society for Neuroscience. 2015;35(2):748-60. doi:10.1523/JNEUROSCI.2405-14.2015.
7. Zhou X, He X, Ren Y. Function of microglia and macrophages in secondary damage after spinal cord injury. Neural regeneration research. 2014;9(20):1787-95. doi:10.4103/1673-5374.143423.
8. Perry VH, Teeling J. Microglia and macrophages of the central nervous system: the contribution of microglia priming and systemic inflammation to chronic neurodegeneration. Seminars in immunopathology. 2013;35(5):601-12. doi:10.1007/s00281-013-0382-8.
9. Girard S, Brough D, Lopez-Castejon G, Giles J, Rothwell NJ, Allan SM. Microglia and macrophages differentially modulate cell death after brain injury caused by oxygen-glucose deprivation in organotypic brain slices. Glia. 2013;61(5):813-24. doi:10.1002/glia.22478.
10. Miron VE, Franklin RJ. Macrophages and CNS remyelination. Journal of neurochemistry. 2014;130(2):165-71. doi:10.1111/jnc.12705.
11. Murray PJ, Allen JE, Biswas SK, Fisher EA, Gilroy DW, Goerdt S et al. Macrophage activation and polarization: nomenclature and experimental guidelines. Immunity. 2014;41(1):14-20. doi:10.1016/j.immuni.2014.06.008.
12. Van Dyken SJ, Locksley RM. Interleukin-4- and interleukin-13-mediated alternatively activated macrophages: roles in homeostasis and disease. Annual review of immunology. 2013;31:317-43. doi:10.1146/annurev-immunol-032712-095906.
13. Baekelandt V, Eggermont K, Michiels M, Nuttin B, Debyser Z. Optimized lentiviral vector production and purification procedure prevents immune response after transduction of mouse brain. Gene therapy. 2003;10(23):1933-40. doi:10.1038/sj.gt.3302094.
14. Geraerts M, Michiels M, Baekelandt V, Debyser Z, Gijsbers R. Upscaling of lentiviral vector production by tangential flow filtration. The journal of gene medicine. 2005;7(10):1299-310. doi:10.1002/jgm.778.
15. Le Blon D, Hoornaert C, Daans J, Santermans E, Hens N, Goossens H et al. Distinct spatial distribution of microglia and macrophages following mesenchymal stem cell implantation in mouse brain. Immunology and cell biology. 2014;92(8):650-8. doi:10.1038/icb.2014.49.
16. Bergwerf I, De Vocht N, Tambuyzer B, Verschueren J, Reekmans K, Daans J et al. Reporter gene-expressing bone marrow-derived stromal cells are immune-tolerated following implantation in the central nervous system of syngeneic immunocompetent mice. BMC biotechnology. 2009;9:1. doi:10.1186/1472-6750-9-1.
17. Praet J, Santermans E, Reekmans K, de Vocht N, Le Blon D, Hoornaert C et al. Histological characterization and quantification of cellular events following neural and fibroblast(-like) stem cell grafting in healthy and demyelinated CNS tissue. Methods in molecular biology. 2014;1213:265-83. doi:10.1007/978-1-4939-1453-1_22.

18. De Vocht N, Reekmans K, Bergwerf I, Praet J, Hoornaert C, Le Blon D et al. Multimodal imaging of stem cell implantation in the central nervous system of mice. Journal of visualized experiments : JoVE. 2012(64):e3906. doi:10.3791/3906.
19. Reekmans K, De Vocht N, Praet J, Le Blon D, Hoornaert C, Daans J et al. Quantitative evaluation of stem cell grafting in the central nervous system of mice by in vivo bioluminescence imaging and postmortem multicolor histological analysis. Methods in molecular biology. 2013;1052:125-41. doi:10.1007/7651_2013_17.
20. Gour N, Wills-Karp M. IL-4 and IL-13 signaling in allergic airway disease. Cytokine. 2015;75(1):68-78. doi:10.1016/j.cyto.2015.05.014.
21. Zurawski G, de Vries JE. Interleukin 13, an interleukin 4-like cytokine that acts on monocytes and B cells, but not on T cells. Immunology today. 1994;15(1):19-26. doi:10.1016/0167-5699(94)90021-3.
22. Yang MS, Park EJ, Sohn S, Kwon HJ, Shin WH, Pyo HK et al. Interleukin-13 and -4 induce death of activated microglia. Glia. 2002;38(4):273-80. doi:10.1002/glia.10057.
23. Won SY, Kim SR, Maeng S, Jin BK. Interleukin-13/Interleukin-4-induced oxidative stress contributes to death of prothrombinkringle-2 (pKr-2)-activated microglia. Journal of neuroimmunology. 2013;265(1-2):36-42. doi:10.1016/j.jneuroim.2013.09.014.
24. Aguzzi A, Barres BA, Bennett ML. Microglia: scapegoat, saboteur, or something else? Science. 2013;339(6116):156-61. doi:10.1126/science.1227901.
25. Gomes-Leal W. Microglial physiopathology: how to explain the dual role of microglia after acute neural disorders? Brain and behavior. 2012;2(3):345-56. doi:10.1002/brb3.51.

Chapter V

Intracerebral transplantation of interleukin 13-producing mesenchymal stem cells limits microgliosis and demyelination in the cuprizone mouse model

5.1. ABSTRACT

Background: Forced alternative activation of neuroinflammation is expected to become a new therapeutic approach for central nervous system (CNS) disorders in which detrimental pro-inflammatory microglia and/or macrophages display a major contribution to the neuropathology. In this study, we present a novel *in vivo* approach using intracerebral grafting of mesenchymal stem cells (MSC) genetically engineered to secrete interleukin 13 (IL13-MSC).

Methods: In the first experimental setup, IL13-MSC were grafted in the *splenium* of the *corpus callosum* of wild type C57BL/6 mice followed by induction of CNS inflammation and demyelination by means of a cuprizone supplemented diet. Next, the influence of IL13-MSC grafting on neuropathological alterations was monitored by non-invasive T_2-weighted magnetic resonance imaging (MRI) and quantitative histological analyses. In order to attribute a specific role to microglia and macrophages, the same experiment was repeated in $CX_3CR1^{eGFP/+}CCR2^{RFP/+}$ transgenic C57BL/6 mice allowing histological discrimination of microglia and macrophages. In the second experimental setup, IL13-MSC were grafted in the CNS of $eGFP^+$ bone marrow chimeric C57BL/6 mice and expression of several markers associated with alternative activation was analysed on MSC graft-recognizing microglia and MSC graft-infiltrating macrophages.

Results: In the first part of this study, we demonstrate that grafting of IL13-MSC, as compared to grafting of control MSC, protects against cuprizone-induced microgliosis and demyelination. In the second part of this study, we demonstrate that MSC graft-associated microglia and MSC graft-infiltrating macrophages are forced into alternative activation upon grafting of IL13-MSC, but not upon grafting of control MSC.

Conclusion: Our study suggests that controlled and localized production of IL13 by means of intracerebral MSC grafting at the onset of neuroinflammation has the potential to modulate cell-graft and pathology-associated microglial/macrophage immune responses and demyelinating events.

5.2. INTRODUCTION

Detrimental inflammatory responses in the central nervous system (CNS) are a hallmark of various neurodegenerative pathologies, with multiple sclerosis (MS), stroke and traumatic brain or spinal cord injury being excellent examples of the complex interplay between CNS-resident microglia and lesion-infiltrating leukocytes[1-4]. Although microglia and CNS-invading peripheral monocytes both act as phagocytic cells of the brain, it is currently becoming accepted that these two cell types are more distinct than generally assumed[2, 5]. This is supported by observations in various models of neuroinflammation in which microglia and bone marrow (BM)-derived macrophages may be present at different time points, may have a different spatial distribution and – more importantly – may display different functions and/or phenotypes during the course of neuroinflammation and neurodegeneration[5]. Nevertheless, in the early stage of neuroinflammatory responses, lesion-associated microglia and/or macrophages are generally described as "classically activated", i.e. displaying a phenotype and function comparable to *in vitro* LPS- and/or IFNγ-activated macrophages[6]. From an emerging therapeutic point of view, it is suggested that forced "alternative activation" of lesion associated microglia and/or macrophages during the development of inflammatory responses can have a beneficial effect on disease outcome[5]. Although dependent on the stimuli applied, several directions of alternative macrophage activation can be achieved *in vitro* and *in vivo [6]*. In this study, we aimed to investigate the potential of interleukin 13 (IL13) [7] to modulate microglia and/or macrophage activation *in vivo* in an attempt to influence pathology-associated neuroinflammation.

One of the major challenges in current CNS immunomodulation research is how to effectively deliver therapeutic proteins (in casu IL13) directly to the site of neuroinflammation. While several methods of delivery can be implemented[8], including (i) direct protein injection, (ii) non-viral and viral gene therapy, and (iii) implantation of genetically engineered cellular grafts, each of them has specific advantages and disadvantages. Whereas direct protein injection would be the most straightforward, it would require multiple injections as - in case of IL13 – sustained therapeutic protein expression may be essential. Alternatively, mechanical or chemical methods (e.g. electroporation, ultrasound or lipoplexes) may be applied to transfer plasmid DNA encoding the therapeutic protein of interest into inflammatory cells at the site of neuroinflammation. Nevertheless, these techniques are still poorly efficient and need

further optimisation for *in vivo* application. Gene transfer in the CNS by means of viral vectors, on the other hand, is highly efficient in rodents, but for obvious reasons, remains controversial in terms of clinical translation to humans. Lastly, transplantation of genetically engineered (stem) cell populations is an emerging methodological approach for *in situ* delivery of therapeutic proteins[9, 10]. Preceding work by our group has already extensively compared the *in vivo* behaviour of neural stem cell (NSC) and mesenchymal stem/stromal cell (MSC) grafts upon implantation in the CNS of mice[11-16]. Based on our published reports, we have a strong preference for MSC as a cellular carrier to deliver therapeutic proteins due to their relatively easy *ex vivo* culture, susceptibility for genetic modification and their more robust survival upon grafting in CNS tissue compared to NSC. In this study we aim to investigate whether *in situ* grafting of MSC genetically engineered to express IL13 can influence neuroinflammatory responses, both on the level of cell graft-associated inflammatory responses, as well as on the level of pathology-associated inflammatory responses.

In order to address these questions, we investigated the behaviour of control MSC and IL13-expressing MSC grafts both under healthy and under inflammatory CNS conditions. For the latter, we used the well-established cuprizone (CPZ) mouse model of CNS inflammation, oligodendrocyte death and subsequent demyelination[17]. Furthermore, in order to separately investigate the behaviour of brain-resident microglia and CNS-invading peripheral macrophages, the majority of the experiments presented in this study were performed in the $CX_3CR1^{eGFP/+}$ $CCR2^{RFP/+}$ transgenic mouse model or in $eGFP^+$ bone marrow (BM) chimeric mice.

5.3. MATERIALS AND METHODS

5.3.1. Mice

Wild type C57BL/6 mice were obtained via Charles River Laboratories (strain code 027). Transgenic C57BL/6-eGFP mice (strain code 003291), $CX_3CR1^{eGFP/eGFP}$ mice (strain code 005582) and $CCR2^{RFP/RFP}$ mice (strain code 017586) were obtained via Jackson Laboratories. $CX_3CR1^{eGFP/+}$ $CCR2^{RFP/+}$ mice were obtained by breeding $CX_3CR1^{eGFP/eGFP}$ mice with $CCR2^{RFP/RFP}$ mice. During the entire study, mice were kept in the animalarium of the University of Antwerp (UA) under normal day-night cycle (12/12) with free access to food and water. All animal

experimental procedures were approved by the Ethics Committee for Animal Experiments of the UA (Approval No 2011–13 and 2012–39).

5.3.2. Lentiviral vector (LVv) production

The pCHMWS-IL13-IRES-Pac LVv plasmid was constructed by replacing the eGFP cDNA insert (SpeI/XbaI digest) from the pCHMWS-eGFP-IRES-Pac plasmid (provided by the Leuven viral vector core, Molmed, KULeuven, Belgium) with the IL13 cDNA (NcoI/NheI digest) from the pORF-mIL13 plasmid (InvivoGen) using standard subcloning techniques. Before proceeding to LVv production, the pCHMWS-IL13-IRES-Pac plasmid was electroporated in K562 cells followed by stable selection by addition of puromycin to the culture medium. Expression of IL13 was confirmed by a murine IL13 ELISA (Peprotech) using the supernatant of stably transfected puromycin-resistant K562 cells. Following confirmation of IL13 expression and Pac functionality, LVv production was outsourced to the Leuven viral vector core[18, 19].

5.3.3. Culture and genetic engineering of MSC

In this study, we used a previously established and characterized C57BL/6 mouse BM-derived MSC line (further named as parental MSC)[20] and a derivative thereof, genetically engineered to express the blue fluorescent protein (further named as BFP-MSC)[13]. For expansion, both MSC lines were cultured in standard cell culture plasticware (well plates and/or culture flasks) in 'complete expansion medium' (CEM)[21] consisting of Iscove's modified Dulbecco's medium (IMDM; Lonza) supplemented with 8% fetal bovine serum (FBS; Invitrogen), 8% horse serum (HS; Invitrogen), 200U/mL + 100µg/mL penicillin/streptomycin (Invitrogen) and 1µg/mL amphotericin B (Invitrogen). Culture medium for BFP-MSC was further supplemented with 1µg/mL puromycin (InvivoGen). MSC cultures were split 1:5 twice a week using 0.05% trypsin-EDTA (Invitrogen) for cell detachment. Both the parental MSC line and the BFP-MSC line were transduced with the pCHMWS-IL13-IRES-Pac LVv, according to previously optimized procedures[21, 13]. Following puromycin selection, the resulting engineered MSC lines were further named as IL13-MSC and IL13/BFP-MSC. Culture medium for both IL13-MSC and IL13/BFP-MSC was further supplemented with 5µg/mL puromycin. IL13-MSC were used in two experiments and IL13/BFP-MSC were used in one experiment out of three in the cuprizone

mouse model. To avoid confusion, both IL13-producing cell lines will be referred to as IL13-MSC further in text.

5.3.4. Bone marrow transplantation experiments

In order to discriminate between microglia and macrophages, $eGFP^+$ BM chimeric mice were generated as previously described[13]. Briefly, wild type C57BL/6 mice received 10Gy total body irradiation using an XRAD320 small animal irradiation device (Precision X-Ray). For this, groups of five non-anesthetised mice were placed in a single cage within the whole irradiation field (without head protection). Six hours post-irradiation, a single intravenous injection of total $eGFP^+$ BM cells ($1.5x10^6$ cells in 100µl phosphate buffered saline) was administered via the tail vein. Total BM cells were isolated from 8-week old C57BL/6-eGFP mice by flushing dissected femurs and tibias with sterile phosphate buffered saline (PBS). Before administration, total BM cells were filtered over a 70 µm sterile mesh (Becton Dickinson), centrifuged and suspended in PBS. During recovery, mice were treated with Enrofloxacin (1µl/mL; Baytril 10%; Bayer) added to the drinking water for 8 weeks post-irradiation.

5.3.5. Cell implantation experiments

All surgical experiments were performed under sterile conditions, as previously described[22-24]. Briefly, mice were anesthetized by an intraperitoneal injection of a ketamine (80 mg/kg, Pfizer) + xylazine (16 mg/kg, Bayer Health Care) mixture in PBS and placed in a stereotactic frame (Stoelting). A midline scalp incision was made and a hole was drilled in the skull using a dental burr drill (Stoelting) at the following coordinates relative to *bregma*:(i) 0.3mm *dextra* and 1.6mm *posterior* for injections in CPZ-treated mice, or (ii) 2.3mm *dextra* for injections in healthy mice. Next, an automatic microinjector pump (kdScientific) with a 10µl Hamilton Syringe was positioned above the exposed *dura*. A 30-gauge needle (Hamilton), attached to the syringe, was placed through the intact *dura* to a depth of 1.3mm in CPZ-treated mice (directly within the right side of the *splenium* of the *corpus callosum)* and to a depth of 2.3mm for injections in healthy mice (directly underneath the *capsula externa*). After 2 minutes of pressure equilibration, a suspension of $2x10^4$ MSCs in a volume of 0.4µl was injected in CPZ-treated mice or a suspension of $2x10^5$ MSCs in a volume of 2µl was injected in healthy mice.

The needle was retracted after another 4 min to allow pressure equilibration and to prevent backflow of the injected cell suspension. Next, the skin was sutured (Vicryl, Ethicon) and 100 µl of a 0.9% NaCl solution (Baxter) was administered subcutaneously in order to prevent dehydration while mice were placed under a heating lamp to recover.

5.3.6. Cuprizone (CPZ) mouse model

For induction of CNS inflammation and demyelination, mice received standard rodent chow mixed with 0.2% w/w CPZ (Sigma-Aldrich) for 4 weeks between the ages of 8 and 12 weeks, as previously described[25, 14, 26, 27].

5.3.7. Magnetic resonance imaging acquisition

In vivo imaging experiments were conducted at 400 MHz on a 9.4T Bruker Biospec system (Biospec 94/20 USR, Bruker Biospin) using a standard Bruker cross coil setup, with a quadrature volume coil for excitation and quadrature mouse surface coil for signal detection. During imaging, mice were anesthetized using 2% isoflurane (Isoflo®, Abbot Laboratories Ltd.) in a mixture of 30% O_2 and 70% N_2O at a flow rate of 600 ml/min. Mice were fixed in an animal restrainer with ear bars and a tooth bar. Respiratory rate was continuously monitored and body temperature was measured and maintained constant at 37°C using a feedback coupled warm air system (MR compatible Small Animal Monitoring and Gating System, SA instruments, Inc.). T_2 values were acquired with the Multi-Slice, Multi-Echo (MSME) sequence that is based on the Carr-Purcell-Meiboom-Gill (CPMG) sequence, where transverse magnetization of a 90º pulse is refocused by a train of 180º pulses generating a series of echoes. The following imaging parameters were used: number of averages (NA) = 1; number of slices (NS) = 6 with a slice thickness of 0.4mm and an interslice thickness of 0.4mm; number of echoes = 10 with echo spacing = 8.5ms (echo times (TE) being 8.5; 17; 25.5; 34; 42.5; 51; 59.5; 68; 76.5; 85); a repetition time (TR) = 4000ms; field of view (FOV) = 2.0 x 2.0cm; matrix size = 256 x 256 (this yields an effective in-plane resolution of 0.078 x 0.078 mm). The total acquisition time per analysis was 12 min 48 seconds.

5.3.8. Magnetic resonance imaging processing

T_2 maps were generated with custom-built programs written in MATLAB (MATLAB R2011b, The MathWorks Inc.) using a monoexponential fit function [$y= A+C*\exp(-t/T_2)$], where A = Absolute bias, C = signal intensity, T_2 = transverse relaxation time. Regions of interest (ROIs) were drawn manually on the T_2-weighted images, according to a mouse brain atlas, with AMIRA software (Mercury Computer systems) and regional average T_2 values were calculated. ROIs included the external capsule (EC) and the *splenium* of the *corpus callosum* (CC), which was further divided in two parts in respect to the brain's midline, and later referred as the right and the left side of the *splenium*.

5.3.9. Immunofluorescence analysis

All immunofluorescence analyses were performed according to previously described procedures[22, 23]. Mice were transcardially perfused with 0.9% NaCl solution followed by 4% paraformaldehyde (PFA) solution. Next, brains were isolated and further fixed in 4% PFA for 3h, then dehydrated through a sucrose gradient of 5%, 10% and 20%. Afterwards, brain tissue was snap-frozen in liquid nitrogen and kept at -80°C until further processing. Ten µm-thick cryosections were made using a microm HM500 cryostat. Immunofluorescence staining was performed on brain slides using the following antibody combinations: a primary goat anti-MBP antibody (10µg/ml, Santa Cruz, sc-13914) with a secondary donkey anti-goat Alexa Fluor 350 antibody (20µg/ml, Invitrogen,A21081); a primary rabbit anti-Iba1 antibody (1µg/ml, Wako, 019-19741) with a secondary donkey anti-rabbit Alexa Fluor 555 (2µg/ml, Invitrogen, A31572); a primary rabbit anti-GFAP antibody (4.5µg/ml, Abcam, ab7779) with a secondary donkey anti-rabbit Alexa Fluor 555 antibody; a primary rat anti-F4/80 antibody (4µg/ml, AbD serotec, MCA497R) with a secondary goat anti-rat Cy5 antibody (10µg/ml, Invitrogen, A10525); a primary rat anti-MHCII antibody (2.5µg/ml, eBioscience, 14-5321-82) with a secondary goat anti-rat Alexa Fluor 555 or goat anti-rat Alexa Fluor 350 antibody (10µg/ml, Invitrogen, A21093); a primary goat anti-Arg1 antibody (4µg/ml, Santa Cruz, sc-18354) with a secondary donkey anti-goat Alexa Fluor 555 (10µg/ml, Invitrogen, A21432) or donkey anti-goat Cy5 antibody (10µg/ml, Abcam, AB6566).

5.3.10. Histological quantification

Quantitative analyses of microglial inflammation and/or demyelination in the cuprizone mouse model were performed using NIH ImageJ analysis software (v1.47), according to previously established procedures [13, 15, 23]. The following parameters were determined for the whole *splenium*, the right side of the *splenium* and the left side of the *splenium*: (i) percentage of eGFP coverage (3 slides per mouse brain analysed), and (ii) percentage of MBP coverage (3 slides per mouse brain analysed). Quantitative analyses of macrophage and/or microglia responses were performed using TissueQuest immunofluorescence analysis software (TissueGnostics GmbH, v3.0), as previously described by our group [12, 13, 15, 23]. For each of the slides analysed, the graft site was manually delineated based on nuclear TOPRO-3 staining. The graft site border was then determined as a region extending 85µm from the MSC graft site. According to previously established procedures, the following parameters were determined for the MSC graft site and the MSC graft site border in $eGFP^+$ bone marrow chimeric mice: the cellular density of (i) $eGFP^+$ macrophages (3 slides per cell graft analysed), (ii) $MHCII^+$ $eGFP^+$ macrophages (1 slide per cell graft analysed), (iii) $Arg1^+$ $eGFP^+$ macrophages (1 slide per cell graft analysed), (iv) $Iba1^+$ cells (1 slide per graft analysed) and (v) $MHCII^+$ $Arg1^+$ cells (1 slide per cell graft analysed).

5.3.11. Statistical analyses

For the results obtained in the cuprizone mouse model, the following statistical analyses were applied: (i) Comparison of mean T_2-relaxation times of the left, right and whole *splenium* of the CC, and the EC between healthy mice, CPZ-treated mice, BFP-MSC grafted CPZ-treated mice and IL13-MSC grafted CPZ-treated mice were analysed using a two-way ANOVA, with the obtained p-values being corrected for multiple testing using the Tukey HSD post-hoc test. (ii) Comparisons of the percentages of eGFP and MBP coverage in the left, right and whole *splenium* of $CX_3CR1^{eGFP/+}$ $CCR2^{RFP/+}$ mice between healthy mice, CPZ-treated mice, BFP-MSC grafted CPZ-treated mice and IL13 -MSC grafted CPZ-treated mice were analysed by using GEE, with the given p-values being corrected for multiple testing using the false discovery rate method. (iii) The dependence between eGFP and MBP coverage percentage, eGFP coverage percentage and T_2 relaxation times, MBP coverage percentage and T_2 relaxation times was

measured using the Spearman's correlation coefficient. A bootstrap procedure was used to construct 95% confidence intervals. Correlation coefficients and confidence intervals are stated in the results section. All of the above data and/or analyses are presented either in dot plots or in graphs showing mean + standard deviation. A p-value of <0.05 was considered statistically significant. All significant p-values are stated in the results section. For the results obtained in healthy eGFP+ bone marrow chimeric mice, the following statistical analyses were applied: (i) Differences in cellular density of $eGFP^+$ macrophages within the implant site and the implant border of BFP-MSC and IL13-MSC grafts were analysed using generalized estimating equations (GEE) [28, 29]. (ii) Differences in cellular density of MHCII- and Arg1-expressing $eGFP^-$ microglia and $eGFP^+$ macrophages within the implant site and the implant border of BFP-MSC and IL13-MSC grafts were analysed using Wilcoxon tests. For both analyses, the given p-values were corrected for multiple testing using the false discovery rate method [30].

5.4. RESULTS

5.4.1. Non-invasive T_2-weighted MRI reveals a neuroprotective effect against CPZ-induced CNS inflammation and demyelination following grafting of IL13-producing MSC

In the first part of this study, we investigated whether grafting of IL13-producing MSC could influence neuro-inflammatory responses. For this, we performed three independent experiments of which the details of employed mouse strains (wt C57BL/6 or C57BL/6 $CX_3CR1^{eGFP/+}$ $CCR2^{RFP/+}$ mice), grafted cell types (BFP-MSC, IL13-MSC or IL13/BFP-MSC) and size of the different experimental groups (healthy control, CPZ control, CPZ + BFP-MSC and CPZ + IL13-MSC) are provided in table 1. Experimentally, eight-week old mice received a BFP-MSC or an IL13-MSC graft at the right side of the *splenium* of the *corpus callosum* followed by a four-week CPZ-supplemented diet. Healthy control mice were kept on normal rodent diet for four weeks, while CPZ control mice received a four-week CPZ-supplemented diet without undergoing surgical intervention. At the age of 12 weeks, T_2-weighted MRI was applied to non-invasively measure CPZ-induced inflammation and demyelination in the *splenium* and the *external capsule* (EC, internal control region)[31]. As no significant differences in the calculated T_2 relaxation times for the *splenium* and the EC were found between wt C57BL/6

(used in experiments 1 and 2) and C57BL/6 $CX_3CR1^{eGFP/+}$ $CCR2^{RFP/+}$ mice (used in experiment 3), under both healthy conditions as well as under CPZ treatment, data from all three experiments were used to increase power in further statistical analyses (figure 1a and 1b, experiment 2 versus experiment 3, healthy control and CPZ control). When comparing the calculated T_2 relaxation time for the whole *splenium* (both right and left side of the midline) and the whole EC (both right and left side) from healthy control mice and non-injected CPZ-treated mice (CPZ control), it is clear that CPZ treatment causes a significant increase of the T_2 relaxation time in both brain regions (figure 1a and 1b, for both $p<0.0001$). This can also be noted on the representative MRI images provided where hyperintensity regions were seen in the *splenium* and EC of CPZ control mice, a finding not observed in healthy control mice (figure 1a and 1b). When comparing the T_2 relaxation times of the whole *splenium* in BFP-MSC with IL13-MSC grafted mice, data indicate that T_2 relaxation times of IL13-MSC grafted mice, but not of BFP-MSC grafted mice, deviate significantly less from healthy control values compared to those obtained from CPZ-treated mice (figure 1a, CPZ control versus CPZ + IL13-MSC, $p=0.0007$). This is indicative of reduced inflammation and demyelination in the *splenium* of IL13-MSC grafted mice. The latter can also be noted on the representative MRI images provided in figure 1a, where the *splenium* in IL13-MSC grafted mice displays less hyperintensity as compared to CPZ control mice. The observation that T_2 relaxation times of the EC remained high and were not significantly different from those obtained in CPZ control mice (figure 1b), indicates that the observed protective effect following grafting of IL13-MSC is due to the performed cell therapeutic intervention and does not result from model failure and/or model variation. Of note, we observed in some of the BFP-MSC grafted mice that this procedure might have led to neuroprotection. However, as this was only observed in part of the mice from one out of three MRI experiments, the results convince that IL13-MSC grafting is superior to control BFP-MSC grafting in establishing protection against inflammation and demyelination in the whole *splenium.* Further analyses over the right and left side of the *splenium*, T_2-weighted MRI data indicate that the protective effect of grafting IL13-expressing MSC is of higher significant importance on the right side of the *splenium* ($p<0.0001$) as compared to the left side of the *splenium* ($p=0.01$) (figure 2).

Exp.	Mouse strain	Cell graft	Healthy control	CPZ control	CPZ + BFP-MSC	CPZ + IL13-MSC
1	C57BL/6 wt	BFP-MSC IL13-MSC	-	-	n = 5	n = 7
2	C57BL/6 wt	BFP-MSC IL13-MSC	n = 10	n = 10	n = 10	n = 10
3	C57BL/6 $CX_3CR1^{eGFP/+}CCR2^{RFP/+}$ tg	BFP-MSC IL13/BFP-MSC*	n = 6	n = 6	n = 5	n = 7
TOTAL number of mice			**n = 16**	**n = 16**	**n = 20**	**n = 24**

Table 1. Experimental outline of the three comparative cell grafting experiments performed in the cuprizone (CPZ) mouse model. Exp: Experiment; wt: wild type, tg: transgenic; MSC: mesenchymal stem cell; BFP-MSC: blue fluorescent protein-expressing MSC; IL13-MSC: interleukin 13-expressing MSC; IL13/BFP-MSC: IL13 + BFP-expressing MSC; n: number of mice. * To avoid confusion, both IL13-producing cell lines, IL13- and IL13/BFP-MSC, will be referred to as IL13-MSC further in text.

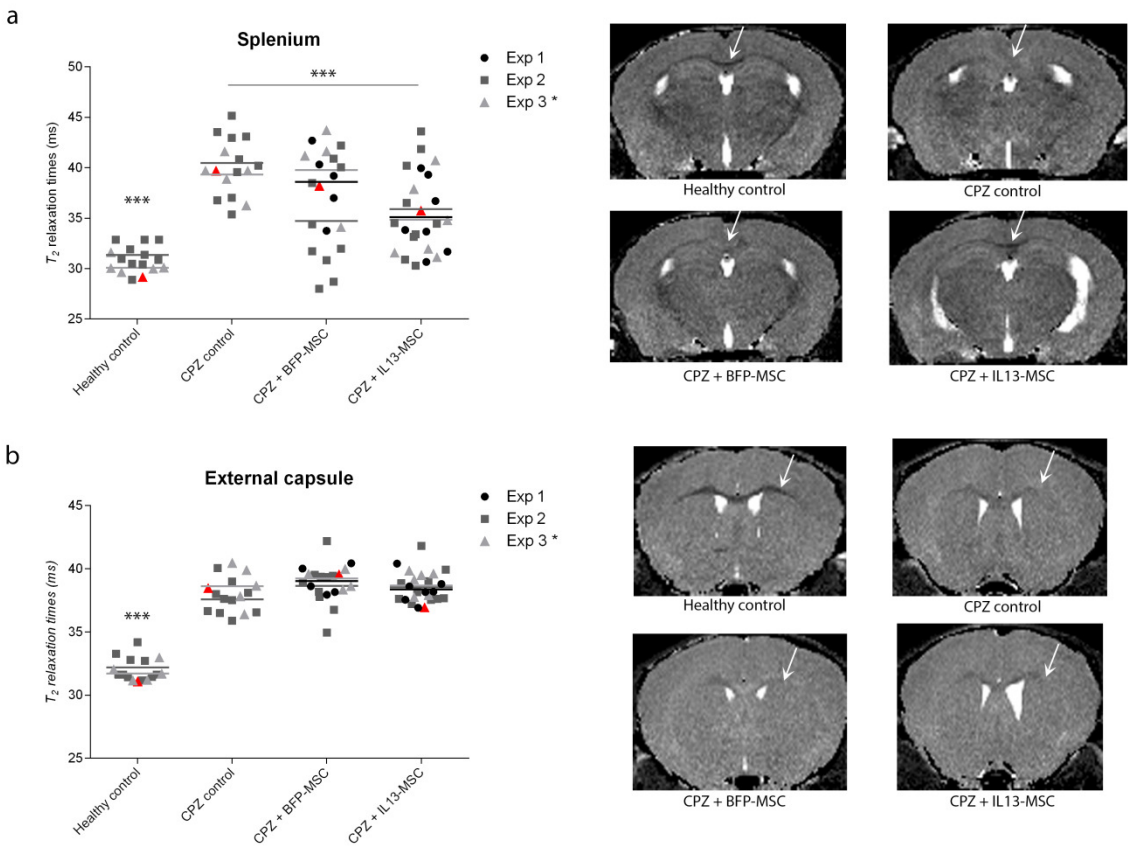

Figure 1. T_2-weighted MRI of the control and experimental groups.

(a) Left side: dot plot showing T_2-relaxation times of the whole *splenium* of the *corpus callosum* (CC) in healthy control mice (n=16), in CPZ-treated mice (CPZ control, n=17), in BFP-MSC grafted CPZ-treated mice (CPZ + BFP-MSC, n=20) and in IL13-MSC grafted CPZ-treated mice (CPZ + IL13-MSC, n=24). Each data point corresponds to the value obtained from an individual mouse of one of the three independent experiments (described in table 1). The mean of each independent experiment is represented by a horizontal line. Right side: representative MRI image demonstrating intensity alterations in the *splenium* for each group (area indicated by arrows). (b) Left side: dot plot showing T_2-relaxation times of the whole external capsule (EC) for each experimental group. The mean

of each independent experiment is represented by a horizontal line. Right side: representative MRI image demonstrating intensity alterations in the EC for each group (area indicated by the arrows). Significant differences versus the CPZ control group are indicated with two (p-value ≤ 0.01) or three (p-value ≤ 0.001) asterisks. Data points indicated in red on figure 1a and 1b correspond with the MRI images provided in figures 1a and 1b and the histological images shown in figure 3a and 4.

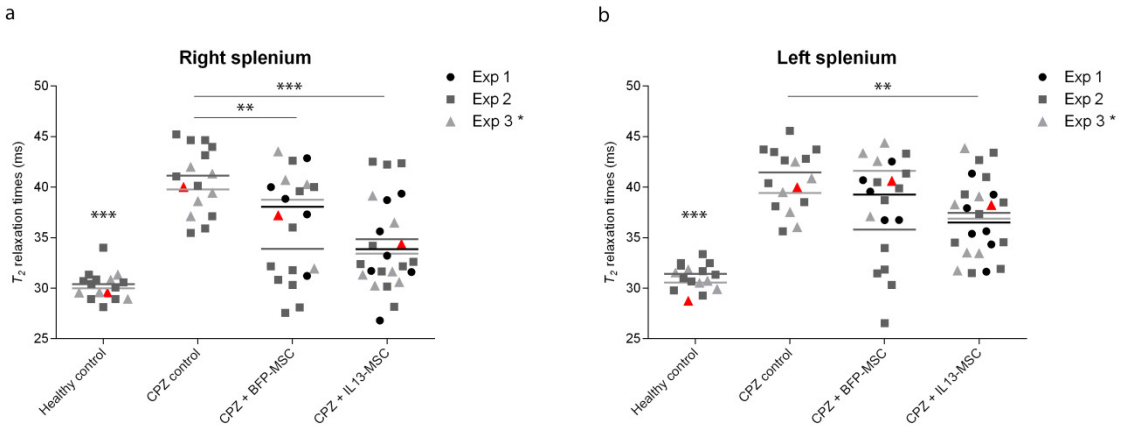

Figure 2. T2-weighted MRI of the right and left splenium of control and experimental groups.
(a) Dot plot showing T_2-relaxation times of the right side of the *splenium* for each experimental group. The mean of each independent experiment is represented by a horizontal line. (b) Dot plot showing T_2-relaxation times of the left side of the *splenium* for each experimental group. The mean of each independent experiment is represented by a horizontal line. Significant differences versus the CPZ control group are indicated with one (p-value <0.05), two (p-value ≤ 0.01) or three (p-value ≤ 0.001) asterisks. Data points indicated in red on figure 2a and 2b correspond with the MRI images provided in figures 1a and 1b and the histological images shown in figure 3a and 4.

5.4.2. Histological evaluation confirms protection against CPZ-induced CNS inflammation and demyelination by IL13-secreting MSC

Next, we performed immunofluorescent stainings for myelin basic protein (MBP) on C57BL/6 $CX_3CR1^{eGFP/+}$ $CCR2^{RFP/+}$ mice for which MRI data were obtained (MRI experiment 3, n=5 for Healthy control, n=5 for CPZ control, n=5 for CPZ + BFP-MSC and n=7 for CPZ + IL13 -MSC), and assessed both the degree of $CX_3CR1^{eGFP/+}$ microglia activity (as determined by the percentage of eGFP coverage) and the degree of myelination (as determined by the percentage of MBP coverage) in the whole *splenium*, the right side of the *splenium* and the left side of the *splenium* (figure 3). As shown by the representative images in figure 3a, it is clear that the *splenium* becomes highly invaded by $CX_3CR1^{eGFP/+}$ microglia following CPZ treatment. As

expected from the above-mentioned MRI data, representative images of IL13-MSC grafted mice show a decrease in $CX_3CR1^{eGFP/+}$ microglia density in the *splenium*, which was not observed in BFP-MSC grafted mice. In agreement with the aforementioned MRI data, further quantitative analysis of microglia activity (Figure 3b) within the whole, the right and the left side of the *splenium* confirms a significant decrease following grafting of IL13-MSC over the whole *splenium* ($p=0.02$), and more specifically at the right side ($p<0.0001$) of the *splenium*, as compared to non-grafted CPZ control mice. In contrast, no overall significant decrease in microglia activity could be detected following grafting of BFP-MSC in the *splenium*, as compared to non-grafted CPZ control mice. Concerning the degree of myelination, it is clear from the representative images provided in figure 3a that severe demyelination can be observed at the site of CX_3CR1^{+} microglia accumulation upon CPZ administration. Moreover, as expected from the MRI and representative images of IL13-MSC grafted mice, protection against demyelination of the *splenium* is suggested. Further quantitative analysis of myelination (Figure 3c) within the whole, the right and the left side of the *splenium* confirms a significant protection against demyelination following grafting of IL13-MSC over the whole *splenium* ($p=0.0011$) and the right side of the *splenium* ($p<0.0001$), as compared to non-grafted CPZ control mice. Again, no overall significant protection against demyelination could be detected following grafting of BFP-MSC in the *splenium*, as compared to non-grafted CPZ control mice.

5.4.3. T_2-weighted MRI results strongly correlate with histology data

As we have obtained a large set of corresponding MRI and histology data, we investigated if non-invasive T_2-weighted MRI observations can be used as a reliable surrogate analysis to assess inflammation and demyelination in the CPZ mouse model. When histologically evaluating $CX_3CR1^{eGFP/+}$ microglia density and MBP myelination, a very strong negative correlation ($r = -0.789$; 95% confidence interval [-0.907 ; -0.500]) was found between the increase in microglia density and the degree of demyelination over the whole *splenium* (Figure 3d, left graph). When evaluating T_2-weighted MRI data with histological data showing $CX_3CR1^{eGFP/+}$ microglia density, a strong positive correlation ($r = 0.635$; 95% confidence interval [0.222 ; 0.858]) was found between the increase in microglia density and the increase of T_2 relaxation time over the whole *splenium* (Figure 3d, middle graph). When evaluating T_2-

weighted MRI data with histological data showing MBP myelin density, a strong negative correlation (r = -0.650; 95% confidence interval [-0.839 ; -0.290]) was found between the decrease in MBP density and the increase of T_2 relaxation time over the whole *splenium* (Figure 3d, right graph). Based on these correlation analyses, we are confident that the observed T_2-weighted MRI images reflect the obtained histological data.

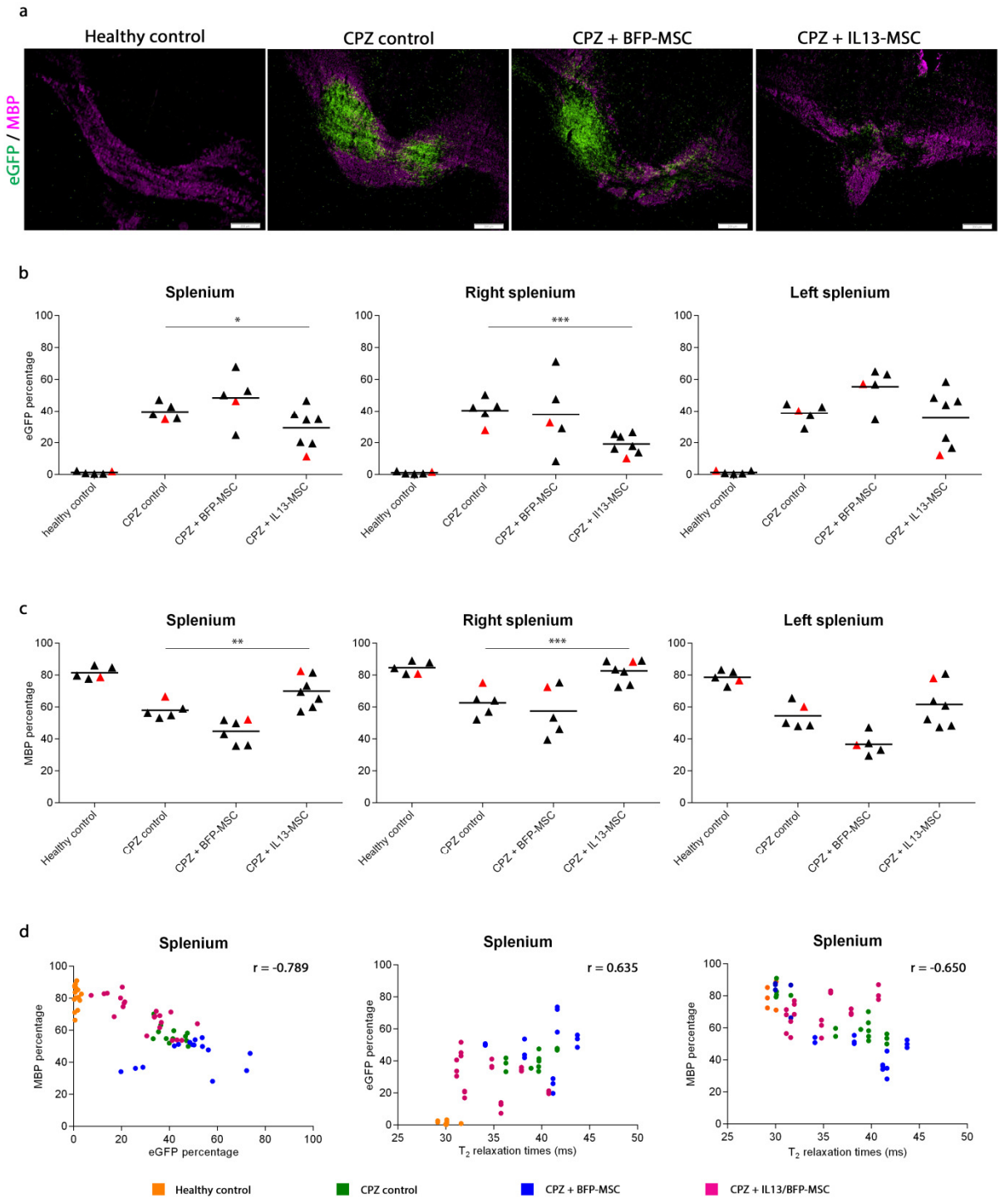

Figure 3. eGFP and MBP in the splenium of the control and experimental groups.

(a) Representative overview images of the *splenium* of the *corpus callosum* in control, CPZ-treated mice and CPZ-treated mice with BFP-MSC grafts or IL13-MSC grafts. Scalebar indicates 200µm. (b) Dot plots showing the coverage percentage of eGFP in the whole *splenium* (left graph), the right *splenium* (middle graph) and the left *splenium* (right graph) for each experimental group. (c) Dot plots showing the coverage percentage of MBP in the whole *splenium* (left graph), the right *splenium* (middle graph) and the left *splenium* (right graph) for each

experimental group. The mean of each independent experiment is represented by a horizontal line. Significant differences are indicated with one (p-value <0.05), two (p-value ≤ 0.01) or three (p-value ≤ 0.001) asterisks. (d) Dot plots showing the correlation between eGFP and MBP coverage percentage (left graph), eGFP coverage percentage and T_2 relaxation times (middle graph), MBP coverage percentage and T_2 relaxation times (right graph) in the *splenium* for each experimental group. Spearman's correlation coefficient (r) is presented on each graph. Data points indicated in red on figure 3b and 3c correspond with the representative MRI images provided in figure 1a and 1b and with the representative histological images shown in figure 3a and 4.

5.4.4. Differential behaviour of microglia and macrophages in IL13-expressing MSC graft-mediated modulation of CPZ-induced neuroinflammation and demyelination

Next, we took advantage of the $CX_3CR1^{eGFP/+}$ $CCR2^{RFP/+}$ mouse model to unravel the contribution and/or phenotypic properties of microglia and macrophages during CPZ-induced inflammation and the effect of IL13-expressing MSC grafts. For this, further histological analyses were performed on C57BL/6 $CX_3CR1^{eGFP/+}$ $CCR2^{RFP/+}$ mice from MRI experiment 3, of which representative overview and detail images of the *splenium* are provided in figure 4. For each of the experimental conditions, images discriminate CX_3CR1^{+} microglia (eGFP fluorescence) from $CCR2^{+}$ infiltrating peripheral macrophages (RFP fluorescence). Additional activation markers, including F4/80, MHCII and Arg1, are shown in blue (figure 4). While in healthy control mice, only small numbers of $CX_3CR1^{eGFP/+}$ microglia are present within the *splenium*, following CPZ treatment, the *splenium* becomes highly invaded by $CX_3CR1^{eGFP/+}$ microglia without noticeable contribution of $CCR2^{RFP/+}$ peripheral macrophages. Representative images of IL13-MSC grafted mice, but not BFP-grafted mice, show a remarkable decrease in $CX_3CR1^{eGFP/+}$ microglia density in the whole *splenium* (figure 4, first and second rows, direct CX_3CR1-eGFP fluorescence and direct CCR-RFP fluorescence, quantification provided in figure 3b). In agreement with our previously published data on the spatial distribution of microglia and BM-derived macrophages following MSC transplantation in the CNS, both MSC graft types in CPZ treated $CX_3CR1^{eGFP/+}$ $CCR2^{RFP/+}$ mice are invaded by $CCR2^{RFP/+}$ peripheral macrophages and surrounded by $CX_3CR1^{eGFP/+}$ brain-resident microglia (figure 4, second row, direct CX_3CR1-eGFP fluorescence and direct CCR2-RFP fluorescence)[13]. Clearly, following MSC grafting in the CPZ model we can thus distinguish two separate inflammatory responses: (i) CPZ-induced activation of $CX_3CR1^{eGFP/+}$ microglia in the *splenium*, which can be modulated following grafting of IL13-expressing MSC, and (ii) MSC graft-associated $CX_3CR1^{eGFP/+}$ microglia and $CCR2^{RFP/+}$ peripheral macrophage activation. Upon

further evaluation of the activation status of microglia and macrophages, by staining for F4/80 in each of the experimental groups, it is clear that CPZ pathology-associated $CX_3CR1^{eGFP/+}$ microglia, as well as MSC graft-associated $CX_3CR1^{eGFP/+}$ microglia and $CCR2^{RFP/+}$ peripheral macrophages, express F4/80 (figure 4, third and fourth rows, blue staining), while expression of this activation marker is absent on steady-state resting microglia in healthy brain tissue. MHCII expression is mainly restricted to $CCR2^{RFP/+}$ peripheral macrophages invading the BFP-MSC graft, whereas MHCII is expressed on both IL13 -MSC graft-infiltrating $CCR2^{RFP/+}$ peripheral macrophages and on graft-surrounding $CCR2^{RFP/+}$ macrophages and $CX_3CR1^{eGFP/+}$ microglia (figure 4, fifth and sixth rows, blue staining). Also note that no MHCII expression was detected on CPZ pathology-associated $CX_3CR1^{eGFP/+}$ microglia (figure 4, fifth and sixth rows). Finally, staining for Arg1 (figure 4, seventh and eighth rows, blue staining) can only be detected on IL13 -MSC graft-infiltrating and graft-surrounding $CCR2^{RFP/+}$ peripheral macrophages and $CX_3CR1^{eGFP/+}$ microglia. These results indicate that IL13 produced by grafted MSC is able to: (i) trigger alternative activation of MSC graft-associated microglia and macrophages; and (ii) diminishes CPZ-induced inflammation and demyelination by its direct action or in combination with the action of alternatively activated macrophages/microglia.

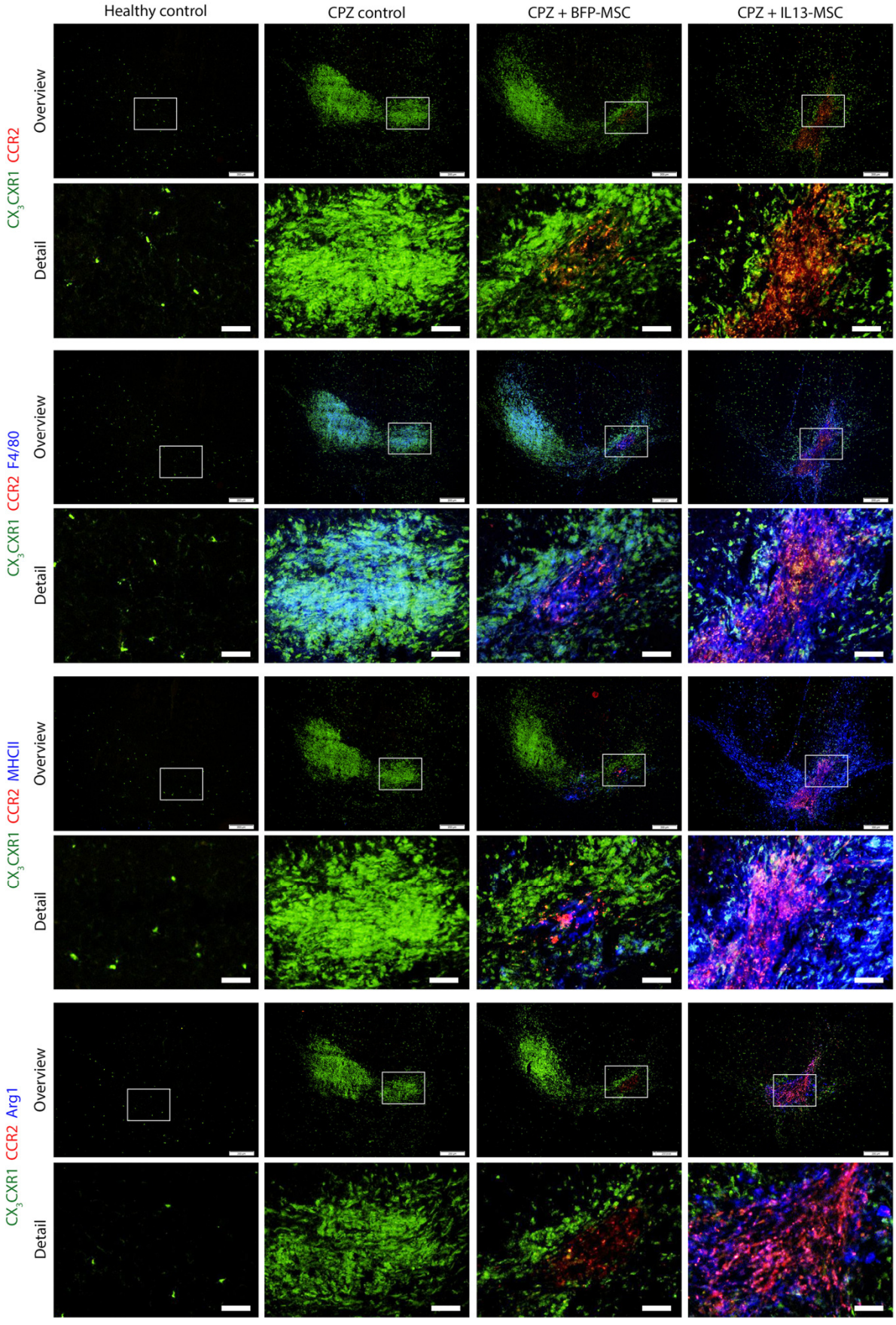
Healthy control
CPZ control
CPZ + BFP-MSC
CPZ + IL13-MSC
CX3CXR1 CCR2
CX3CXR1 CCR2 F4/80
CX3CXR1 CCR2 MHCII
CX3CXR1 CCR2 Arg1
Overview
Detail

Figure 4. Representative images illustrating multiple phenotypes of microglia and macrophages in the control and experimental groups.

Representative overview images (odd rows, scale bar indicates 200 µm) of the *splenium* of the *corpus callosum* (CC) in control mice (first column), CPZ-treated mice (second column) and CPZ-treated mice with BFP-MSC grafts (third column) or IL13-MSC grafts (fourth column). Representative detail images (even rows, scale bar indicates 50 µm) from the BFP-MSC or IL13-MSC graft site or from the corresponding areas in healthy control or CPZ control mice. First and second rows: in green direct eGFP fluorescence from CX3CR1$^{+/eGFP}$ brain resident microglia and in red direct RFP fluorescence from peripheral CCR2$^{+/RFP}$ macrophages. Third and fourth rows: additionally in blue immunofluorescent staining for F4/80 marking activated eGFP^{+} brain-resident microglia and RFP^{+} peripheral macrophages. Fifth and sixth rows: additionally in blue immunofluorescent staining for MHCII marking activated eGFP^{+} brain-resident microglia and RFP^{+} peripheral macrophages. Seventh and eighth rows: additionally in blue immunofluorescent staining for Arg1 marking alternatively activated eGFP^{+} brain-resident microglia and RFP^{+} peripheral macrophages.

5.4.5. IL13-producing MSC grafts induce the appearance of alternative activation phenotypes in graft-associated macrophages and microglia

In order to further investigate the observed phenotypic differences between BFP-MSC and IL13-MSC graft-associated microglia and macrophages, we performed additional immunofluorescent stainings to determine the expression of the activation markers MHCII and Arginase1 (Arg1). Since we encountered limitations in C57BL/6 CX$_3$CR1$^{eGFP/+}$ CCR2$^{RFP/+}$ transgenic mice in the histological quantification of multiple cell activation phenotypes, we used the bone marrow transplantation mouse model to distinguish between microglia and macrophages in this part of the study. MHCII expression could be detected on eGFP^{+} macrophages and eGFP^{-} microglia within both MSC grafts (figure 5a, indicated by arrows and arrowheads respectively). Furthermore, while MHCII expression was rarely detected on eGFP^{+} macrophages and eGFP^{-} microglia in the border of BFP-MSC grafts (figure 5a, indicated by arrows and arrowheads respectively), its expression is clearly visible on both eGFP^{+} macrophages and eGFP^{-} microglia in the border of IL13-MSC grafts (figure 5a, indicated by arrows and arrowheads respectively). Further quantification provided in figure 2B confirms that the highest density of MHCII^{+} cells can be detected among eGFP^{+} macrophages and eGFP^{-} microglia within the BFP- and IL13-MSC grafts, without significant differences between both graft types (figure 5b). However, the density of MHCII^{+} eGFP^{+} macrophages and MHCII^{+} eGFP^{-} microglia in the IL13-MSC graft border is significantly higher than in the BFP-MSC graft border (figure 5b, both p=0.0346). Next, we found that Arg1 was not expressed on eGFP^{+} macrophages or eGFP^{-} microglia within or surrounding the BFP-MSC grafts (figure 5c).

However, in the case of IL13-MSC grafts, it can clearly be noted that Arg1^{+} eGFP^{+} macrophages and Arg1^{+} eGFP^{-} microglia can be detected both in and around the graft (figure 5c, indicated by arrows and arrowheads respectively). Further quantification provided in figure 5d indeed confirms that Arg1^{+} cells can be detected among eGFP^{+} macrophages and eGFP^{-} microglia within and surrounding the IL13-MSC graft (for all p=0.0233).

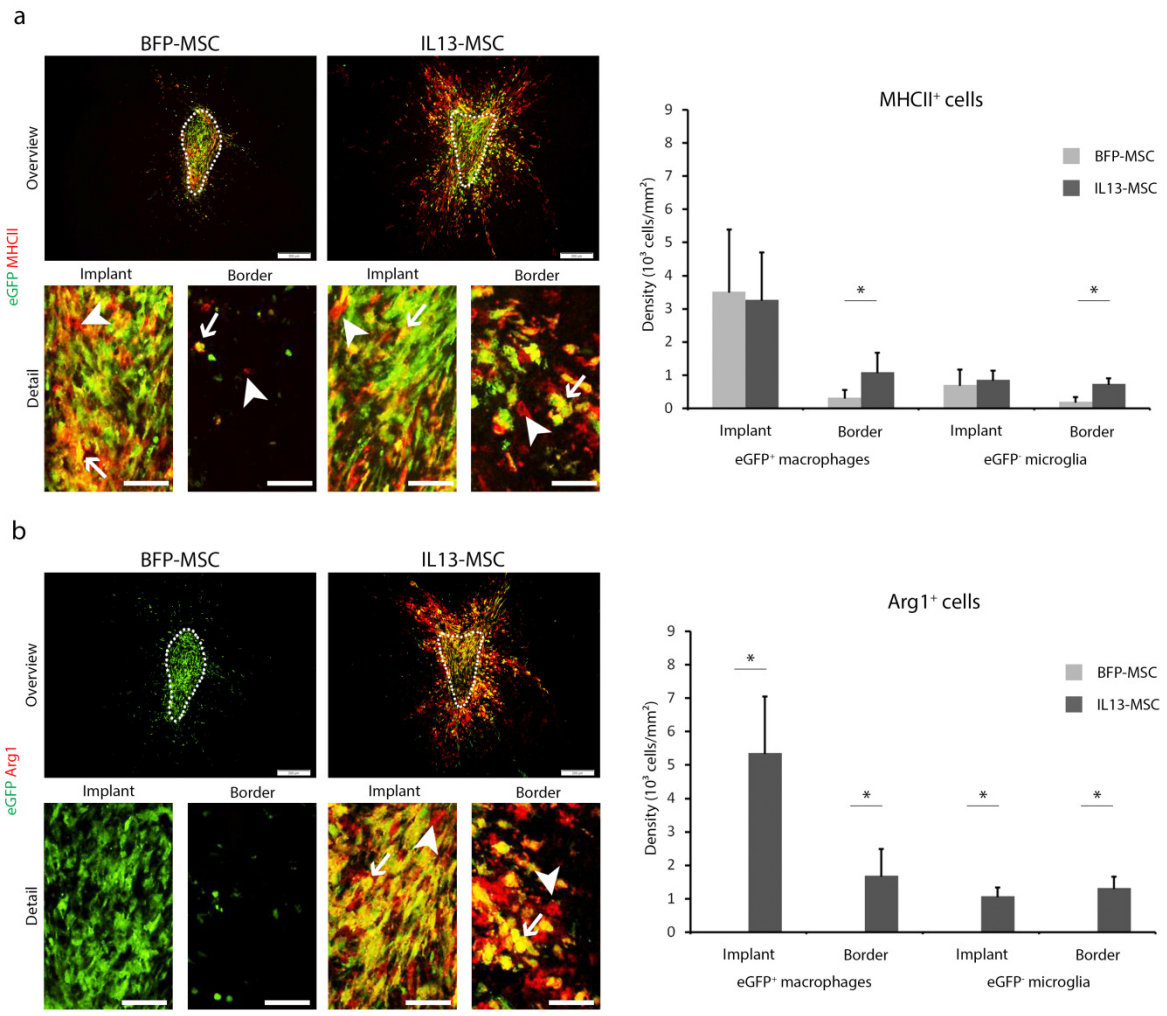

Figure 5. Activation phenotype of macrophages and microglia in BFP- and IL13-MSC grafts in the CNS of eGFP^{+} bone marrow chimeras.

(a) Overview of a BFP- and IL13-MSC graft, showing graft-infiltrating macrophages (green) and MHCII-expressing eGFP^{-} brain-resident microglia and eGFP^{+} peripheral macrophages (red). Details of the BFP- and IL13-MSC implant and border are provided, showing activated MHCII^{+}eGFP^{+} macrophages (arrows) and activated MHCII^{+}eGFP^{-} microglia (arrowheads). (b) Cell densities of MHCII^{+}eGFP^{+} BM-derived macrophages and MHCII^{+}eGFP^{-} microglia within the implant and border of BFP- and IL13-MSC grafts. Values are given as mean ± standard deviation. Significant differences (p-value ≤ 0.05) are indicated with an asterisk. (c) Overview of a BFP- and IL13-MSC graft, showing graft-infiltrating macrophages (green) and Arg1-expressing eGFP^{-} microglia and eGFP^{+} macrophages. Details of the BFP- and IL13-MSC implant and border are provided, showing alternatively activated Arg1^{+}eGFP^{+}

macrophages (arrows) and Arg1^{+}eGFP^{-} microglia (arrowheads). (d) Cell densities of Arg1^{+}eGFP^{+} BM-derived macrophages and Arg1^{+}eGFP^{-} microglia within the implant and border of BFP- and IL13-MSC grafts. Values are given as mean ± standard deviation. Significant differences (p-value <0.05) are indicated with an asterisk.

5.4.6. Influence of IL13 on the occurrence and spatial distribution of classically and alternatively activated microglia and macrophage phenotypes following MSC grafting

In the final part of our study, we wanted to investigate the modulatory capacity of IL13, produced by MSC grafts, in more detail. More precisely, we examined whether microglia, macrophage or astrocyte behavior was altered upon implantation of IL13-MSC (n=5) compared to implantation of BFP-MSC (n=6) in the CNS of healthy mice. As shown by the representative immunofluorescence images in figure 6a, a GFAP^{+} astroglial scar delineates both BFP-MSC and IL13-MSC grafts. No noticeable differences were observed at the level of astroglial scarring. Within the MSC graft site, a clear side-by-side presence of grafted BFP-MSC or IL13-MSC (figure 6b; arrowheads) and eGFP^{+} BM-derived peripheral macrophages (figure 6b; arrows) can be noted. As expected, the majority of BFP-MSC and IL13-MSC graft-invading eGFP^{+} peripheral macrophages reside within the astroglial scar (figure 6a). However, upon IL13-MSC grafting, the location of eGFP^{+} BM-derived macrophages seems to be less restricted to the implant site as compared to BFP-MSC grafts (figure 6a). In this transplantation model, microglia and macrophages can be distinguished following Iba1 staining (figure 6c). As shown, the majority of Iba1^{+} cells within both the BFP-MSC and the IL13-MSC grafts are eGFP^{+} macrophages (figure 6c; arrows), whereas the majority of Iba1^{+} cells within the implant border are eGFP^{-} microglia (figure 6c; arrowheads). Further quantification indeed confirms that the density of eGFP^{+} macrophages is higher within both the BFP-MSC and the IL13-MSC graft as compared to the graft-surrounding border (both $p<0.0001$). However, more Iba1^{+} eGFP^{+} macrophages are found in the implant border in the case of IL13-MSC grafts as compared to BFP-MSC grafts (figure 6c; arrows) ($p=0.0121$). In order to further characterize phenotypic properties of both microglia and macrophages we performed MHCII/Arg1 double immunofluorescence stainings. As shown in figure 6d, double staining for MHCII and Arg1 clearly shows that in the case of IL13-MSC grafting multiple subtypes of both eGFP^{-} brain-resident microglia and eGFP^{+} peripheral macrophages can be visualized in and around IL13-MSC grafts. Based on these MHCII (in blue) and Arg1 (in red) double stainings, following

populations can be identified: eGFP$^+$ MHCII$^+$ Arg1$^-$ macrophages (cyan), eGFP$^+$ MHCII$^-$ Arg1$^+$ macrophages (yellow), eGFP$^+$ MHCII$^+$ Arg1$^+$ macrophages (white), eGFP$^+$ MHCII$^-$ Arg1$^-$ macrophages (green), eGFP$^-$ MHCII$^+$ Arg1$^-$ microglia (blue), eGFP$^-$ MHCII$^-$ Arg1$^+$ microglia (red), and eGFP$^-$ MHCII$^+$ Arg1$^+$ microglia (magenta). Note that with this staining combination, eGFP$^-$ MHCII$^-$ Arg1$^-$ microglia (black background), which are also present, cannot be visualized in these images. When evaluating the phenotypic properties of control BFP-MSC graft-associated microglia and macrophages, only the following populations can be distinguished: eGFP$^+$ MHCII$^+$ macrophages (cyan), eGFP$^+$ MHCII$^-$ macrophages (green) and eGFP$^-$ MHCII$^+$ microglia (blue). Again, eGFP$^-$ MHCII$^-$ microglia (black background), which are also present, cannot be visualized on these images. Following quantitative analysis of MHCII- and/or Arg1-expressing cells on eGFP$^+$ macrophages and eGFP$^-$ microglia (figure 5a and 5b), we calculated an approximate biodistribution of the different microglia and macrophage phenotypes observed within and surrounding the BFP- and IL13-MSC grafts (figure 6e). Note the following important similarities and/or differences: (i) macrophages are the major immune cell population within the BFP- and IL13-MSC grafts, (ii) microglia are the major immune cell population surrounding the BFP- and IL13-MSC grafts, (iii) the number of macrophages surrounding the IL13-MSC grafts is significantly higher than the number of macrophages surrounding the BFP-MSC grafts (see above; $p=0.0121$), (iv) around 50% of macrophages within the BFP-MSC grafts express MHCII, while the majority (80%) of macrophages within the IL13-MSC grafts express Arg1 with half of them co-expressing MHCII, (v) the small population of microglia within the BFP-MSC grafts expresses MHCII, whereas microglia within the IL13-MSC grafts display a heterogeneous expression of MHCII and/or Arg1, (vi) in the BFP-MSC graft border, only a small population of microglia and macrophages express MHCII, and (vii) in the IL13-MSC graft border, the majority of both microglia and macrophages display a heterogeneous expression of MHCII and/or Arg1. These results summarize that IL13 secretion by MSC grafts induces a broad spectrum of alternatively activated brain-resident microglia and graft-infiltrating peripheral macrophages, both within as around the MSC grafts.

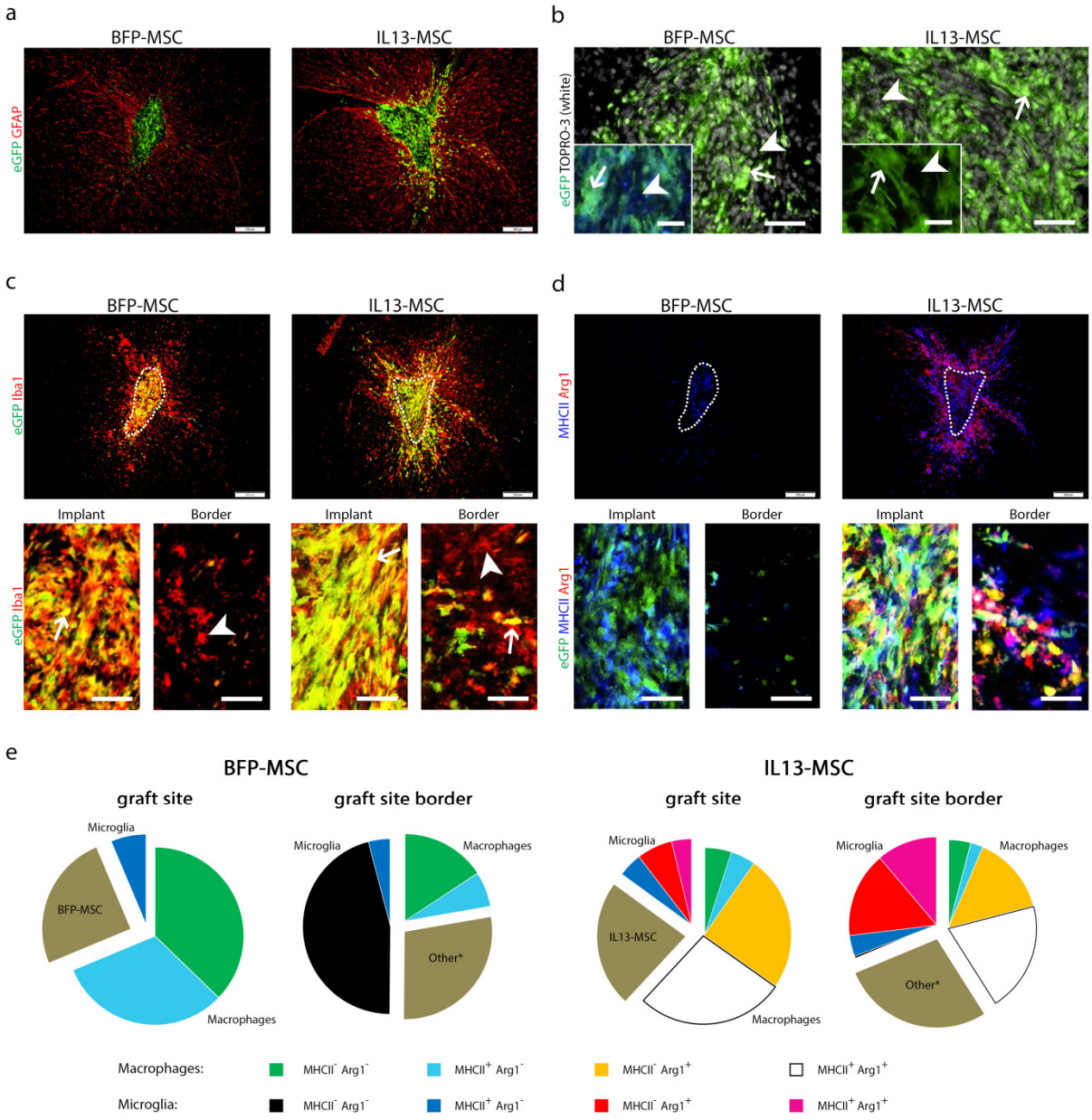

Figure 5. Analysis of BFP- and IL13-MSC graft remodelling in CNS of eGFP⁺ bone marrow chimeras.
(a) Overview of a BFP- and IL13-MSC graft. Green: eGFP fluorescence from bone marrow-derived macrophages indicating infiltration at the graft. Red: GFAP staining indicates astrogliosis around the graft. (b) Detail of the BFP- and IL13-MSC graft. White: TOPRO-3 marking all nuclei. Green: eGFP fluorescence from graft-infiltrating macrophages (arrows). eGFP⁻ nuclei (arrowheads) are grafted MSC or (few) graft-infiltrating microglia. Insets show BFP fluorescence (blue) or no fluorescence (black) from grafted BFP-MSC or IL13-MSC (arrowheads). Green: eGFP fluorescence from graft-infiltrating macrophages (arrows). Scale bars indicate 20 µm. (c) Overview of a BFP- and IL13-MSC graft. Green: eGFP fluorescence from graft-infiltrating macrophages. Red: Iba1 staining marks both eGFP⁻ microglia and eGFP⁺ macrophages. Details of the BFP- and IL13-MSC implant and border show Iba1⁺eGFP⁺ peripheral macrophages mainly within the implant (arrows) andIba1⁺eGFP⁻ microglia mainly within the border (arrowheads). (d) Overview of a BFP- and IL13-MSC graft, showing MHCII-expressing (blue) and Arg1-expressing microglia and macrophages (red). Details of the BFP- and IL13-MSC implant and border are provided,

showing graft-infiltrating macrophages (green) in combination with Arg1- (red) and MHCII-expressing (blue) microglia and macrophages. The following cell populations can be distinguished: $eGFP^+MHCII^+Arg1^-$ macrophages (cyan), $eGFP^+MHCII^-Arg1^+$ macrophages (yellow), $eGFP^+MHCII^+Arg1^+$ macrophages (white), $eGFP^+MHCII^-Arg1^-$ macrophages (green), $eGFP^-MHCII^+Arg1^-$ microglia (blue), $eGFP^-MHCII^-Arg1^+$ microglia (red), $eGFP^-MHCII^+Arg1^+$ microglia (magenta). $eGFP^-MHCII^-Arg1^-$ microglia (black background) cannot be visualised using this setup. Dotted lines delineate the actual implants. The border is an area extending 85 µm. All overview scale bars indicate 200 µm and all detail scale bars indicate 50 µm. (e) Pie graphs showing mean representation of each microglia and macrophage phenotype within the BFP-MSC and IL13-MSC graft and border. For the graft site, the fraction of BFP-MSC or IL13-MSC is indicated. For the border, the fraction of other cells is indicated (* = neurons, oligodendrocytes and/or astrocytes). The colours of differentially activated microglia and macrophage correspond to those in figure 4f.

5.5. DISCUSSION

It is currently well described that several stimuli can trigger alternative activation phenotypes in microglia and macrophages, with IL4/13 (M2a type polarisation) and IL10 (M2c type polarisation) currently being the best characterized[7, 6]. Specifically focussing on M2a-polarisation, we hypothesize that influencing complex immune cascades within the CNS, which are mostly initiated and/or orchestrated by a misbalanced macrophage and/or microglia function, can be achieved by triggering alternative activation pathways solely in macrophages and/or microglia. Consequently, as IL13R expression is absent on T cells[32] - in contrast to IL4R expression – the choice of IL13 over IL4 allows for a more restricted therapeutic intervention without potentially influencing adaptive immunity. In the present study, we therefore focussed on providing a thorough pre-clinical analysis of MSC graft-mediated IL13 delivery as an effective approach to modulate both pathology-associated and MSC graft-induced immune responses in the CNS of mice.

In the first part of our manuscript, we highlight that IL13 production by grafted MSC, potentially aided by the appearance of alternatively activated microglia and macrophages at the MSC graft site, prevents microgliosis and demyelination in the CPZ mouse model. Note that the therapeutic approach presented here is significantly different from several previously published reports using non-engineered MSC. A study by Nessler and colleagues was unable to report any clinical benefit of both intravenously or intranasally administered MSC[33], most likely due to limited cell migration to the CNS. In addition, our own preceding work on cell grafting in the CPZ model at the peak of inflammation and demyelination was also unable to demonstrate any contribution of mesenchymal, neural or hematopoietic cells to

remyelination[14]. The latter observation was recently confirmed by a study performed by Salinas Tejedor et al. showing that MSC injected at the onset or the peak of oligodendrocyte proliferation during cuprizone induced demyelination do not exert beneficial effects on remyelination[34]. Comparing our new study with these previously published reports, the therapeutic delivery of IL13 by means of MSC grafting represents an achievable goal in the further development of cell-based therapies to counteract neuroinflammatory processes. Based on our current knowledge, and in agreement with several literature reports we propose the following working hypothesis to explain the neuroprotective character of MSC-mediated IL13 delivery in the CNS. At one hand, it has been described by Yang et al. that IL13 can directly induce apoptosis in activated microglia[35]. It is not unlikely that this feature of IL13 highly contributes to the reduced microgliosis, and subsequent reduced demyelination, observed in this study. On the other hand, M2a polarised macrophages/microglia, which are effectively introduced in the CNS by means of local transplantation of IL13-producing MSC, may also contribute to the observed neuroprotection. In this context it has previously been reported that M2 polarised macrophages are able to promote oligodendrocyte differentiation and enhance remyelination[36]. However, as the field on CNS immunomodulation is highly complex and continuously evolving, a highly complex interplay between both proposed mechanisms is not unlikely.

In the second part of the study, we focused more on the characterization of the MSC graft site remodelling by IL13. Over the past years, we have reported extensively on the cellular remodelling of neural and mesenchymal cell grafts in the CNS of healthy mice. It is clear now that - especially in case of mesenchymal (stem) cell grafts - this intervention is a highly complex interplay between hypoxia- induced apoptosis of the grafted cells, neutrophil invasion, neo-angiogenesis, microglia/macrophage recruitment, astrogliosis, and eventually survival of a limited number of grafted cells[11-15]. In previous studies we also reported that graft-infiltrating macrophages display a pro-inflammatory phenotype as shown by the temporary expression of CD11b and MHCII. It should be noted however that at this time we were unable to experimentally distinguish brain-resident microglia from CNS-invading macrophages [12]. In this new study, we highlight the potential of IL13 secretion by grafted MSC to induce alternative activation in graft-surrounding microglia and in graft-infiltrating macrophages *in vivo*, as indicated by the expression of MHCII and/or Arg1. During the past decade, pro-

inflammatory microglia and macrophages have generally been associated with tissue destruction, thereby characterising them as M1-oriented[9]. On the other hand, alternatively activated microglia and macrophages have generally been associated with immune modulation and tissue repair, thereby characterising them as M2-oriented[9]. Clearly, the underlying biology is more complex as distinct compounds can induce multiple subtypes ranging from M1 to M2 activation[6]. Moreover, depending on the pathology, M1-oriented microglia and/or macrophages can exert a beneficial effect, whereas M2-oriented microglia and/or macrophages can also be detrimental[37]. From our study, it is clear that IL13 priming of macrophages and microglia *in vivo* does not result in a single, clearly distinguishable cell population. We speculate that each of the microglia or macrophage phenotypes described, either single positive for MHCII, single positive for Arg1 or double positive, may exert a different effector function, however this remains to be further investigated.

5.6. CONCLUSION

With this study, we propose a novel approach for effective modulation of detrimental *in vivo* inflammatory responses in the CNS, where IL13 production by grafted MSC and potentially aided by the appearance of alternatively activated microglia and macrophages at the MSC graft site, induces microglial quiescence at the onset of inflammatory responses. In this context, we believe our approach is worth further evaluating in clinically relevant mouse models of neuro-trauma displaying a gradual increase in inflammatory responses, e.g. models of spinal cord injury or stroke.

5.7. REFERENCES

1. Benakis C, Garcia-Bonilla L, Iadecola C, Anrather J. The role of microglia and myeloid immune cells in acute cerebral ischemia. Frontiers in cellular neuroscience. 2014;8:461. doi:10.3389/fncel.2014.00461.
2. Morganti JM, Jopson TD, Liu S, Riparip LK, Guandique CK, Gupta N et al. CCR2 antagonism alters brain macrophage polarization and ameliorates cognitive dysfunction induced by traumatic brain injury. The Journal of neuroscience : the official journal of the Society for Neuroscience. 2015;35(2):748-60. doi:10.1523/JNEUROSCI.2405-14.2015.
3. Yamasaki R, Lu H, Butovsky O, Ohno N, Rietsch AM, Cialic R et al. Differential roles of microglia and monocytes in the inflamed central nervous system. The Journal of experimental medicine. 2014;211(8):1533-49. doi:10.1084/jem.20132477.
4. Zhou X, He X, Ren Y. Function of microglia and macrophages in secondary damage after spinal cord injury. Neural regeneration research. 2014;9(20):1787-95. doi:10.4103/1673-5374.143423.
5. Shechter R, Schwartz M. Harnessing monocyte-derived macrophages to control central nervous system pathologies: no longer 'if' but 'how'. The Journal of pathology. 2013;229(2):332-46. doi:10.1002/path.4106.
6. Murray PJ, Allen JE, Biswas SK, Fisher EA, Gilroy DW, Goerdt S et al. Macrophage activation and polarization: nomenclature and experimental guidelines. Immunity. 2014;41(1):14-20. doi:10.1016/j.immuni.2014.06.008.
7. Van Dyken SJ, Locksley RM. Interleukin-4- and interleukin-13-mediated alternatively activated macrophages: roles in homeostasis and disease. Annual review of immunology. 2013;31:317-43. doi:10.1146/annurev-immunol-032712-095906.
8. Ibraheem D, Elaissari A, Fessi H. Gene therapy and DNA delivery systems. International journal of pharmaceutics. 2014;459(1-2):70-83. doi:10.1016/j.ijpharm.2013.11.041.
9. De Vocht N, Praet J, Reekmans K, Le Blon D, Hoornaert C, Daans J et al. Tackling the physiological barriers for successful mesenchymal stem cell transplantation into the central nervous system. Stem cell research & therapy. 2013;4(4):101. doi:10.1186/scrt312.
10. Bergwerf I, Tambuyzer B, De Vocht N, Reekmans K, Praet J, Daans J et al. Recognition of cellular implants by the brain's innate immune system. Immunology and cell biology. 2011;89(4):511-6. doi:10.1038/icb.2010.141.
11. Costa R, Bergwerf I, Santermans E, De Vocht N, Praet J, Daans J et al. Distinct in vitro properties of embryonic and extraembryonic fibroblast-like cells are reflected in their in vivo behavior following grafting in the adult mouse brain. Cell transplantation. 2015;24(2):223-33. doi:10.3727/096368913X676196.
12. De Vocht N, Lin D, Praet J, Hoornaert C, Reekmans K, Le Blon D et al. Quantitative and phenotypic analysis of mesenchymal stromal cell graft survival and recognition by microglia and astrocytes in mouse brain. Immunobiology. 2013;218(5):696-705. doi:10.1016/j.imbio.2012.08.266.
13. Le Blon D, Hoornaert C, Daans J, Santermans E, Hens N, Goossens H et al. Distinct spatial distribution of microglia and macrophages following mesenchymal stem cell implantation in mouse brain. Immunology and cell biology. 2014;92(8):650-8. doi:10.1038/icb.2014.49.
14. Praet J, Reekmans K, Lin D, De Vocht N, Bergwerf I, Tambuyzer B et al. Cell type-associated differences in migration, survival, and immunogenicity following grafting in CNS tissue. Cell transplantation. 2012;21(9):1867-81. doi:10.3727/096368912X636920.
15. Praet J, Santermans E, Daans J, Le Blon D, Hoornaert C, Goossens H et al. Early inflammatory responses following cell grafting in the CNS trigger activation of the sub-ventricular zone: a proposed model of sequential cellular events. Cell transplantation. 2014. doi:10.3727/096368914X682800.
16. Reekmans K, De Vocht N, Praet J, Fransen E, Le Blon D, Hoornaert C et al. Spatiotemporal evolution of early innate immune responses triggered by neural stem cell grafting. Stem cell research & therapy. 2012;3(6):56. doi:10.1186/scrt147.
17. Praet J, Guglielmetti C, Berneman Z, Van der Linden A, Ponsaerts P. Cellular and molecular neuropathology of the cuprizone mouse model: clinical relevance for multiple sclerosis. Neuroscience and biobehavioral reviews. 2014;47:485-505. doi:10.1016/j.neubiorev.2014.10.004.

18. Baekelandt V, Eggermont K, Michiels M, Nuttin B, Debyser Z. Optimized lentiviral vector production and purification procedure prevents immune response after transduction of mouse brain. Gene therapy. 2003;10(23):1933-40. doi:10.1038/sj.gt.3302094.
19. Geraerts M, Michiels M, Baekelandt V, Debyser Z, Gijsbers R. Upscaling of lentiviral vector production by tangential flow filtration. The journal of gene medicine. 2005;7(10):1299-310. doi:10.1002/jgm.778.
20. Tambuyzer BR, Bergwerf I, De Vocht N, Reekmans K, Daans J, Jorens PG et al. Allogeneic stromal cell implantation in brain tissue leads to robust microglial activation. Immunology and cell biology. 2009;87(4):267-73. doi:10.1038/icb.2009.12.
21. Bergwerf I, De Vocht N, Tambuyzer B, Verschueren J, Reekmans K, Daans J et al. Reporter gene-expressing bone marrow-derived stromal cells are immune-tolerated following implantation in the central nervous system of syngeneic immunocompetent mice. BMC biotechnology. 2009;9:1. doi:10.1186/1472-6750-9-1.
22. Praet J, Santermans E, Reekmans K, de Vocht N, Le Blon D, Hoornaert C et al. Histological characterization and quantification of cellular events following neural and fibroblast(-like) stem cell grafting in healthy and demyelinated CNS tissue. Methods in molecular biology. 2014;1213:265-83. doi:10.1007/978-1-4939-1453-1_22.
23. Reekmans K, De Vocht N, Praet J, Le Blon D, Hoornaert C, Daans J et al. Quantitative evaluation of stem cell grafting in the central nervous system of mice by in vivo bioluminescence imaging and postmortem multicolor histological analysis. Methods in molecular biology. 2013;1052:125-41. doi:10.1007/7651_2013_17.
24. De Vocht N, Reekmans K, Bergwerf I, Praet J, Hoornaert C, Le Blon D et al. Multimodal imaging of stem cell implantation in the central nervous system of mice. Journal of visualized experiments : JoVE. 2012(64):e3906. doi:10.3791/3906.
25. Guglielmetti C, Praet J, Rangarajan JR, Vreys R, De Vocht N, Maes F et al. Multimodal imaging of subventricular zone neural stem/progenitor cells in the cuprizone mouse model reveals increased neurogenic potential for the olfactory bulb pathway, but no contribution to remyelination of the corpus callosum. NeuroImage. 2014;86:99-110. doi:10.1016/j.neuroimage.2013.07.080.
26. Praet J, Orije J, Kara F, Guglielmetti C, Santermans E, Daans J et al. Cuprizone-induced demyelination and demyelination-associated inflammation result in different proton magnetic resonance metabolite spectra. NMR in biomedicine. 2015;28(4):505-13. doi:10.1002/nbm.3277.
27. Orije J, Kara F, Guglielmetti C, Praet J, Van der Linden A, Ponsaerts P et al. Longitudinal monitoring of metabolic alterations in cuprizone mouse model of multiple sclerosis using 1H-magnetic resonance spectroscopy. NeuroImage. 2015;114:128-35. doi:10.1016/j.neuroimage.2015.04.012.
28. Liang KY, Zeger SL. Longitudinal Data-Analysis Using Generalized Linear-Models. Biometrika. 1986;73(1):13-22. doi:DOI 10.1093/biomet/73.1.13.
29. Zeger SL, Liang KY. Longitudinal data analysis for discrete and continuous outcomes. Biometrics. 1986;42(1):121-30.
30. Benjamini Y, Hochberg Y. Controlling the False Discovery Rate - a Practical and Powerful Approach to Multiple Testing. J Roy Stat Soc B Met. 1995;57(1):289-300.
31. Thiessen JD, Zhang Y, Zhang H, Wang L, Buist R, Del Bigio MR et al. Quantitative MRI and ultrastructural examination of the cuprizone mouse model of demyelination. NMR in biomedicine. 2013;26(11):1562-81. doi:10.1002/nbm.2992.
32. Graber P, Gretener D, Herren S, Aubry JP, Elson G, Poudrier J et al. The distribution of IL-13 receptor alpha1 expression on B cells, T cells and monocytes and its regulation by IL-13 and IL-4. European journal of immunology. 1998;28(12):4286-98.
33. Nessler J, Benardais K, Gudi V, Hoffmann A, Salinas Tejedor L, Janssen S et al. Effects of murine and human bone marrow-derived mesenchymal stem cells on cuprizone induced demyelination. PloS one. 2013;8(7):e69795. doi:10.1371/journal.pone.0069795.
34. Salinas Tejedor L, Berner G, Jacobsen K, Gudi V, Jungwirth N, Hansmann F et al. Mesenchymal stem cells do not exert direct beneficial effects on CNS remyelination in the absence of the peripheral immune system. Brain, behavior, and immunity. 2015. doi:10.1016/j.bbi.2015.06.024.

35. Yang MS, Park EJ, Sohn S, Kwon HJ, Shin WH, Pyo HK et al. Interleukin-13 and -4 induce death of activated microglia. Glia. 2002;38(4):273-80. doi:10.1002/glia.10057.
36. Miron VE, Boyd A, Zhao JW, Yuen TJ, Ruckh JM, Shadrach JL et al. M2 microglia and macrophages drive oligodendrocyte differentiation during CNS remyelination. Nature neuroscience. 2013;16(9):1211-8. doi:10.1038/nn.3469.
37. Chakrabarty P, Tianbai L, Herring A, Ceballos-Diaz C, Das P, Golde TE. Hippocampal expression of murine IL-4 results in exacerbation of amyloid deposition. Molecular neurodegeneration. 2012;7:36. doi:10.1186/1750-1326-7-36.

Chapter VI

General conclusions and future perspectives

6.1. GENERAL CONCLUSIONS

Throughout this thesis, resolving several technical challenges has led to a number of scientific observations and conclusions, which are briefly summarized and discussed below.

6.1.1. Technical achievements

A. Successful implementation of bone marrow transplantation (BMT) procedures to generate eGFP+ chimeric mice in order to distinguish peripheral macrophages from brain-resident microglia in the CNS.

Although brain-resident microglia and bone marrow-derived macrophages are highly comparable, as they display expression of similar phenotypic markers and exert similar functions[1, 2], they are different cell types which can display different functions during CNS inflammatory responses[3, 4]. In order to investigate whether microglia and macrophages also effectively act differentially during MSC graft remodeling, we applied the BMT procedure using $eGFP^+$ bone marrow cells isolated from $eGFP^+$ transgenic mice before grafting MSC in the CNS. During this thesis, the procedure of BMT was successfully optimized following determination of the amount and timing of irradiation, the amount of bone marrow stem cells for injections and the after-care for the transplanted mice. At 8 weeks after BMT, flow cytometric analysis (see p. 46) revealed that nearly all bone marrow-derived nucleated blood cells expressed eGFP, demonstrating a successful BMT.

This procedure was successfully applied in several experiments, both presented in this thesis (see chapter 2 and [5]) and beyond[6]. The latter study involves a specific set of experiments highly similar to the results presented in chapter 2 but applying direct lentiviral vector injection of IL13 instead of implantation of IL13-producing stem cells.

B. Successful implementation of the $CX_3CR1^{eGFP/+}$ $CCR2^{RFP/+}$ transgenic mouse model to distinguish between brain-resident microglia and infiltrating peripheral macrophages.

While BMT is a well-established method for labelling infiltrating blood-borne macrophages in the CNS, the technique requires mice to be irradiated and completely depleted from their bone marrow, preferentially at the age of 8 weeks. Furthermore, as after BMT the mice need several weeks (minimum 4-5 weeks[7] and 8 weeks according to our protocol[5]) in order to achieve nearly full recovery, we felt certain limitations concerning

the timeline. Especially as administration of a cuprizone-supplemented diet is most optimal to achieve CNS inflammation and demyelination when applied at 8 weeks of age[8-10]. Although it is ascribed by Guglielmetti et al. [6] that BMT and CPZ-treatment can be combined, we preferred to overcome these limitations by investing in the transgenic $CX_3CR1^{eGFP/+}$ $CCR2^{RFP/+}$ mouse model. These transgenic mice were bred in-house by cross-breeding $CX_3CR1^{eGFP/eGFP}$ mice with $CCR2^{RFP/RFP}$ mice. In these crossed transgenic mice have one allele of the CX_3CR1 gene replaced by eGFP and one allele of the CCR2 gene replaced by RFP[11], thereby presenting microglia as green fluorescent and infiltrating macrophages as red fluorescent cells (see p. 115).

This transgenic mouse model was successfully applied in several experiments, both presented in this thesis (see chapter 5 and [12]) and beyond (Dooley et al., manuscript in progress). The latter study involves the implantation of IL13 producing stem cells in a mouse model of spinal cord injury that was subjected in the $CX_3CR1^{eGFP/+}$ $CCR2^{RFP/+}$ mouse model to discriminate between microglia and macrophages.

C. Successful implementation of TissueQuest histological analysis software to determine cellular densities of different cell types in the CNS.

Since immunofluorescence analysis of MSC grafts in healthy $eGFP^+$ BM chimeras and $CX_3CR1^{eGFP/+}$ $CCR2^{RFP/+}$ transgenic cuprizone-treated mice revealed many differently activated microglia and macrophage phenotypes, we were able to quantify each portion of the identified cell types by using TissueQuest software (see p. 104). This software tool made it relatively easy to determine cell densities of grafted MSC, astrocytes and differentially activated microglia and macrophages phenotypes within and surrounding the MSC cell graft. A specific advantage of this tool over the well-known ImageJ-based analyses and/or visual scoring methods is the highly quantitative nature of the obtained data, which in current biomedical science becomes of increased scientific value. Therefore, TissueQuest analyses have become a standard research tool in our laboratory, of which we published 2 methodological manuscripts[13, 14].

D. Successful implementation of magnetic resonance imaging to determine the therapeutic effect of IL13-producing MSC.

After selecting IL13 as a potential therapeutic cytokine for immunomodulation of neuroinflammatory processes, a mouse model was selected in order to pre-clinically evaluate the therapeutic potential of IL13. Since the cuprizone mouse model is a highly standardized model for induction of neuroinflammation and demyelination at the level of the splenium of the corpus callosum, it is also highly suitable for non-invasive imaging using magnetic resonance imaging (MRI) tools[9, 15]. By quantification of the T_2 relaxation time at the splenium, a comparison of the IL13-treated group could easily be performed between healthy and cuprizone control groups, as well as to determine the effect of IL13 on neuropathological events. Moreover, MRI results were correlated with quantitative histological analyses (see Chapter 5 and [12]). Due to our strong collaboration with the BioImaging laboratory at the University of Antwerp (prof. Annemie Van der Linden), we believe that our data presented in this thesis, validated by two independent and different research methodologies, i.e. non-invasive imaging and quantitative histological analyses, lead to highly similar results.

6.1.2. Scientific achievements

A. Description of a distinct spatial organization of brain-resident microglia and blood-borne macrophages during MSC graft remodeling.

Most studies investigating CNS inflammatory responses label brain-resident microglia and blood-borne macrophages as one and the same cell type due to overlapping phenotype markers and functions[1, 2]. However, more recently it has become clear that both populations demonstrate specific roles in neuro-inflammatory processes[3, 4]. Also in this thesis we describe that microglia and macrophages are able to express distinct markers upon activation, but can also differ in their spatial distribution (see p. 46) upon MSC implantation into the CNS. These observations not only indicate that both cell types can act differently in terms of neuro-inflammatory processes, but may also indicate that therapeutic intervention against neuro-inflammatory responses might need specific orientation toward microglia and/or macrophages[3, 16]. Further exploration of their

distinct roles – and eventually manipulation – may lead to better treatment options for patients with severe neuro-inflammatory disorders.

B. Efficient in vivo induction of M2 alternatively activated microglia and macrophages following transplantation of IL13 producing MSC.

Numerous *in vitro* studies have previously demonstrated the effect of IL13 on the activation status of microglia and macrophages. In these former studies, macrophages/microglia were always activated by LPS and/or IFNγ, creating highly pro-inflammatory M1-activated immune cells. Addition of IL13 to cell cultures led to the conversion of M1 towards M2 activation of microglia/macrophages[17, 18]. However, this in vitro setup does not completely resemble the in vivo situation, as many other factors should be considered during MSC graft-induced immune responses or pathology-induced inflammation in the CNS. In this thesis, we provide the first evidence that IL13, secreted by grafted MSC, is able to induce M2 activation of macrophages and microglia in the healthy and inflamed CNS *in vivo* (see p. 113). Moreover, we indicate that a wide range of microglia/macrophage activation phenotypes is induced via IL13 secreted by MSC in the CNS (see p. 122), thereby implicating that the M1/M2 paradigm is not so absolute as generally assumed. Therefore, this study is fully in line with other reports describing a wide range of M2-like activation phenotypes[18], which most likely all may contribute in a specific manner to dampen neuro-inflammatory responses.

C. Establishment of the neuroprotective effect of IL13-producing MSC on cuprizone – induced inflammation and demyelination in the CNS.

In the second part of this thesis, our findings demonstrate for the first time that IL13-producing MSC, grafted near the splenium of the corpus callosum, are able to reduce inflammation and demyelination in the CPZ mouse model (see Chapter 5 and [12]). These results are of high importance for future investigation, as this approach might lead to novel strategies to modulate neuroinflammation in CNS disease and injury. Moreover, we would like to stress that these observations were re-validated in several ways as determination of therapy effect was established both by MRI and quantitative histological analyses (see p. 106-109), as well as by the application of lentiviral vector technology to directly express IL 13 in the splenium of CPZ treated mice[5].

6.2. FUTURE PERSPECTIVE

Previous PhD theses within the Laboratory of Experimental Hematology already highly contributed to our current understanding of immunological responses following MSC, NSC and MEF grafting in the CNS[19-29]. With a specific focus on discriminating between microglia and macrophages as well as investigating the immunotherapeutic potential of IL13, this thesisis an evident continuation of these preceding efforts and again creates a strong basis for various new research questions briefly discussed below:

A. What is the mechanism behind the beneficial effects of IL13, observed in inflamed and demyelinated CNS?

In Chapter 5 p.123, we discussed the results obtained following grafting of IL13-MSC in the CNS of cuprizone-treated mice. As both MRI and quantitative histological analyses within the splenium showed diminished inflammation and demyelination, a major question with regard to how IL13 exactly exerts this effect remains. The most plausible mechanisms discussed, are either by the direct action of IL13 through inducing death of activated microglia, or alternatively by the indirect action of M2-activated macrophages induced by IL13, or by a combination of both. In order to investigate potential mechanisms of action, in future experiments we will perform transplantation of IL13-producing MSC in IL4 receptor type II knockout ($IL4RII^{-/-}$) mice[30]. This receptor binds both IL4 and IL13[31], so the effect of IL13 on brain-resident microglia and blood-borne macrophages could be investigated in this mouse model. However, to observe the effect specifically on microglia, $IL4RII^{-/-}$ mice should receive a wild type (or $eGFP^{+}$) bone marrow transplantation, in order for the BM-derived macrophages to express IL4RII. Inversely, to investigate the indirect IL13 effect specifically on BM-derived macrophages, wild type mice should receive BM isolated from $IL4RII^{-/-}$ mice. For this experimental setup, BMT procedures are already available within the laboratory and the IL4R KO mouse model has recently been introduced. Furthermore, several *in vitro* experiments could be set up to validate at one hand that IL13 is capable of inducing microglia cell death, e.g. by co-culture of LPS-activated microglia with IL13-producing MSC, or on the other hand that IL13-induced M2-activated macrophages are able to suppress microglial activation, e.g. by co-culture of IL13-MSC-primed macrophages with LPS-activated microglia. Unraveling the true mode of

action for in vivo IL13 mediated modulation of neuroinflammation is currently top priority in future research projects.

B. Do IL13-producing MSC exert similar neuroprotective effects in other CNS disease or injury models?

In order to validate whether IL13-MSC grafts are potential therapeutics for other pathologies characterized by neuroinflammation, additional disease or injury mouse models, more closely resembling human pathology, should be investigated. We are aware of this issue and in order to investigate this topic, we convinced several laboratories to jointly investigate this topic. At first, a long-lasting collaboration with prof. Sven Hendrix (Department of Morphology, University of Hasselt) has led to successful application and demonstration of the therapeutic benefit of IL13-MSC grafting in a mouse model of spinal cord injury in mice (Dooley et al., manuscript in progress). Currently we are also investigating in collaboration with prof. Stefanie Dedeurwaerdere (Experimental Laboratory of Translational Neuroscience and Otolaryngology, University of Antwerp) whether grafting of IL13-MSC in the hippocampus can alter the course and/or severity of epileptogenesis in a kainic acid-induced mouse model of epilepsy. Finally, we have planned an additional study in collaboration with prof. Matthias Hoehn (Max Planck Institute for Metabolism Research, Cologne) in order to evaluate the therapeutic benefit of IL13-secreting MSC in the middle cerebral artery occlusion mouse model of stroke. Within the next 1-2 years we hope to provide a clear answer whether transplantation of IL13-MSC has a future in human medicine.

C. Are there better alternatives available for the local administration of IL13 in the CNS?

In this thesis we used autologous MSC that were genetically transduced in order to produce IL13. However, future application of IL13-producing MSC in human CNS disease or injury, especially in case of urgent need, may require the use of allogeneic cells. An alternative research line within our laboratory is currently investigating whether grafting of allogeneic off-the-shelf MSC genetically engineered to secrete IL13 can achieve the same neuroprotective results. Currently we have learned that IL13-production by allogeneic MSC grafts can prolong their immunological survival in immune competent hosts as compared to non-engineered allogeneic MSC[32], but we still need to establish

whether the latter also results in therapeutic efficacy. Another possibility to avoid the use of cell grafts altogether is the direct administration of lentiviral vector encoding IL13 lentiviral vector for in vivo gene delivery into the CNS. This method was investigated in parallel to this thesis[5]. While the therapeutic effects on demyelination and inflammation were comparable to those presented in this thesis, over-activation of microglia and macrophages was observed. This effect is most likely due to the TLR-stimulation induced by the lentiviral particle[33]. Therefore, as demonstrated in this thesis, we are in favor of autologous, or eventually allogeneic, MSC grafts as a potential tool for the delivery of IL13 to counteract severe inflammatory responses following CNS injury or disease.

6.3. REFERENCES

1. Durafourt BA, Moore CS, Zammit DA, Johnson TA, Zaguia F, Guiot MC et al. Comparison of polarization properties of human adult microglia and blood-derived macrophages. Glia. 2012;60(5):717-27. doi:10.1002/glia.22298.
2. Hickman SE, Kingery ND, Ohsumi TK, Borowsky ML, Wang LC, Means TK et al. The microglial sensome revealed by direct RNA sequencing. Nature neuroscience. 2013;16(12):1896-905. doi:10.1038/nn.3554.
3. Shechter R, Schwartz M. Harnessing monocyte-derived macrophages to control central nervous system pathologies: no longer 'if' but 'how'. The Journal of pathology. 2013;229(2):332-46. doi:10.1002/path.4106.
4. Jung S, Schwartz M. Non-identical twins - microglia and monocyte-derived macrophages in acute injury and autoimmune inflammation. Frontiers in immunology. 2012;3:89. doi:10.3389/fimmu.2012.00089.
5. Le Blon D, Hoornaert C, Daans J, Santermans E, Hens N, Goossens H et al. Distinct spatial distribution of microglia and macrophages following mesenchymal stem cell implantation in mouse brain. Immunology and cell biology. 2014;92(8):650-8. doi:10.1038/icb.2014.49.
6. Guglielmetti C, Le Blon D, Santermans E, Salas-Perdomo A, Daans J, De Vocht N et al. Interleukin-13 immune gene therapy preventssevere inflammation and demyelination in the cuprizone mouse model via alternative activation of microglia and macrophages. **Submitted** to Molecular Therapy.
7. Larochelle A, Bellavance MA, Michaud JP, Rivest S. Bone marrow-derived macrophages and the CNS: An update on the use of experimental chimeric mouse models and bone marrow transplantation in neurological disorders. Biochimica et biophysica acta. 2015. doi:10.1016/j.bbadis.2015.09.017.
8. Praet J, Guglielmetti C, Berneman Z, Van der Linden A, Ponsaerts P. Cellular and molecular neuropathology of the cuprizone mouse model: clinical relevance for multiple sclerosis. Neuroscience and biobehavioral reviews. 2014;47:485-505. doi:10.1016/j.neubiorev.2014.10.004.
9. Guglielmetti C, Praet J, Rangarajan JR, Vreys R, De Vocht N, Maes F et al. Multimodal imaging of subventricular zone neural stem/progenitor cells in the cuprizone mouse model reveals increased neurogenic potential for the olfactory bulb pathway, but no contribution to remyelination of the corpus callosum. NeuroImage. 2014;86:99-110. doi:10.1016/j.neuroimage.2013.07.080.
10. Torkildsen O, Brunborg LA, Myhr KM, Bo L. The cuprizone model for demyelination. Acta neurologica Scandinavica Supplementum. 2008;188:72-6. doi:10.1111/j.1600-0404.2008.01036.x.
11. Mizutani M, Pino PA, Saederup N, Charo IF, Ransohoff RM, Cardona AE. The fractalkine receptor but not CCR2 is present on microglia from embryonic development throughout adulthood. Journal of immunology. 2012;188(1):29-36. doi:10.4049/jimmunol.1100421.
12. Le Blon D, Guglielmetti C, Hoornaert C, Dooley D, Daans J, Lemmens E et al. Intracerebral transplantation of interleukin 13-producing mesenchymal stem cells limits microgliosis and demyelination in the cuprizone mouse model. **Submitted** to Journal of Neuroinflammation.
13. Praet J, Santermans E, Reekmans K, de Vocht N, Le Blon D, Hoornaert C et al. Histological characterization and quantification of cellular events following neural and fibroblast(-like) stem cell grafting in healthy and demyelinated CNS tissue. Methods in molecular biology. 2014;1213:265-83. doi:10.1007/978-1-4939-1453-1_22.
14. Reekmans K, De Vocht N, Praet J, Le Blon D, Hoornaert C, Daans J et al. Quantitative evaluation of stem cell grafting in the central nervous system of mice by in vivo bioluminescence imaging and postmortem multicolor histological analysis. Methods in molecular biology. 2013;1052:125-41. doi:10.1007/7651_2013_17.
15. Wu QZ, Yang Q, Cate HS, Kemper D, Binder M, Wang HX et al. MRI identification of the rostral-caudal pattern of pathology within the corpus callosum in the cuprizone mouse model. Journal of magnetic resonance imaging : JMRI. 2008;27(3):446-53. doi:10.1002/jmri.21111.
16. Corraliza I. Recruiting specialized macrophages across the borders to restore brain functions. Frontiers in cellular neuroscience. 2014;8:262. doi:10.3389/fncel.2014.00262.

17. Van Dyken SJ, Locksley RM. Interleukin-4- and interleukin-13-mediated alternatively activated macrophages: roles in homeostasis and disease. Annual review of immunology. 2013;31:317-43. doi:10.1146/annurev-immunol-032712-095906.
18. Murray PJ, Allen JE, Biswas SK, Fisher EA, Gilroy DW, Goerdt S et al. Macrophage activation and polarization: nomenclature and experimental guidelines. Immunity. 2014;41(1):14-20. doi:10.1016/j.immuni.2014.06.008.
19. Bergwerf I, Tambuyzer B, De Vocht N, Reekmans K, Praet J, Daans J et al. Recognition of cellular implants by the brain's innate immune system. Immunology and cell biology. 2011;89(4):511-6. doi:10.1038/icb.2010.141.
20. Praet J, Reekmans K, Lin D, De Vocht N, Bergwerf I, Tambuyzer B et al. Cell type-associated differences in migration, survival, and immunogenicity following grafting in CNS tissue. Cell transplantation. 2012;21(9):1867-81. doi:10.3727/096368912X636920.
21. Tambuyzer BR, Bergwerf I, De Vocht N, Reekmans K, Daans J, Jorens PG et al. Allogeneic stromal cell implantation in brain tissue leads to robust microglial activation. Immunology and cell biology. 2009;87(4):267-73. doi:10.1038/icb.2009.12.
22. Praet J, Santermans E, Daans J, Le Blon D, Hoornaert C, Goossens H et al. Early inflammatory responses following cell grafting in the CNS trigger activation of the sub-ventricular zone: a proposed model of sequential cellular events. Cell transplantation. 2014. doi:10.3727/096368914X682800.
23. Praet J, Santermans E, Reekmans K, de Vocht N, Le Blon D, Hoornaert C et al. Histological characterization and quantification of cellular events following neural and fibroblast(-like) stem cell grafting in healthy and demyelinated CNS tissue. Methods in molecular biology. 2014;1213:265-83. doi:10.1007/978-1-4939-1453-1_22.
24. Reekmans K, De Vocht N, Praet J, Fransen E, Le Blon D, Hoornaert C et al. Spatiotemporal evolution of early innate immune responses triggered by neural stem cell grafting. Stem cell research & therapy. 2012;3(6):56. doi:10.1186/scrt147.
25. Reekmans K, De Vocht N, Praet J, Le Blon D, Hoornaert C, Daans J et al. Quantitative evaluation of stem cell grafting in the central nervous system of mice by in vivo bioluminescence imaging and postmortem multicolor histological analysis. Methods in molecular biology. 2013;1052:125-41. doi:10.1007/7651_2013_17.
26. Costa R, Bergwerf I, Santermans E, De Vocht N, Praet J, Daans J et al. Distinct in vitro properties of embryonic and extraembryonic fibroblast-like cells are reflected in their in vivo behavior following grafting in the adult mouse brain. Cell transplantation. 2015;24(2):223-33. doi:10.3727/096368913X676196.
27. De Vocht N, Lin D, Praet J, Hoornaert C, Reekmans K, Le Blon D et al. Quantitative and phenotypic analysis of mesenchymal stromal cell graft survival and recognition by microglia and astrocytes in mouse brain. Immunobiology. 2013;218(5):696-705. doi:10.1016/j.imbio.2012.08.266.
28. De Vocht N, Praet J, Reekmans K, Le Blon D, Hoornaert C, Daans J et al. Tackling the physiological barriers for successful mesenchymal stem cell transplantation into the central nervous system. Stem cell research & therapy. 2013;4(4):101. doi:10.1186/scrt312.
29. De Vocht N, Reekmans K, Bergwerf I, Praet J, Hoornaert C, Le Blon D et al. Multimodal imaging of stem cell implantation in the central nervous system of mice. Journal of visualized experiments : JoVE. 2012(64):e3906. doi:10.3791/3906.
30. Ndlovu H, Brombacher F. Role of IL-4Ralpha during acute schistosomiasis in mice. Parasite immunology. 2014;36(9):421-7. doi:10.1111/pim.12080.
31. Gour N, Wills-Karp M. IL-4 and IL-13 signaling in allergic airway disease. Cytokine. 2015;75(1):68-78. doi:10.1016/j.cyto.2015.05.014.
32. Hoornaert C, Luyckx E, Reekmans K, Dhainaut M, Dooley D et al. In vivo IL13-primed macrophages contribute to reduced alloantigen-specific T cell activation and prolong immunological survival of allogeneic mesenchymal stem cell implants. **Submitted** to Stem cells.

33. Matrai J, Chuah MK, VandenDriessche T. Recent advances in lentiviral vector development and applications. Molecular therapy : the journal of the American Society of Gene Therapy. 2010;18(3):477-90. doi:10.1038/mt.2009.319.

Curriculum vitae

Personal details

Debbie Le Blon
02-03-1988
Belgian
+32 495 42 13 72
LeBlon.Debbie@gmail.com

Frans Pauwelslei 31 b5
2970 Schilde
Belgium

Professional experiences

Since I have done my Master thesis in the laboratory of experimental hematology (Cell transplantation group), I was pleased to start my PhD here after achieving an IWT grant, in order to continue the interesting work on stem cell transplantation in the central nervous system. I was able to expand my knowledge and expertise in cell biology and animal studies regarding neuro-inflammation, while at the same time I was given the opportunity to participate at international conferences and publish my first research articles.

Education

PhD in medical sciences — University of Antwerp (2012-2015)

Doctoral thesis: *In situ* analysis of cellular and molecular interactions following cell transplantation in the central nervous system in mice.

Master in biomedical sciences — University of Antwerp (2009-2011)
With great honor

Master thesis: *In vivo* survival and characterization of NSC-derived neuronal cells following intracerebral transplantation in mice.
Acquired the Felasa C certificate

Bachelor in biomedical sciences — University of Antwerp (2006-2009)
With honor

Academic accomplishments

Publications

Nathalie de Vocht, Kristien Reekmans, Irene Bergwerf, Jelle Praet, Chloé Hoornaert, **Debbie Le Blon**, Jasmijn Daans, Zwi Berneman, Annemie Van Der Linden, Peter Ponsaerts. Multimodal imaging of stem cell implantation in the central nervous system of mice.
Journal of Visualized Experiments 2012; 64: e3906. (IF 2014: 1.325)

Nathalie de Vocht, Dan Lin, Jelle Praet, Chloé Hoornaert, Kristien Reekmans, **Debbie Le Blon**, Jasmijn Daans, Patrick Pauwels, Herman Goossens, Niel Hens, Zwi Berneman, Annemie Van Der Linden, Peter Ponsaerts. Quantitative and phenotypic analysis of mesenchymal stromal cell graft survival and recognition by microglia and astrocytes in mouse brain.
Immunobiology 2013; 218: 696-705. (IF 2014: 3.18)

Kristien Reekmans, Nathalie de Vocht, Jelle Praet, Erik Fransen, **Debbie Le Blon**, Chloé Hoornaert, Jasmijn Daans, Herman Goossens, Annemie Van Der Linden, Zwi Berneman, Peter Ponsaerts. Spatiotemporal evolution of early innate immune responses triggered by neural stem cell grafting.
Stem Cell Research & Therapy 2012; 3: 56. (IF 2014: 3.37)

Kristien Reekmans, Nathalie de Vocht, Jelle Praet, **Debbie Le Blon**, Chloé Hoornaert, Jasmijn Daans, Annemie Van Der Linden, Zwi Berneman, Peter Ponsaerts. Quantitative evaluation of stem cell grafting in the central nervous system of mice by in vivo bioluminescence imaging and postmortem multicolor histological analysis.
Methods in Molecular Biology 2013; 1052: 125-141. (IF pending)

Nathalie de Vocht, Jelle Praet, Kristien Reekmans, **Debbie Le Blon**, Chloé Hoornaert, Jasmijn Daans, Zwi Berneman, Annemie Van Der Linden, Peter Ponsaerts. Tackling the physiological barriers for successful mesenchymal stem cell transplantation into the central nervous system.
Stem Cell Research & Therapy 2013; 4: 101. (IF 2014: 3.7)

Roberta Costa, Irene Bergwerf, Eva Santermans, Nathalie de Vocht, Jelle Praet, Jasmijn Daans, **Debbie Le Blon**, Chloé Hoornaert, Kristien Reekmans, Niel Hens, Herman Goossens, Zwi Berneman, Ornella Parolini, Francesco Alviano, Peter Ponsaerts. Distinct in vitro properties of embryonic and extra-embryonic fibroblast-like cells are reflected in their in vivo behaviour following grafting in the adult mouse brain.
Cell Transplantation 2015;24(2):223-33. doi:10.3727/096368913X676196. (IF 2014: 3.13)

Debbie Le Blon, Chloé Hoornaert, Jasmijn Daans, Eva Santermans, Niel Hens, Herman Goossens, Zwi Berneman, Peter Ponsaerts. Distinct spatial distribution of microglia and macrophages following mesenchymal stem cell implantation in mouse brain.
Immunology & Cell Biology 2014; 92(8):650-8. (IF 2014: 4.15)

Jelle Praet, Eva Santermans, Kristien Reekmans, Nathalie de Vocht, **Debbie Le Blon**, Chloé Hoornaert, Jasmijn Daans, Herman Goossens, Zwi Berneman, Niel Hens, Annemie Van der Linden, Peter Ponsaerts. Histological characterization and quantification of cellular events following neural and fibroblast(-like) stem cell grafting in healthy and demyelinated CNS tissue.
In: *Bruno Christ et al. (eds.) Animal Models for Stem Cell Therapy, Methods in Molecular Biology, 2014; vol. 1213:265-83.* DOI 10.1007/978-1-4939-1453-1_22

Jelle Praet, Eva Santermans, Jasmijn Daans, **Debbie Le Blon**, Chloé Hoornaert, Herman Goossens, Niel Hens, Annemie Van der Linden, Zwi Berneman, Peter Ponsaerts. Early inflammatory responses following cell grafting in the CNS trigger activation of the sub-ventricular zone: a proposed model of sequential cellular events.
Cell Transplantation 2014. doi:10.3727/096368914X682800. (IF 2014: 3.13)

Chloé Hoornaert, Evi Luyckx, Kristien Reekmans, Maxime Dhainaut, Dearbhaile Dooley, **Debbie Le Blon**, Erik Fransen, Jasmijn Daans, Louca Verbeeck, Nathalie De Vocht, Evi Lemmens, Herman Goossens, Annemie Van der Linden, Valerie Roobrouck, Catherine Verfaillie, Sven Hendrix, Muriel Moser, Zwi Berneman, Peter Ponsaerts. In vivo IL13-primed macrophages contribute to reduced alloantigen-specific T cell activation and prolong immunological survival of allogeneic mesenchymal stem cell implants.
Accepted for publication in Stem Cells. (IF 2014: 6.52)

Debbie Le Blon, Chloé Hoornaert, Jan R. Detrez, Sanne Bevers, Jasmijn Daans, Herman Goossens, Winnok H. De Vos, Zwi Berneman, Peter Ponsaerts. Immune remodeling of stromal cell grafts in the central nervous system: therapeutic inflammation or (harmless) side effect?
Accepted for publication in Journal of Tissue Engineering and Regenerative Medicine. (IF 2016: 5.20)

Debbie Le Blon, Caroline Guglielmetti, Chloé Hoornaert, DearbhaileDooley, Jasmijn Daans, Evi Lemmens, Nathalie De Vocht, Kristien Reekmans, Eva Santermans, Niel Hens, Herman Goossens, Marleen Verhoye, Annemie Van der Linden, Zwi Berneman, Sven Hendrix and Peter Ponsaerts. Intracerebral transplantation of interleukin 13-producing mesenchymal stem cells limits microgliosis and demyelination in the cuprizone mouse model.
Under review at Journal of Neuroinflammation.(IF 2014: 5.41)

Caroline Guglielmetti, **Debbie Le Blon**, Eva Santermans, Angelica Salas-Perdomo, Jasmijn Daans, Nathalie De Vocht, Disha Shah, Chloé Hoornaert, Jelle Praet, Jurgen Peerlings, Firat Kara, Christian Bigot, Zhenhua Mai, Niel Hens, Sven Hendrix, Marleen Verhoye, Anna Planas, Zwi Berneman, Annemie van der Linden, Peter Ponsaerts. Interleukin-13 immune gene therapy preventssevere inflammation and demyelination in the cuprizone mouse model via alternative activation of microglia and macrophages.
Under review at Molecular Therapy. (IF 2014: 6.23)

Scientific activities

INMiND 'Animal models of neuro-inflammation' course. October 2012, Barcelona (Spain) - Training

National symposium: Cell-Based Therapies in Central Nervous System Pathology. April 2013, Hasselt (Belgium) – Poster presentation

> Abstract: Cell transplantation into CX3CR1-eGFP mice reveals two distinct microglia/macrophage populations recognizing mesenchymal stem cell grafts in mouse brain. (Debbie Le Blon, Chloé Hoornaert, Nathalie De Vocht, Jasmijn Daans, Kristien Reekmans, Zwi Berneman and Peter Ponsaerts.)

XIth European Meeting on Glial Cells in Health and Disease. July 2013, Berlin (Germany) – Poster presentation

> Abstract: Cell transplantation into CX3CR1-eGFP mice reveals two distinct microglia/macrophage populations recognizing mesenchymal stem cell grafts in mouse brain. (Debbie Le Blon, Chloé Hoornaert, Nathalie De Vocht, Jasmijn Daans, Kristien Reekmans, Zwi Berneman and Peter Ponsaerts.)

BSCDB October meeting 'Experimental models of human diseases'. 2013, Luik (Belgium) – Poster presentation.

> Abstract: Expression of IL13 by grafted mesenchymal stromal cells modulates activation state of graft-infiltrating macrophages, and not microglia, in the central nervous system of immune competent mice. (Debbie Le Blon, Nathalie De Vocht, Dearbhaile Dooley, Chloé Hoornaert, Jasmijn Daans, Herman Goossens, Kristien Reekmans, Evi Lemmens, Zwi Berneman, Sven Hendrickx and Peter Ponsaerts.)

The ESGCT and SETGyC collaborative Congress. October 2013, Madrid (Spain) – Poster presentation

> Abstract: Expression of the M2-type cytokines IL4 and IL13 prevents mesenchymal stem cell graft infiltration by microglia/macrophages in the central nervous system of immune competent mice. (Debbie Le Blon, Nathalie De Vocht, Dearbhaile Dooley,

Chloé Hoornaert, Jasmijn Daans, Herman Goossens, Kristien Reekmans, Evi Lemmens, Zwi Berneman, Sven Hendrickx, Peter Ponsaerts.)

EMBL Conference: Microglia: Guardians of the brain? March 2014, Heidelberg (Germany) – Poster presentation

Abstract: Transplantation of IL13-secreting mesenchymal stem cells protects against cuprizone-induced inflammation and demyelination in mouse brain via the introduction of M2-type macrophages. (Debbie Le Blon, Chloé Hoornaert, Caroline Guglielmetti, Nathalie De Vocht, Kristien Reekmans, Jasmijn Daans, Herman Goossens, Annemie Van der Linden, Zwi Berneman, Sven Hendrix, Peter Ponsaerts.)

Lentiviral Vectors Symposium. April 2014, Brussel (Belgium) - Poster presentation

Abstract: Lentiviral vector-mediated expression of interleukin 13 by mesenchymal stem cell grafts in chronic inflammatory CNS tissue promotes the conversion of an M1 pro-inflammatory environment towards an M2 anti-inflammatory environment. (Debbie Le Blon, Caroline Guglielmetti, Chloé Hoornaert, Eva Santerman, Dearbhaile Dooley, Evi Lemmens, Jasmijn Daans, Nathalie de Vocht, Niel Hens, Annemie van der Linden, Zwi Berneman, Sven Hendrix, Peter Ponsaerts.)

WOG-MS Symposium. April 2014, Leuven (Belgium) - Poster presentation

Abstract: Neo-expression of interleukin 13 by mesenchymal stem cell grafts in healthy and demyelinating mouse brain induces the M2-phenotype in graft- and lesion-infiltrating microglia and/or macrophages. (Debbie Le Blon, Chloé Hoornaert, Caroline Guglielmetti, Nathalie De Vocht, Kristien Reekmans, Jasmijn Daans, Herman Goossens, Annemie Van der Linden, Zwi Berneman, Sven Hendrix, Peter Ponsaerts.)

BSCDB and BSBMB joint meeting. October 2014, Antwerp (Belgium) – Oral presentation

Abstract: Genetic engineering of mesenchymal stem cells with interleukin 13 improves their immunotherapeutic efficacy in the cuprizone mouse model of multiple sclerosis. (Debbie Le Blon, Caroline Guglielmetti, Chloé Hoornaert, Eva Santermans, Dearbhaile Dooley, Jasmijn Daans, Evi Lemmens, Niel Hens, Annemie Van der Linden, Sven Hendrix, Zwi Berneman and Peter Ponsaerts.)

Interuniversity Stem Cell Meeting. April 2015, Leuven (Belgium) – Oral presentation

Abstract: Genetic engineering of mesenchymal stem cells with interleukin 13 improves their immune modulating capacity in the cuprizone mouse model of CNS inflammation. (Debbie Le Blon, Caroline Guglielmetti, Chloé Hoornaert, Eva Santermans, Dearbhaile Dooley, Jasmijn Daans, Evi Lemmens, Niel Hens, Annemie Van der Linden, Sven Hendrix, Zwi Berneman and Peter Ponsaerts.)

Dankwoord

Hier zijn we dan eindelijk! Vier jaar geleden leek dit nog verre toekomst, maar zoals ze zeggen: Time flies when you're having fun! En leuk was het zeker, een beetje cellen kweken hier, een paar muizen injecteren daar, afgewisseld met wat coupes kleuren en schrijfwerk tussendoor. Uiteraard had ik hier niet gestaan zonder de begeleiding, hulp en steun van vele mensen rondom mij, die ik dan ook graag even zou bedanken.

Vooraleerst zou ik mijn promotoren Peter Ponsaerts en Zwi Berneman willen bedanken om mij de mogelijkheid te geven te doctoreren in jullie onderzoeksgroep. In het bijzonder bedank ik Peter nog graag even voor de fantastische begeleiding tijdens mijn doctoraat en de fijne wetenschappelijke gesprekken die me gemotiveerd hielden wanneer het wat stroef ging. Wanneer de helft van mijn testgroep het na transplantatie al begeven had, of wanneer ik dure producten had besteld die achteraf niet bleken te werken, zelfs wanneer ik mezelf per ongeluk met difteria toxine had geïnjecteerd, je deur stond altijd open! Dan hielp je wel altijd om een plan B te bedenken. Of me naar de spoed te sturen…

Mijn lieve collega's,
Uiteraard zouden al deze resultaten niet mogelijk zijn zonder jullie. Jasmijn die heel wat hersentjes gesneden heeft voor mij, Chloé die insprong wanneer nodig bij injecties of bij celkweek, Alessandra who helped with perfusions. Thank you all! I always loved eating chocolates, homemade cakes, drinking caipirinhas, or having lunches in the sun and just chatting with you about anything!
Anne, hoewel je maar een relatief korte tijd bij ons was, ben ik toch blij om met je te hebben kunnen samenwerken!
Merci à Caroline, la madame d'IRM, je te remercie mille fois pour toutes les fois que tu m'as aidé, même quand tu étais à l'autre bout du monde! Ainsi que toutes nos conversations scientifiques et non-scientifiques, je ne les oublierai jamais!
Ook alle ex-collega's, Nathalie, Kristien, Nele en Jelle, wil ik heel graag bedanken omdat ik altijd met al mijn vragen bij jullie terecht kon. Ook voor al de research en optimalisatie die jullie al gedaan hadden, dat heeft het mij zeker en vast een stuk gemakkelijker gemaakt! Bart en Irene, een beetje de grondleggers van het onderzoek over MSC modulatie in de hersenen,

ik heb niet, of maar korte tijd met jullie samengewerkt, maar jullie harde werk heeft ook mede de basis gevormd voor mijn thesis, waarvoor dank!

Veel van het onderzoek binnen deze thesis had uiteraard ook niet mogelijk geweest zonder de expertise en/of de infrastructuur van andere labo's.
De onderzoeksgroep van Prof. Hendrickx, met Evi en Derv, heel erg bedankt voor de leuke samenwerking en vergaderingen met de lekkere taarten en aardbeien!
And thank you Derv, me and Chloé will never forget the traumatizing day we had to empty the bladders for the first time! ;-) Although the mice were surely even more traumatized…
Bedankt aan Prof. Van der Linden en het Bio-Imaging Lab voor alle MRI experimenten die werden uitgevoerd en geanalyseerd binnen mijn onderzoek. Bedankt ook aan het MICA en het Laboratorium voor Oncologie voor alle hulp bij het optimaliseren en uitvoeren van het bestralingsexperiment. Bedankt aan Prof. Hens en Eva van CENSTAT voor het analyseren van de vele data en ervoor te zorgen dat alles statistisch correct berekend werd. Bedankt ook aan Prof. De Vos en Jan Detrez van het Laboratorium voor Celbiologie en Histologie voor de prachtige 3D beelden van onze MSC grafts.

Mocht ik hier toch nog mensen vergeten zijn, alvast mijn excuses, maar alsnog bedankt!

Tot slot wil ik nog enkele heel belangrijke personen bedanken die er altijd waren om op terug te vallen tijdens mijn doctoraat.

Mijn partner in crime, Wai Ping, ik kon altijd bij jou terecht met frustraties of om gewoon eens goed te tetteren en lachen. Jouw mailtjes konden mij altijd opfleuren ;-)
You always made my day!

Mijn lieve, geweldige ouders, dankzij jullie was het in de eerste plaats mogelijk om dit doctoraat te beginnen. Jullie steun tijdens mijn volledige studieverloop betekent erg veel voor mij. Niet enkel door het financieren van mijn studies, maar vooral ook door altijd interesse te tonen en oprecht trots te zijn op mijn prestaties. Bedankt voor alles! Hou van jullie!

Stefan, Dirk en Aline, mijn voltallige schoonfamilie en al mijn vrienden, jullie vroegen geregeld naar mijn doen en laten op het labo en ik vond het altijd erg leuk om mijn project in begrijpbare taal uit te leggen aan jullie (al was het een drietal keer). Ontzettend bedankt voor alle steun en interesse!

Als allerlaatste wil ik mijn fantastische man bedanken om er altijd voor mij te zijn. Om mijn enthousiasme te delen wanneer ik mijn IWT moest gaan verdedigen, een presentatie moest geven, een artikel had gepubliceerd, en om me altijd op te beuren wanneer het wat moeilijker ging. Ons weekend in de Ardennen, zo perfect getimed na het BSCDB congres, zal ik dan ook nooit vergeten. Alle stress van die week was in één tel volledig verdwenen. Je bent de perfecte man voor mij, ik hou ontzettend veel van jou.